Doctoral Thesis

博士論文

Uncertainties in tsunami risk management:

A case study for the southern coasts of Iran

(津波リスクマネジメントにおける不確定性：イラン南部の海岸を例として)

Parastoo Salah

パラストー　サラ

UNCERTAINTIES IN TSUNAMI RISK MANAGEMENT:

A CASE STUDY FOR THE SOUTHERN COASTS OF IRAN

A Dissertation

by

PARASTOO SALAH 47-177652

in Partial Fulfillment

of the Requirements for the Degree

Doctor of Philosophy

Advisor: Professor Jun Sasaki

Graduate Program in Sustainability Science – Global Leadership Initiative

Graduate School of Frontier Sciences

THE UNIVERSITY OF TOKYO

February 2021

UNCERTAINTIES IN TSUNAMI RISK MANAGEMENT:

A CASE STUDY FOR THE SOUTHERN COASTS OF IRAN

ABSTRACT

Tsunami Risk Management is a very complex process which requires knowledge of tsunami sources, wave propagation, subsequent inundation, and geographical condition of the affected area along with socio-economic factors. To date the outcome of various risk management implemented in the world have been less effective than hoped by their planners. It is mostly because of the uncertain nature of hazards and individuals. Based on world's experience from previous disasters there are various sources of uncertainties that may cause failure on the implication of a risk management. These uncertainty indicators are scattered in different fields (e.g. engineering, sociology, and psychology), and a holistic perspective is needed to connect various disciplines and stakeholders in order to develop a universal framework to minimize the uncertainties.

To this purpose, in this study, after introduction in Chapter 1, a systematic literature review from different subjects was conducted in Chapter 2 to evaluate the most important uncertainty indices and factors which caused failure on the previous disaster risk managements. Accordingly, a holistic framework of uncertainty indicators that includes the failure roots and their drivers was developed. It is concluded that the inefficiency of protection infrastructures (i.e. hard measures), awareness and experience, belief system, normalcy bias, too much reliance on warning system and sea walls, demographic characteristics (e.g. aging society and gender discrimination), and trust are the main sources causing the failure. Furthermore, it is indicated that to propose an optimal mitigation measure, mitigation strategies have to acknowledge heterogeneity in each community characteristics. This remains an important gap in regions where risk probability is low and the lack of empirical data are considered a serious shortcoming. Thus, Makran region was selected as the study area that is – due to the relatively infrequent coastal disasters and its low population – not as important in literature as other tsunami prone areas. The identified uncertainty indicators for Makran were evaluated in order to promote resilience and minimize the prolonged uncertainty.

Chapter 3 provides a general methodology to how to incorporate each uncertainties. In Chapter 4 an interdisciplinary approach to tsunami hazard assessment in Makran Subduction Zone (MSZ) was illustrated via developing a methodology that incorporates uncertainties

stemming from the lack of researcher knowledge and the random nature of the hazards. Former is represented by epistemic uncertainty in literature while the latter is known as aleatory variability. The method combines statistical, geological, historical tsunami assessment and simulation modeling. The threat of tsunami hazard posed to the coast of Iran by the MSZ were assessed and a comprehensive probabilistic tsunami hazard assessment for the entire coast regardless of population density was presented. The sources of epistemic uncertainties were taken into account by employing event tree and ensemble modeling. Aleatory variability was also considered through probability density function. Further, the contribution of small to large magnitudes was considered and multitude of scenarios were created as initial conditions using the developed event trees. `Funwave-TVD` was employed to propagate these scenarios. The results of this chapter are of vital for various stakeholders for developing and implementing tsunami risk activities such as insurance activity, land use, critical facility design, and guiding risk-aware city planning.

On the other hand a mere reliance on engineering measures, i.e. hard, could lead to more vulnerability since people at risk neglect self-protection. Furthermore, implication of this type of measures is very costly yet not efficient enough. Hence, the importance of soft measures to minimize vulnerability should be taken into account and more research has to be done along these lines. Accordingly, a cost-benefit disaster management should be applied in developing countries like Iran, where there is a limited budget for developing hard measures in the area. Having said that, one of the challenges nowadays is how to apply the methods of performance of soft measures to disaster preparedness. A very first step is to assess local awareness, knowledge, perception, and willingness to evacuate, which is discussed in Chapter 5. In order to asses the aforementioned factors in Makran region, a mixed methodology was used, using questionnaire survey, interviews and group discussion amongst the local residents, beach users and authorities. Some initial steps were taken including systematic literature review and expert's consultation. The questions were distributed to 6 experts in the field of disaster from Iran by email and their comments were applied on the questionnaire. In addition, the questionnaire was first tested on 10 residents through face to face interviews. The modified questionnaire covers the following topics: knowledge, awareness, experience, trust, evacuation

behavior, socio-demographic factors (age, income, gender, occupation, religion, and education), family composition, vulnerable groups and sense of belonging. The survey was conducted by various convenience sampling methods at four locations along the Makran coast in the period September 10-30, 2018. In total, 198 valid questionnaires were collected. 24 households' face to face surveys, three group discussions (about 3 hours and 45 minutes in total) were held in 3 fishery ports. Finally, the quantitative and qualitative analysis were done.

From the analysis of both questioners and interviews, it was learned that the solid faith in destiny and lack of belief in their will and determination are among the personal characteristics of individuals living in the area. The improper belief in destiny and neglecting one's part (ability) to change his or her situation lead to have less plans and almost dismiss the role of mitigation strategies. It should be noted that getting used to any circumstances blindly together with "actions" that come with no action, make any change and acceptance of new thoughts and methods difficult. Also, the results showed that the level of people's trust to government for disaster education and information is very low. This is comparable with the SVS framework (Salient Value Sharing Framework) that was furthermore modified to incorporate this study'd findings.

The results, limitations and future direction were discussed in chapter 6. Finally, this research's findings were concluded and summarized in Chapter 7. The results of this study shed light on the uniqueness of the community characteristic in a less known region (Makran), expands upon the empirical evidence of them, provides accurate and reliable tsunami hazard maps, and help policy-makers to understand how to shape a cost-effective and sustainable tsunami risk planning and provide valuable information for diverse stakeholders to underpin tsunami activities, and risk-aware city planning, and mitigation measure design.

ACKNOWLEDGMENTS

I would foremost like to thank my advisor Prof. Jun Sasaki for his trust, continuous support, and encouragement through my study period in Japan. Our discussions have always been a pleasure and I wish to thank him for sharing his thoughts with me. I am also indebted to Prof. Hiromi Yokoyama for commenting on the social aspects of this thesis and for several illuminating conversations.

I would also like to extend my gratitude to the thesis examination committee members, Professor Honda Riki, Professor Hiromi Yokoyama, Associate Professor Tanaka Toshinori, and Associate Professor Takenori Shimozono for their valuable comments and critical discussions. I am thankful to all the members of Sasaki Lab for providing me endless help and sharing an enjoyable study environment with me.

I would like to kindly acknowledge the support of the Japanese Ministry of Education, Culture, Sports, Science and Technology (MEXT), for providing me the great opportunity and experience in a wonderful country, Japan.

A big thank you goes to the people who have helped me during my field survey in Tehran and Chabahar, Eng. Abbas Sheikhi, my brother, Peyman and sister in law, Hedieh.

I would like to express my deepest gratitude towards my brother for his love, support and for always believing in me. I would not have made it to this point without him.

Last but for most, I cannot begin to express my unfailing gratitude and love to my coming soon husband! and my best friend, Morteza, who constantly supported and encouraged me when the tasks seemed arduous and insurmountable. He made the PhD life an enjoyable and sweet challenge for me. I will continue admiring him and getting inspiration from him in my academic journey (though it seems impossible to be as good as he!).

DEDICATION

To my parents, Yousef and Shahnaz,

who have always supported me, stood by my side, and encouraged me to seek my dreams in a man dominated society. I am the woman I am today because of them.

TABLE OF CONTENTS

LIST OF FIGURES

LIST OF TABLES

1 INTRODUCTION

In this chapter, first, the background and motivation of this study are provided. Then, based on what is discussed in these sections, the main and sub-objectives of the research are described.

1.1 Disaster risk management

"It may be said that the twenty first century is the age not so much of the 'revolt of the masses' as the 'revolt of nature' (Starrs, 2014a)."

Risk is the probability of loss that takes place at three levels of sophistication: hazard, vulnerability, and exposure. The probability of loss changes as any elements change (Crichton, 1999). Hazard is a potentially destructive physical phenomenon (e.g. earthquake, tsunami, flood). Hazard assessment is the process of identifying what hazards have threatened an area, how often specified hazards have occurred, and with what intensity. Succinctly, it is the probability and severity of a destructive physical phenomenon. Exposure is the value of asset that could be affected by a hazard (e.g. population, structures, historical and natural attractions). Vulnerability describes the characteristics of people, structure and any system and their circumstances due to the damaging effects of a hazard. There are various factors of vulnerability, like physical, environmental, economic, and social (Wisner et al., 2004).

Disaster risk management is a multidisciplinary research field since its assessment cannot solely be reduced by an evaluation of the physical hazard itself and socio-economic factors play a prominent role to decrease or increase it. Fig. 1 shows the diagram of the key elements of risk.

Risk management mainly consists of risk assessment and risk evaluation. Risk assessment is dealing with scientific outputs of modeled parameters and vulnerable factors. Risk evaluation employs perceived risk to a practical and sensible way of analysis, such as cost benefit relationship and socio economic or/and cultural impact.

In risk management, evaluation and assessment of all the three pillars (see Fig. 1) are inevitable. Besides, any disaster risk reduction effort require intersections among different disciplines involved. The Sendai framework for disaster risk reduction 2015 – 2030 underlines

that for disaster risk reduction and promoting disaster resilience, knowledge of the hazards and vulnerability factors (i.e. physical, social, cultural, economic, and environmental is infrangible (UNISDR, 2015).

On the other hand, disasters can have a devastating impact on the long-term sustainability of human settlements. Thus, disaster risk reduction is one of the crucial topics in sustainability science (Esteban et al., 2020). Moreover, five sustainable development goals (SDGs) namely, 11.b, 2.4, 11.5, 1.5 and 13.1 concern about disaster risk reduction and are linked directly to reduce risk disaster. Moreover, SDG3 – population health outcomes – cannot be achieved without risk reduction than can cause health problems.

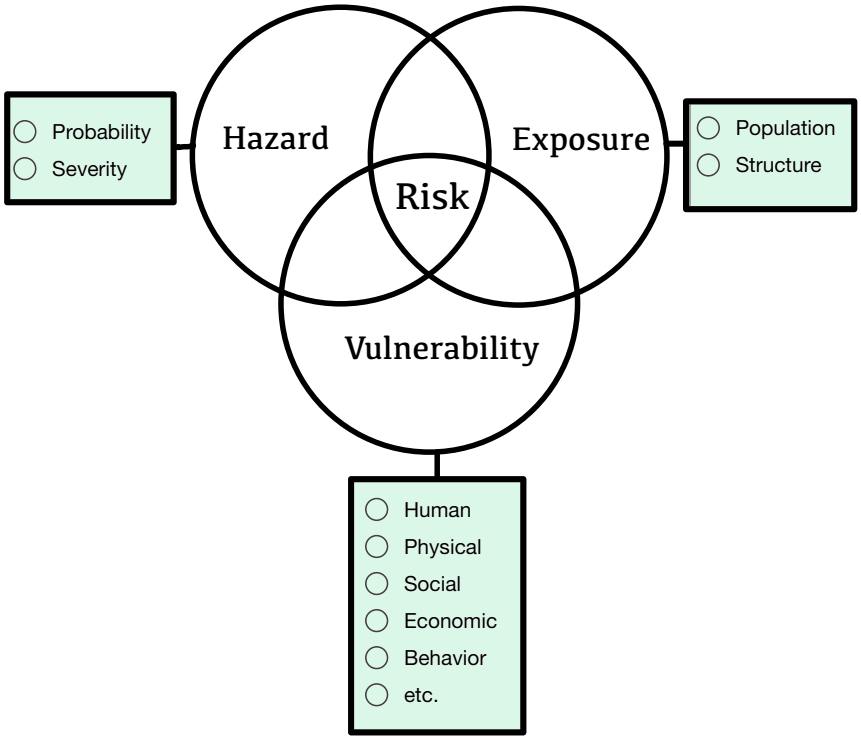

Fig. 1 Three pillars of Risk: Hazard, Vulnerability, and Exposure.

1.2 Tsunami risk management

The global population continues to increase and so does the number of people living in disaster prone regions without strong risk awareness. *Tsunamis* are a representative natural threat that can lead to significant casualties and widespread destruction, homelessness, and poverty.

Although tsunamis are not frequent around the world, their damages are significant and not negligible owing to their destructive forces as well as many other impacts after it, namely, displaced populations, health risks, food scarcity, emotional after shocks and etc.

Tsunami Risk Management is a very complex process which requires knowledge of the tsunami resources, the wave propagation and subsequent inundation, geographical condition of the affected area, social and economic aspects and etc. Also, it is a highlighted subject since the three key elements of sustainability science are directly affected by it (society, environment and economy). In addition, holistic point of view is needed to connect various disciplines in order to develop approaches that can reduce the tsunami risk.

The initial step toward a comprehensive tsunami risk management is the hazard assessment. In particular, the importance of a comprehensive tsunami hazard assessment (THA) is highlighted when a disastrous tsunami occurs. Recent devastating tsunamis such as the Sumatra tsunami of 2004, with more than 200,000 fatalities (Starrs, 2014b), and the 2011 Tohoku tsunami in Japan, which caused more than 15,000 fatalities and was responsible for the Fukushima Nuclear Power Plant accident (Fujii et al., 2011a), are representative examples. Following these disasters, there has been a remarkable development in tsunami risk management to reduce the effect of future tsunamis. For recent reviews of these developments, including full lists of references, see (Løvholt et al., 2015; Ward et al., 2020).

The assessment of vulnerability in the concept of risk management is a complex area, by considering its wide variety parameters and being scattered in different fields. It constitute a multidisciplinary research field and can be classified as human, physical, socio economic, environmental, behavioural and etc. A review of available global risk management analyses reveals that greater focus has been on potential of hazards and other aspects are yet under - studied. In the other word, in addition to the view that the world needs more engineering measures, there is actually a ”knowledge gap“ built on the relative lack of knowledge regarding other risk factors such as social and human behavior. This can lead to a massive vulnerability in any tsunami prone areas.

Hence, comprehensive management in disaster confrontation systems and mitigation strategies should be considered as beneficial approaches that no harm can come out of them and for the sake of coastal areas they should be deeply and carefully investigated all the factors.

1.3 Uncertainty in tsunami risk management

Uncertainty is a prerequisite and constant element of risk (Vasvári et al., 2015). To date the outcome of various risk management implemented in the world have been less effective than hopped by their planners. It mostly is because of the uncertain nature of hazards and individuals. Based on world's experience from previous disasters there are different types of uncertainties that may cause failure on the implication of the risk management. These uncertainty indicators are ubiquitous and scattered in different field (e.g. engineering, social, psychology) and even the definition of uncertainty is not consistent across different disciplines. This makes identifying and covering all of the indicators in a risk management a complicated process.

Uncertainty is mainly because of the lack of data, and/or predictability of a major event (Argote, 1982). The less data and information on the study area, the more uncertainty involve in risk managements. To overcome and minimize these uncertainties in any events, gathering and analysing more data about potentially affected areas is the keystone for decision makers (Comfort, 2007). Besides of lack of information, uncertainty can stem from a lack of understanding of the information among both residents and decision makers. Hence, decision makers need to understand that they must work together with other stakeholders rather than simply "educate" them. Moreover, ignoring the heterogeneity in community characteristics and individuals' behaviour may lead to a situation in which decision makers are not aware of the uncertain factors in their community. Furthermore, a poor historical data can lead to a significant uncertainties and a technique is needed to be applied to overcome this shortcoming. Other uncertainties due to inherent randomness of an event, are like throwing a coin. These kind of uncertainties can be best considered by probability studies.

In tsunami risk management various factors such as the ones related to the hazard itself (e.g. maximum magnitude, and arrival time), knowledge, awareness, psychological factors, socio-cognitive process, cultural, and personality causes uncertainties. A comprehensive and

holistic view is needed to identify the uncertainties, gather data (be it evidence or modeled), and develop approaches and frameworks to minimize them in tsunami risk management.

1.4 Tsunami risk management in Iran

Tsunamis can hamper the development of developing countries, and recovery is arduous and expensive. Historically, Iran has been affected by tsunamis; in both the Caspian sea and Oman sea.[1] The historical tsunami events are shown in Fig. 2. From historical records there were no significant tsunami that could affect coast of Caspian sea in the northern part of Iran. However, The most significant one happened in 1945 in the Makran subduction zone (MSZ), causing upwards of 4000 casualties along the southern coasts of Iran and Pakistan (Murty and Rafiq, 1991).

In Iran coastal hazards are infrequent, which leads to a false sense of safety among leaders, decision makers and residents. Besides, according to the country's economic report (census, 2016) Makran is one of the areas with the highest poverty rate. These two together make the MSZ more vulnerable to an unexpected natural hazard. However, considering tsunami hazard and risk assessment, Makran remains one of the under-studied regions in the world. Moreover, there is no local warning system, inundation map, evacuation map, measures to reduce vulnerability of coastal Disaster in the prone areas. In this regard, a comprehensive study is needed to assess both hazard and vulnerability in the MSZ. because damages can be minimized by sufficient mitigation plans and initial preparations.

1.5 Thesis objectives

The main objective of this study is to identify and consider uncertainties in tsunami risk management stemming from the nature of hazard itself and the social vulnerability factors, taking southern coast of Iran as a case study. More categorically the sub-objectives are to:

(i) comprehensively investigate, determine and classify the important factors playing a role in risk and vulnerability assessment in the presence of major uncertainties to provide a holistic framework of uncertainties indicators.

[1] Or the Gulf of Oman, Makran sea.

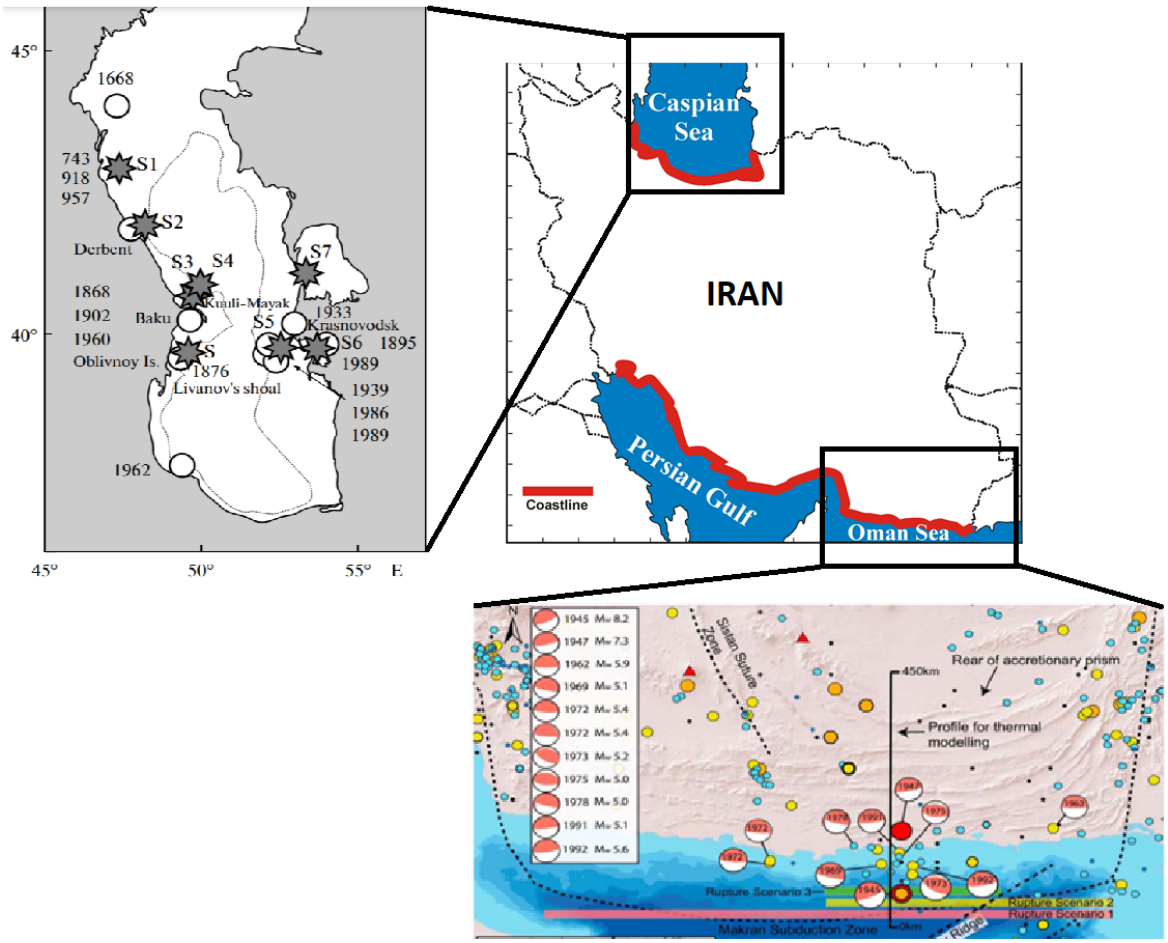

Fig. 2 Historical tsunami happened in the coast of Iran both in the Caspian and Oman sea. References: Caspian sea (Kulikov et al., 2014) and Oman sea (Smith et al., 2013)

(ii) illustrate an interdisciplinary approach to Tsunami hazard assessment integrate uncertainties dealing with the hazard itself. The approach combines statistical, geological, historical tsunami assessment and simulation modeling and provides hazard maps. It includes covering limitation in historical data as well as considering all the stakeholder's interests.

(iii) evaluate the identified uncertainty factors in the MSZ study area addressing how people perceive risks and underpinning risk perception, shed light on the uniqueness of the community characteristic and in this way expands upon the empirical evidence of them, and propose alternative measures considering the priority of approaches for reducing the risk and increasing preparedness mitigation with less cost and effort.

Research findings could be applied in other areas with the similar feature (e.g. incompleteness historical data, similar community characteristics) and other hazards than tsunami.

1.6 Thesis outline

After Introduction provided here in Chapter 1, a systematic literature review to evaluate the most important uncertainty indices and factors which caused failure on the risk management is shown in Chapter 2. Chapter 3 provides a general methodology on both hazard and vulnerability factors assessment in the study area. In chapter 4 uncertainties assessment of hazard and its results are presented. Chapter 5 provides the vulnerability assessment of residents addressing the uncertainties and uniqueness of community. In Chapter 6 discussion, recommendation, and limitations of the study is provided. Finally, all the results are concluded in Chapter 7.

2 SYSTEMATIC LITERATURE REVIEW

In this chapter a systematic literature review to evaluate the most important uncertainty indices and factors which caused failure on the risk management in the previous natural hazards around the world is provided. First, to recognise the most relevant resources and indicators a review of the literature on tsunami risk managements using various keywords published from 1900 to the present had been done. Then, a framework of the most important and used keywords in literature is illustrated. Finally, a detailed review is provided on the filtered academic resources and based on the developed framework.

2.1 Literature mining

A literature search was conducted to identify the relevant studies and articles based on abstract and title words and citation relation. Data were collected from the Web of Science Core Correction in the period of 1900–2020. Various keywords were used to increase the chance of finding more relevant publications. Tsunami + risk management", "Tsunami + failure cause ", "Tsunami + uncertainty" and "Tsunami + lessons" are used as keywords. More than 2000 results were found.

The results were then filtered based on their relevance, and frequency. Fig. 3 shows the density map of the most repeated keywords extracted from the filtered publications. `VOS-viewer` software was used for the visualization (Van Eck and Waltman, 2010). As it was expected, the keywords map shows a vast range of disciplines and are scattered in different fields of research (e.g. engineering, social studies, management studies, probability analysis).

There are two approaches to increase coastal resilience against natural hazards such as tsunamis or storm surges: hard (i.e., structural) and soft (i.e., non-structural) measures. soft measures are "any measures not involving physical construction that uses knowledge, practice or agreement to reduce risk and impacts, in particular through policies and laws, public awareness-raising, training, and education." (UNISDR, 2015). The former includes protection and accommodation in infrastructures while soft measures are any measures not involving physical construction. However, the most highlighted and repeated keywords have focused on the

uncertainties in the physics of the hazard itself, rather than other socio-economic, environment and etc. aspects.

Hence, after a full-text screen and removing the publications without presenting any indicators of uncertainties and failure roots of tsunami risk managements, publications were divided into (i) studies focusing on hard measures and uncertainties in the physics of hazard, and (ii) studies focusing on soft measures and uncertainties in individuals and people.

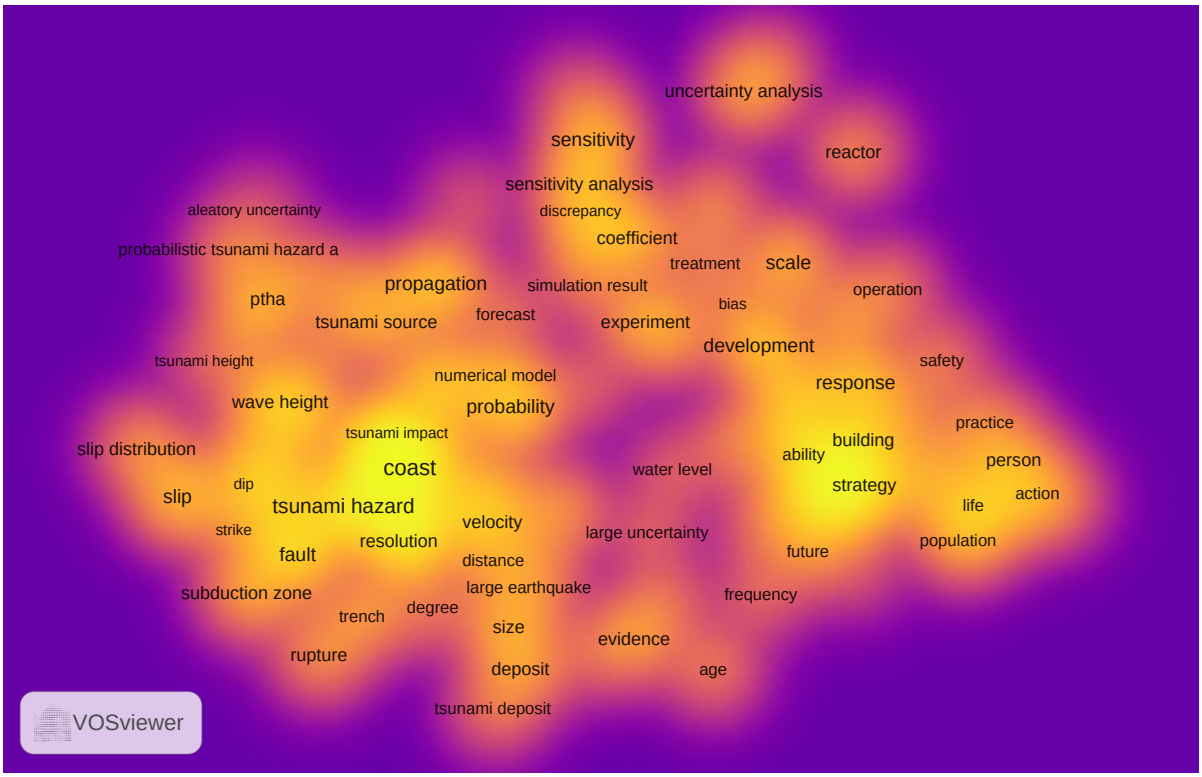

Fig. 3 The density map of the most repeated keywords extracted from the filtered publications. Filtering was based on their relevance, and frequency. Search engine: Web of Science Core and Correlation; Keywords: " Tsunami + risk management", "Tsunami + failure cause ", "Tsunami + uncertainty" and "Tsunami + lessons"; `VOS-viewer` software was used for visualization. The transparency of colors is determined by the weight of the keyword. The higher the weight, the darkest the keyword and its color.

2.2 Literature review – hard uncertainties

The 2004 and 2011 tsunamis lead to the unprecedented role of uncertainty in tsunami hazard assessment in tsunami-prone areas. The failure of hard measures (e.g. sea walls, dikes) in some areas of Japan during the 2011 tsunami, made communities more vulnerable. New concept for

tsunami mitigation measures (i.e., levels 1 and level 2) was considered in Japan (Suppasri et al., 2016).

Tsunami hazard assessment includes sensitivity analyses (see e.g. (Goda et al., 2014, 2019)) as well as deterministic (see e.g. (Heidarzadeh et al., 2009; Lynett et al., 2016; Salah and Soltanpour, 2014)) and probabilistic approaches. The latter approach– called the probabilistic tsunami hazard assessment (PTHA) –has received substantially increased attention after the 2004 and 2011 tsunamis (Kagan and Jackson, 2013; Lorito et al., 2015; Løvholt et al., 2014; Satake, 2014). Unlike deterministic approaches that consider specific scenarios (commonly including the worst case scenario) to calculate tsunami hazard metrics (such as run up height and arrival time), PTHA calculates the likelihood of tsunami impact employing multiple possible scenarios consisting of the contributions from small to large events along with all quantifiable uncertainties (Geist and Lynett, 2014). Hence, PTHA can overcome the limitation of incomplete or insufficient historical records, and extend the return periods from hundreds to thousands of years. Furthermore, this approach considers the uncertainties. PTHA was developed by adopting the probabilistic seismic hazard analysis (PSHA) (Cornell, 1968; Downes and Stirling, 2001; Rikitake and Aida, 1988), and much progress has been built upon it see (Grezio et al., 2017) and the references therein. Notwithstanding that PTHA is a relatively new method, it has been widely used in tsunami-prone areas owing to its diverse range of applications (e.g., (Bayraktar and Ozer Sozdinler, 2020; Davies and Griffin, 2019; Mori et al., 2018; Sepúlveda et al., 2019; Thio et al., 2014)), each of them covers different uncertainties, methods, and level of accuracy. A reliable PTHA must consider the epistemic uncertainty and aleatory variability simultaneously.

Epistemic uncertainties are stemming from the lack of researcher knowledge and is related to the lack of understanding and limited knowledge of the process. while aleatory variability expresses the innate variability of the physical process and the random nature of hazards. Epistemic uncertainty can be reduced by collecting new data and new knowledge about hazards and modeling the process. Whereas the unpredictability of a hazard (i.e. aleatory variability) does not reduce with additional data.

Many authors believe that no theoretical significance exists for this separation because, as long as our knowledge increases, all uncertainties become epistemic (Marzocchi et al., 2015). The main epistemic uncertainty and aleatory variability sources in tsunami hazards are following:

(i) **Source mechanism (zone):** the spatial distribution of earthquakes is heterogeneous. A big challenge is to define a subduction where there is a constrained historical data. Low activity rates mean that a lot of intraplate faults may be unidentified (Grezio et al., 2017) and it is not accurate to not consider them in PTHA studies.

(ii) **Recurrence model:** The magnitude density functions give the relative rate of different magnitude levels on a source. Earthquake catalogues are limited at large magnitudes for a particular fault zone and it imposes uncertainties in frequency distribution. Return periods of large earthquakes are at most of the time undefined.

(iii) **Slip distribution:** slip distribution significantly affects tsunami heights nearshore. In THA studies it has been typical to use uniform slip instead of heterogeneous distributions. Recently, different studies have shown that maximum nearshore wave height varies by a factor of 2 or more due to heterogeneity in earthquake slip (Butler et al., 2017; Goda et al., 2014; Løvholt et al., 2012; Mueller et al., 2015; Sugino et al., 2015).

(iv) **Tide stage:** the tide level at tsunami arrival time is unknown. In most tsunami models the sea level can be adjusted to see the effect of the tsunami at different tide stages. Tide level is one of the main aleatory variability sources (González et al., 2009). (Mofjeld et al., 2007) computed the probability density function of the maximum wave height of tsunami plus the tidal stage. The results area approximated by the least squares fit the Gaussian distribution. (Adams et al., 2015) suggested a method in which the effect of tide can be included by calculating the exceedance probability of tide level.

(v) **Modeling and bathymetry:** Because PTHA have usually multitude scenarios included (cf. deterministic approach),the modeled tsunami metrics (such as run up height and arrival time) are not expected to give a highly accurate representation of the once's in real events.

(vi) **Rupture area:** Given the earthquake magnitude, rupture length and width can varies largely and it is one of the main sources of uncertainties.

(vii) **Intensity (magnitude)** considering maximum magnitude ($M_{\max}$) event due to their short records is one of the main sources of uncertainty (Thio, 2010)

(viii) **Earthquake epicenter:** the location of earthquakes is unknown. Short historical data makes the prediction of exact location of next earthquake impossible.

Fig. 4 shows all the above-mentioned uncertainties. As it was discussed there is no theoretical significance between epistemic uncertainty and aleatory variability. In different studies the boundary of incorporating aleatory and epistemic in to PTHA has been blurry. The method used in this study is explained in Chapter 4. Fig. 4 is restructured with distinguishing epistemic uncertainty and aleatory variability and the approach used in this work (see Fig. 8).

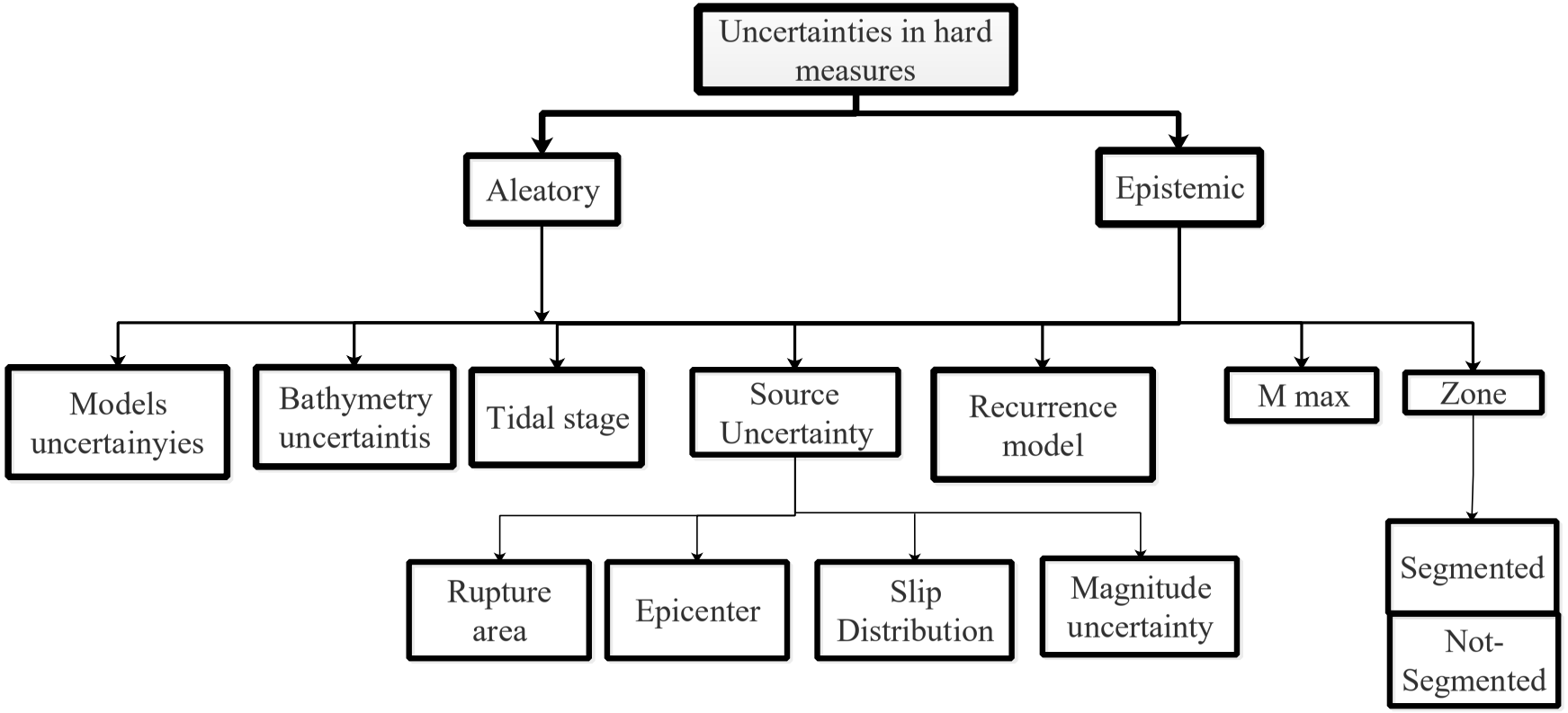

Fig. 4 Two types of uncertainties in THA: epistemic and aleatory.

2.3 Literature review – soft measures

After an in deep review, the publications with the most relevance to uncertainties and failures of soft measures were extracted. Fig. 5 shows the network map of the keywords with more than 5 times repeats in abstract of the extracted literature. Lines colors represent links between keywords and the cluster to which the keyword belongs, respectively. the stronger two keywords relatedness, they located closer to each other. The strongest co-citation links between keywords are represented by lines.

Overall the keywords such as local knowledge, experience, willingness of evacuation, normalcy bias, trust, leader, culture are among the most repeated keywords in publications targeting soft measures and their failure. They can be categorized into (i) people's knowledge and awareness and (ii) their perception and attitude towards a hazard. A more detailed review on these topics is provided in due sections.

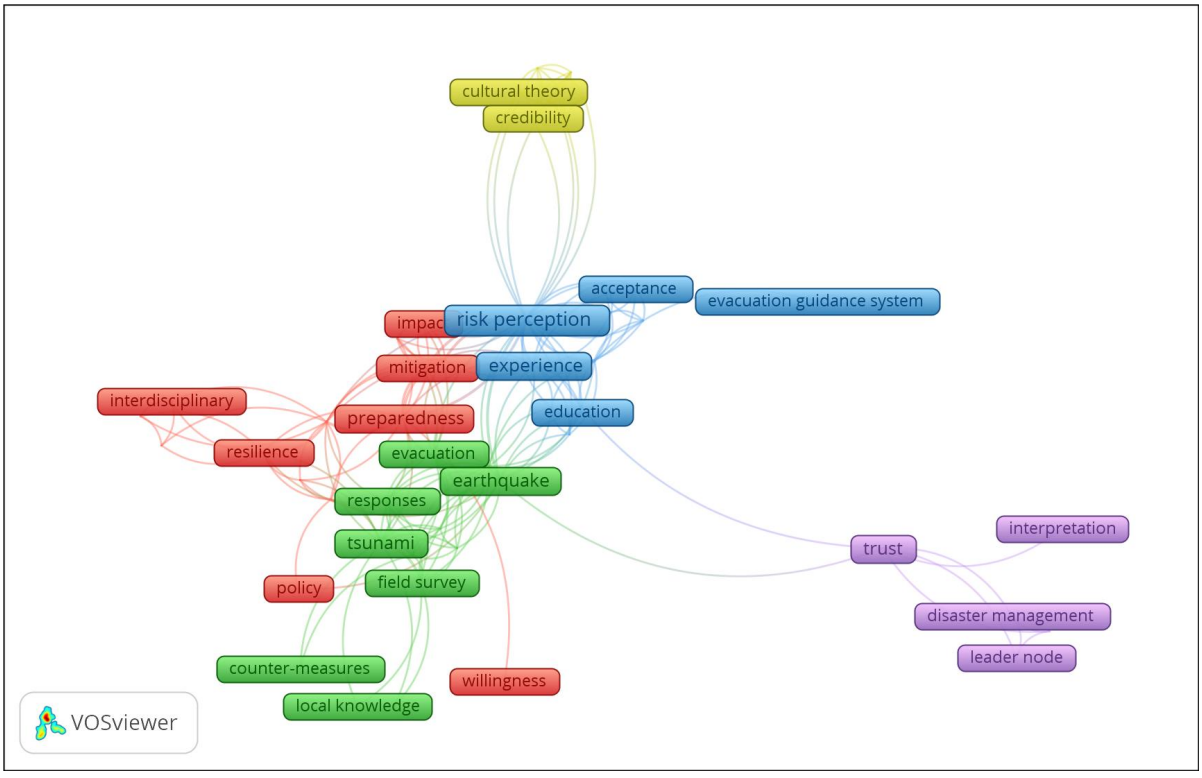

Fig. 5 The network map of the keywords with more than 5 times repeats in abstract of literature on soft measures uncertainties and failure roots. `VOS-viewer` software was used for visualization.

2.3.1 In deep literature review

Usually, after any coastal disaster there is a major drive to construct and/or improve the hard measures in the prone areas. These structures may reduce the tsunami awareness of residents by leading them to believe that the structures fully protect them rather than simply reducing damages. However, an over-reliance on engineering construction, that is, hard measures alone, can still lead to mass casualties as the at-risk population neglects self-protection strategies. A simple example is that of the 2011 Tohoku tsunami, more specifically in Taro town that this thinking occurred (Suppasri et al., 2013). Moreover, implication of this type of measures are very costly yet not efficient enough. Despite the expensive exercise for preventing, predicting, and protecting vulnerable communities in the United States against natural hazards, people have still faced staggering helplessness (Science and Council, 2003). All these together raises the question as to whether hard measures are sustainable and can support the socio-economic development of local communities. This is because the effect of disasters can be exacerbated when socio-economic factors are not addressed (Esteban et al., 2015a; Mileti et al., 1995). Hence, soft measures should also be considered to minimize vulnerability and studied more extensively (Shibayama et al., 2013a; Yun and Hamada, 2012). Accordingly, cost benefit and disaster management analyses should be applied in developing countries such as Iran, where the budget for developing hard measures is limited.

Having said that, still one of the most formidable challenges nowadays is how to apply the concepts and methods of performance of soft measures to disaster preparedness.

To propose optimal mitigation measures, decision makers and education strategies must acknowledge community heterogeneity (Paton and Johnston, 2001).

2.3.1.1 knowledge and awareness

On general grounds, awareness and knowledge influence disaster preparedness. First, literature concerning this topic were briefly reviewed. Awareness in this sense has been defined as the extent to which people think and talk about a specific hazard (Paton, 2003). the authors in (Tavares et al., 2010) assumed that awareness depends on general knowledge of residents and their access to the information sources. However, (Esteban et al., 2013a) pointed out that

awareness of people is location specific and depends on different factors, such as education, policies, and culture. These indices have been separately targeted in unique locations prone to different natural hazards; for example, typhoons (Esteban et al., 2015c, 2016), hurricanes (Ukkusuri et al., 2017; Whitehead et al., 2000), and floods (Esteban et al., 2013a; Mabuku et al., 2018; Takagi et al., 2016). Tsunamis, however, have received comparatively less attention. Some studies have established the level of community awareness in tsunami prone areas (ANH et al., 2017; Esteban et al., 2013b; Gregg et al., 2006; Takabatake et al., 2018a). Researches on knowledge, awareness, and willingness have been carried out in Vietnam (ANH et al., 2017; Esteban et al., 2014), Trinidad and Tobago (La Daana et al., 2016), Samoa (Lindell et al., 2015), and Japan (Kakimoto et al., 2016; Nomoto, 2016; Takabatake et al., 2018a; Yun and Hamada, 2015). Gregg *et al.* in (Gregg et al., 2006) summarized that people knowledge about tsunami in Hilo is low, hence, changes in disaster education is needed to increase understanding among locals. Esteban *et al.* (Esteban et al., 2013b) investigated indices in Japan, Chile, and Indonesia that can reflect the degree of awareness at the authority, institution, or citizen levels. Cubelos *et al.*(Cubelos et al., 2019) established the level of tsunami awareness through community mapping in Chile.

Some studies have further analyzed awareness and proposed new directions for tsunami mitigation and evacuation (Hein, 2014; Shibayama et al., 2013b). For example, the idea conceptualized by Esteban *et al.*(Esteban et al., 2015b) showed how a given event can quickly raise awareness; however, this increased awareness often fades with each successive generation. Hence, repeated education and regular evacuation drills by local government (Suppasri et al., 2015), and storytelling across generations, may maintain this level of awareness (Viglione et al., 2014).

Global awareness about tsunamis and the risk associated with it has increased owing to the recent events, including the 2004 Indian Ocean tsunami, the 2010 Samoa and Chile tsunami, and the 2011 Tohoku earthquake tsunami (Esteban et al., 2018). Due to the high casualties and destruction forces of these events, a conception of "tsunami culture" has developed in vulnerable communities. Furthermore, the mass media coverage following tsunamis has impacted areas that are not often affected by such events.These yield a renewed interest among researchers.

Some studies investigated factors of failures and successes of tsunami mitigations through post-survey: (Gregg et al., 2006) studied socio-cognitive indices of tsunami's warnings based on the 2004 Indian ocean tsunami experience; (Kanai and Katada, 2011) identified issues among residents' preparedness resulting from 2010 Chile tsunami; (Suppasri et al., 2013) found self-evacuation is very important through post-survey after 2011 tsunami; Toshitaka Katada – known as the tsunami hero – showed "children's power to survive" from tsunami education before 2011 Tohoku tsunami (Katada and Kanai, 2016); furthermore, (Esteban et al., 2013a) compared preparedness among Indonesia, Chile and Japan after tsunami. All studies have reported increase awareness and knowledge about tsunami in recent years; however, there is likely an upper limit regarding mass media's influence in areas without tsunami experiences . In addition, the uniqueness of each community, cultural and local factors, play pivotal roles in the context of awareness and knowledge. Accordingly, the MSZ provides a novel case study to be further investigated.

2.3.1.2 Attitude and Perception

Although factors related to the hazard – physics of tsunamis – largely dictate impact, knowledge and awareness affect a community's vulnerability. Other factors like socio-cognitive, personality, cultural are inevitable and yet poorly understood. In the 2011 Tohoku tsunami, only 57% of people evacuated immediately in some areas (MAS et al., 2012), even though owing to different experiences, regular drills were conducted, and educational awareness and general knowledge were relatively high.

(Pidgeon et al., 1992) defined risk perception as "people's beliefs, attitudes judgment and feelings, as well as the broader social or cultural values that people adopt against risks." Risk perception can therefore be considered a cognitive process capable of guiding people's behavior to reduce the impact of a uncertain event. Various factors such as psychological and cultural, which are usually correlated can influence perception assessment.

The importance role of risk perception in evacuation behavior has been showed in the literature, but empirical data are lacking (Sugiura et al., 2019). In addition, although evacuation behavior have been discussed in literature for other types of natural hazards, like, earthquakes

and volcanoes, and hurricanes (Dash and Gladwin, 2007; Lindell and Perry, 2012; Vicente et al., 2014), it is yet to be addressed for tsunami. some studies have been carried out on investigating reasons of failure/success in evacuation in the affected areas (Sugiura et al., 2019; Yasuda et al., 2016) and identified factors related to intention to evacuate by considering a hypothetical scenario in areas not experiencing a major tsunami. Some examples for the former one are: (Sugiura et al., 2019) in which the authors addressed psychological and personality factors by applying hierarchical regression analysis to survey data from survivors of 2011 Tohoku earthquake. (Ohno and Isagawa, 2012; Yasuda et al., 2016) and (Suwa and Kato, 2009) tried to answer how residents behave after 2011 earthquake and 2006 Kuril island tsunami, respectively. Moreover, (Nakasu et al., 2018) investigated reasons behind high death toll of Rikuzentakata in 2011 tsunami. People's experience, belief systems, normalcy bias, too much reliance on warning system and engineering infrastructures, trust, some demographic characteristics such as age and gender have been considered the main failure factors for evacuation (Basolo et al., 2009; Nakasu et al., 2018). Normalcy bias is a tendency to underestimate the risk of a warned hazard, which affects appropriate evacuation.

Regarding the latter subject, i.e. willingness and intention behavior to evacuate, there have been some studies focusing on variety of coastal hazards in different countries. For example, (Fraser et al., 2013) addressed the intended evacuation behavior of residents at Napier city in the event of tsunami. (Whitehead et al., 2000) investigated the intended or hypothetical evacuation willingness from hurricanes in the United States. Other studies have been conducted on the willingness of specific groups (e.g., older (Gray-Graves et al., 2010) and tourist (Faulkner, 2001; Rittichainuwat, 2013) populations) to evacuate. Finally, some studies went one step further and provided predict modelings including actual behavior of residents, employing data appeared already in the literatures (Takabatake et al., 2017, 2018b; Yamashita et al., 2014).

The consideration of evacuation behavior for tsunami events in areas without frequent tsunami experience is poorly studied in the literature; and, remarkably no studies have been carried out in the MSZ regarding this issue.

2.4 Summary

This chapter shows a systematic literature review that had been conducted to find the uncertainty indicators and failure roots in tsunami risk managements. There were rather two branches of indicators and failure roots: the ones dealing with hard measures and those dealing with soft measures. In regards to hard measures uncertainties were mostly stemming from the physics of hazard itself (the lack of data and knowledge, epistemic and unpredictability nature of it, aleatory). They were scattered in different fields, geophysics, numerical modeling, statistical approach, earth science, and etc. Soft measures failure roots were mostly connected to community's knowledge, awareness, attitude, perception, and heterogeneity of each. Hence, both "hard" and "soft" protection measures should be applied in an interactive and simultaneous way to design a cost-benefit and sustainable disaster management.

3 GENERAL METHODOLOGY

In this chapter, the general methodology to account and incorporate uncertainties in both hard and soft measures in Makran, Iran is explained. The identified indicators from literature review in Chapter 2 are taking into account using described method here.

3.1 Study area

As it was shown in Chapter 2, section 1.4, historical records of tsunami show the potential of tsunami in both the north (Caspian sea) and the south (Makran) of Iran. However, Makran was selected as a case study in this research owing to its more vulnerability and uniqueness of the area that it shall be discussed in this section.

The Makran region, located along the southeastern coast of Iran and the southern coast of Pakistan. It should be taken into consideration that area is one of the closest and best access point to the open sea for landlocked countries (e.g., Uzbekistan, Afghanistan, and Mongolia) and is one of the most significant intersections of North-South world business Corridor (see Fig. 6). Moreover, it is benefiting from numerous historical and natural attractions in addition to its valuable Geo-economics advantageous. the Iranian government approved the "Makran sustainable development" plan in 2016, naming Chabahar, the most populated city in the region, a free economic zone and unrestrained migration after the development will happen.

The Makran coast is covered by two province in Iran, Hormozgan and Sistan and Baluchestan and from Gwadar bay to Jask is around 600 km. There are five major port in the area namely, Gwadar, Chabahar, Tis, Konarak and Jask. The Human Development Index (HDI) with 0.682 in Sistan and Baluchestan is the lowest among other provinces in Iran.

Notably, historically, the area has been affected by tsunamis as it was shown in Fig. 2; the most disastrous of which occurred in 1945, with upwards of 4000 casualties reported in Pakistan and Iran.

(Heidarzadeh et al., 2008; Salah and Soltanpour, 2014) carried out studies in Makran to simulate tsunami waves, inundation areas , and predict possible scenarios for future tsunami events (Heidarzadeh and Kijko, 2011; Salah et al., 2020). These studies mainly focused on the

the hazard itself; however, social factors play an important role in the concept of sustainable risk management. Moreover, uncertainties had not been account in the area.

Fig. 6 Study area, Makran shown in red rectangular. It is located at the southern part of Iran. It is covered by two provinces, Hormozgan and Sistan and Baluchestan. it is benefiting from numerous historical and natural attractions in addition to its valuable Geo-economics advantageous.

3.2 Incorporating hard uncertainties

For a region that lacks an extensive historic record of tsunamis and earthquakes, such as Makran, it is utmost important to provide a valuable tool for assessing tsunami hazard. As it was already discussed in Chapter 2, PTHA can overcome the limitation of incomplete or insufficient historical records, and extend the return periods from hundreds to thousands of years. Furthermore, having a sustainability point of view a tsunami hazard assessments should be a very comprehensive one. Accordingly, Probabilistic approaches are highly preferred to deterministic ones since all of the stakeholder's interests and objectives should be taken into account. Moreover, PTHA approach is needed to better quantify the uncertainties, namely Aleatory and Epistemic one.

The MSZ is a tsunami risk zones as attested by compiled tsunami catalogues and recent paleotsunami studies (Kakar et al., 2015) that exhibits risks for the neighboring countries of Iran, Oman, and Pakistan. This region is not as prominent in scientific literature as other tsunami-prone subduction zones owing to its low population density, and it remains as one of the least studied regions. The authors of (Heidarzadeh and Kijko, 2011) performed the first generation of PTHA in the MSZ. Their results are not reliable for return period far from the typical recurrence time of magnitude $M_{\mathrm{w}} = 8.1$ because only three earthquakes were considered in their study. Furthermore, the rough discretization of sources used may have affected the final results. (Hoechner et al., 2016) conducted a PTHA along the MSZ based on a synthetic earthquake catalogue. In their study, a simple geometry model along with a uniform (cf. heterogeneous) slip distribution were used because their primary focus was identifying the consequences of maximum magnitude assumptions. Finally, (El-Hussain et al., 2016) performed a logic tree approach for assessing the hazard only for Oman coasts. Of particular importance is the absence of aleatory variability in the aforementioned studies. For any tsunami probability study, it is critical to understand how uncertainty affects probability estimation. Thus, this study aim to fill the gaps of previous PTHA studies in the MSZ via developing a methodology that incorporates both aleatory and epistemic uncertainties. This work overcomes the limitation in the integration of uncertainties, namely, tidal level, heterogeneity in slip distribution and rupture size, numerical and geometry models, earthquake recurrence rate, and maximum magnitude.

The methodology aims to calculate the probability of exceeding a /set of tsunami heights at the Makran coast, considering both epistemic and aleatory uncertainties. In order to incorporate epistemic uncertainties two event trees were developed based on scientific facts and historical data. Later, to select the true hazard ensemble modeling was applied. Aleatory variability was considered by incorporating directly to the probabilistic equations.

First, the seismicity area and generated synthetic scenarios similar to that described by (Davies and Griffin, 2019) were determined. Then, for each scenario, a fully nonlinear tsunami model `Funwave-TVD` (Kirby et al., 1998; Shi et al., 2012) was ran to obtain the maximum wave heights along the coastline. Additionally, the epistemic uncertainties by developing two event

trees and ensemble modeling were incorporated. Finally, the tsunami height exceedance rate considering the aleatory variability was calculated.

3.2.1 Epistemic incorporation

Epistemic uncertainties can be incorporated by developing event trees. The event tree framework was first considered for PSHA (Cornell, 1968) and then was adapted to assess PTHA (Annaka et al., 2007; Burbidge et al., 2008) and was recognized as a comprehensive method for PTHA. Each node of event tree represents a specific uncertainty and collects a series of alternative models, represented by the different branches. Different branches of event trees may make the analysis expensive in terms of computation time and storage yet it is better than Monte carlo approach. each path of event tree represents one hazard curve, thus the number of path in event trees results the same number of hazard curves.

3.2.1.1 Ensemble model

The selection of true hazard has been subjective of an argument among practitioners. Some argues the mean hazard of event tree is the hazard and hazard distributions of all the paths do not have probabilistic meaning. In contrast, others describe the hazard using the distribution of all event tree hazard curves. (Marzocchi et al., 2015) claims that interpretation of all event tree's outcomes is more appropriate and meaningful from probabilistic point of view. With an example of coin toss with two persons. Probability tree of it is shown in Fig. 7. The mean value of this tree (in this case it is equal to 0.54) has no frequentist interpretation as it would expected one coin with one person will happen every time.

In this study a more general method was used in addition to event trees was used: ensemble model which is based on a method initially introduced for PSHA studies.

To estimate the true hazard, the approach that considers the mean hazard should be abounded and it does not represent a long-term probability of exceedances as the true hazard. Ensemble modeling presumes that epistemic uncertainty is greater than that evaluated by one event tree, and treats the branches of the event tree as an unbiased sample from a parent distribution (Marzocchi et al., 2015). In this way and it solves some drawbacks of logic trees such as the

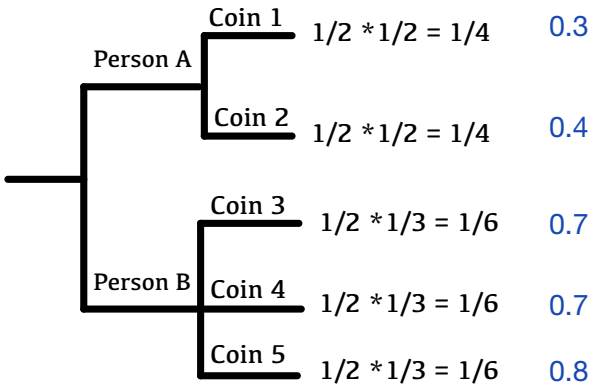

Fig. 7 Probability tree for coin toss. In this tree there are two persons and 5 coins. Each branches of the tree is weighted bu blue color. The mean value of this tree is 0.54, and do not represent any meaningful description as it is expected the outcome of this event be one specific person and coin each time.

interpretation of outcomes. To build an ensemble model of alternatives a parent distribution was fit to the set of event branches' probability outcomes. A natural choice is the beta distribution with parameters of (α, β). Parameters α and β are the average and variance of each branch.

3.2.2 Aleatory variability

Aleatory variability was directly incorporated in probability equations. In the analysis, three main contributions to the aleatory variability have been identified: (i) The mismatch between tsunami height model and observed caused by the numerical and bathymetric model error, (ii) The stochasticity in the earthquake dimensions imposed by the scaling relations, (iii) The tide variation at tsunami arrival time. Fig. 4 is restructured with distinguishing epistemic uncertainty and aleatory variability and the approach used to incorporate each (see Fig. 8).

3.2.3 Generation and propagation model

To calculate generation waves some steps were taken as follow:

(i) First, the vertical co-seismic dislocation of each segments (see Chapter 4 section 4.5.1 for more details about construction of the segments over the MSZ) was calculated via a homogeneous elastic half-space model (Okada, 1985). Okada model is derived from a

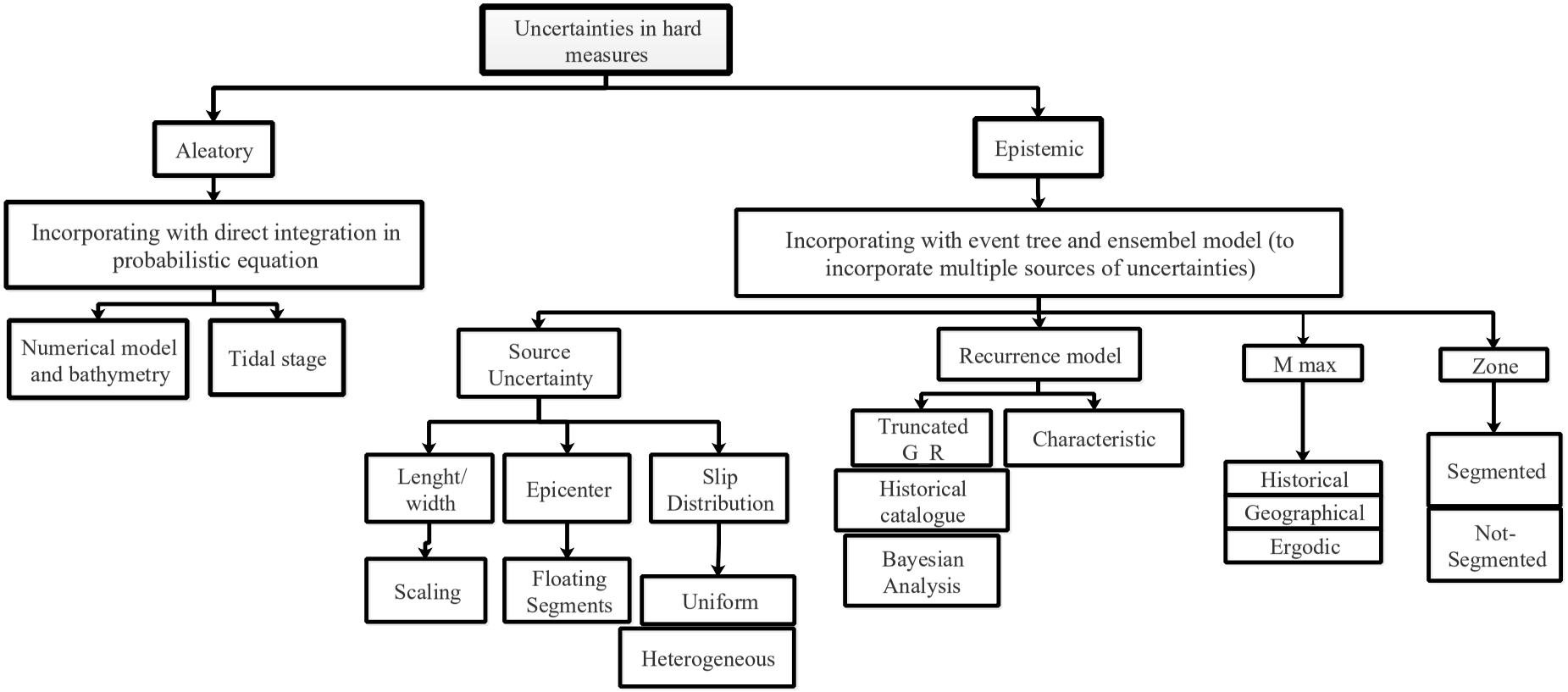

Fig. 8 Methodology used to incorporate uncertainties in tsunami hazard assessments shown in Fig. 4.

Green's function solution to the elastic half space problem. It calculates the displacements at the free surface given rectangular fault geometry, namely fault length (L), fault width (W), depth, dip, and strike, as well as two parameters of dislocation amplitude, rake angle, and slip (see Fig. 9).

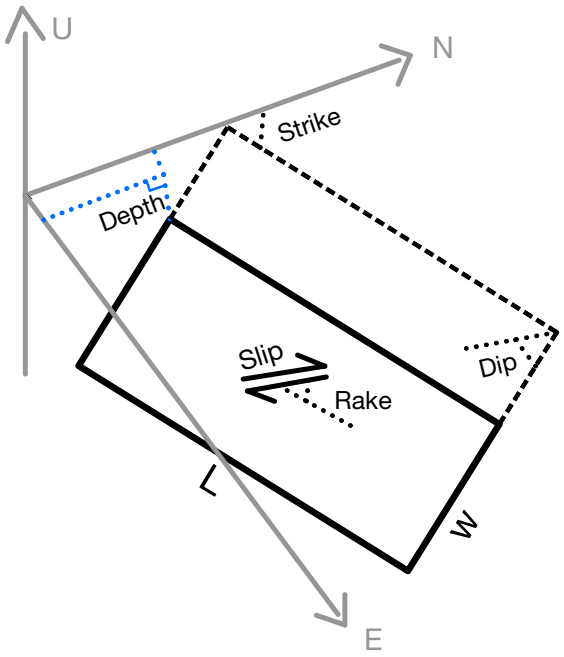

Fig. 9 Seismic parameters of the Okada model (Okada, 1985) to generate the the vertical co-seismic dislocation.

(ii) Then, the Kajiura filter (Kajiura, 1963) was used for the ocean surface deformation of the dislocation to calculate the initial conditions. Kajiura filter represents the three-dimensional non-hydrostatic response of the water column to seafloor uplift, leading to smoothing of the co-seismic dislocation over spatial scales of a the ocean depth.

(iii) Finally, all the active segments were combined linearly considering their associated slips (see Chapter 4, section 4.5.3 for slip calculation approach for each segment). This method is mathematically valid as the Okada model is linear in slip and Kajiura filter is a linear convolution integral (Glimsdal et al., 2013).

Regarding the simulation of tsunami propagation a fully nonlinear and dispersive Boussinesq long wave model, FUNWAVE-TVD (Kirby et al., 1998; Shi et al., 2012), was employed. It features accurate dissipation by considering the breaking wave and bottom friction processes, and has been systematically validated against experimental studies and benchmarks (Tehranirad et al., 2011). The code was parallelized using the message passing interface (MPI). This salable algorithm (using more than 90% of the number of cores in a computer cluster (Shi et al., 2012)) has been paved the way for modeling multitude scenarios.

3.2.3.1 Governing equations

FUNWAVE-TVD, the fully nonlinear Boussinesq equations relying on (Wei et al., 1995), with various parameters is implemented. It considers bottom friction, breaking, and shoreline run-up effects proposed by (Chen et al., 2000; Kennedy et al., 2000) have been applied. The volume conservation and momentum equations are defined as follows,

$$\beta \eta_t + \nabla \cdot \mathbf{M} = 0\,, \tag{3.1}$$

where η_t represents water surface elevation relative to the ocean mean depth h, ∇ is gradient in horizontal coordinates. $\mathbf{M}$ is depth integrated horizontal volume flux given by Eq. (3.2):

$$\mathbf{u}_{\alpha,t} + (\mathbf{u}_\alpha \cdot \nabla)\mathbf{u}_\alpha + g\nabla\eta + \mathbf{V}_1 + \mathbf{V}_2 + \mathbf{R}_f - \mathbf{R}_b = 0\,, \tag{3.2}$$

$\mathbf{V}_1$ and $\mathbf{V}_2$ are terms representing the dispersive Boussinesq terms and are given by (Grilli et al., 2007, Eq.(5) and Eq.(6)).

$$\begin{aligned}
\mathbf{V_1} &= \left\{ \frac{z_\alpha^2}{2}\nabla B + z_\alpha \nabla A \right\}_t - \nabla\left[\frac{\eta^2}{2} B_t + \eta A_t \right], \\
\mathbf{V_2} &= \nabla\left\{ (z_\alpha - \eta)(\mathbf{u}_\alpha \cdot \nabla)A + \frac{1}{2}(z_\alpha^2 - \eta^2)(\mathbf{u}_\alpha \cdot \nabla)B + \frac{1}{2}[A + \eta B]^2 \right\}.
\end{aligned} \tag{3.3}$$

$\mathbf{R}_b$ and $\mathbf{R}_f$ are forces related to the wave breaking and bottom friction, respectively, and $\mathbf{M}$ is the horizontal volume flux:

$$\mathbf{M} = \Lambda \left[\mathbf{u}_\alpha + \left(\frac{z_\alpha^2}{2} - \frac{1}{6}(h^2 - h\eta + \eta^2) \right) \nabla A + \left(z_\alpha + \frac{1}{2}(h-\eta)\nabla B \right) \right], \tag{3.4}$$

Here, $\mathbf{u}_\alpha$ is horizontal velocity at an elevation z_α taken to be $z_\alpha = 0.531h$ following (Wei et al., 1995). A and B are functions of velocity given as follows,

$$A = \nabla \cdot \mathbf{u}_\alpha \,. \tag{3.5}$$

$$B = \nabla \cdot (h\mathbf{u}_\alpha) \,. \tag{3.6}$$

The factors β and Λ were implemented to simulate a porous beach method for calculation of run up on dry shorelines. These factors are shown as follows:

$$\beta = \begin{cases} 1\,, & \eta \geq z^* \\ \delta + (1-\delta)e^{\lambda(\eta - z^*)/h_0}\,, & \eta \leq z^* \end{cases}, \tag{3.7}$$

$$\Lambda = \begin{cases} (\eta - z^*) + \delta(z^* + h_0) + \frac{(1-\delta)h_0}{\lambda}\left(1 - e^{-\lambda(1+z^*/h_0)}\right), & \eta \geq z^* \\ \delta(\eta + h_0) + \frac{(1-\delta)h_0}{\lambda} e^{\lambda(\eta - z^*)/h_0}\left(1 - e^{-\lambda(1+z^*/h_0)}\right), & \eta \leq z^* \end{cases}, \tag{3.8}$$

Here, h_0 is the porous layer depth. It must be deeper than depth of maximum wave rundown during a calculation. The selection of z^* is explained by (Kennedy et al., 2000) . According to the number of tsunami run-up events investigated by (Day et al., 2005; Grilli et al., 2007) $\delta = 0.08$ and $\lambda = 25$ were used.

Boundary condition In this study an absorbing boundary condition introduced by (Larsen and Dancy, 1983) was implemented. In this approach, the variables $\phi(\eta, u, v)$ are directly attenuated at every time step, $\phi = \phi / C_s$. C_s is a damping coefficient defined as:

$$C_s = \alpha_s^{\gamma_x^{i-1}}, \qquad i = 1, 2, \ldots n\,. \tag{3.9}$$

where α_s and γ_s are free parameters and i represents grid numbers. (Chen et al., 1999) suggested $\alpha_s = 2$, $\gamma_s \in [0.88, 0.92]$, and $n \in [50, 100]$. The length of the sponge layer was selected in the process of validating the model (see section 4.6).

3.2.4 Return periods

In PTHA method, the various return periods, ΔT could be used by different purpose and stakeholders. In this study, return periods are set to $\Delta T = \{50, 100, 250, 500, 1000\}$ years; each choice interests different stakeholders and provides information on a specific aspect of the tsunami hazard in the MSZ.

50-year return period hazard curves are shown for understanding threaten of a short term hazard. The failure of coastal defense structures during 2011 Japan tsunami led to a new concepts for tsunami mitigation measures, levels 1 and 2 in Tohoku region. The new generation of coastal embankments have been designed to prevent a tsunami with a return period of up to 100-year (level 1) from over topping, tsunamis that are larger than this (level 2) are expected to cause over topping (Suppasri et al., 2016).

500-year was suggested by UNSIDR (Wright, 2013) for designing airports to provide country wise and global statistics. 1000-year return period hazard curves are shown for understanding threaten of a long term hazard, this can be used by insurance company and designing critical facilities such as nuclear power plant. Moreover, for the facilities located at the coastline such as desalination systems, sea water purifier and etc. Results for different return periods introduced in this section are investigated and provided in hazard curves and probability maps in Chapter 4.

3.3 Incorporating soft uncertainties

There were uncertainties in soft measures of tsunami mitigation measures that had been caused failure in risk managements. The main indicators were discussed and shown in section 2.3. In areas with low tsunami risk probability, mitigation plans are unlikely to resonate with individuals. Evidence and data about local's knowledge, awareness, and attitudes toward tsunamis is a keystone for an optimal risk management and improving the preparedness. In this

chapter, the aforementioned factors in 4 places in the southern part of Iran has been investigated through field survey.

To do so a mixed methodologies approach was used, including distributing the questionnaire and interviewing locals. Moreover, 3 focus group discussions were carried out for further discussion on the findings of the questionnaire survey and interviews.

3.3.1 Samples and analysis

The survey was conducted using different convenience sampling methods at each sites in September of 2018 . Responses were collected at different times of day throughout the week to obtain a better distribution. For Chabahar, questionnaires were administered by two trained enumerators using a random sampling method In Konarak, a GPS random spatial sampling was used to select households in the tsunami prone area. In Tis and Ramin, due to the relatively low level of education, face to face interview was utilised.

3 focus group discussion (3 hours and 45 minutes) were held at 3 fishery ports, namely Beris, Ramin, and Shahid Beheshty with local fishers and beach users. Audio data collected from the focus group discussions were transcribed, and coded analysis to determine the suitability of the study. See Table 1.

Samples were compared with the latest census data (where available) to evaluate their representative. In addition to tabulating the results using descriptive statistics, and ANOVA and chi-squared tests were used to analyze the significance of the relationship between variables using the `scipy.stats` package in `Python`.

3.3.2 Questionnaires

(Plomp, 2013) suggested, typical steps were taken for the creation of the questionnaire, including a systematic literature review shown in Chapter 2 and expert consultation. First, The questions were distributed to 6 Iranian disaster resilience experts. They were selected based on their familiraty about the area, resilience topic, and availability. Their comments were applied to the questionnaire. The approach introduced by Lawshe (Lawshe, 1975) were used to select the number of experts and how to apply their suggestions on the existing questionnaire.

Table 1 Sampling methods and the number of samples.

Area	Chabahar	Konarak	Ramin and Tis	Fisheries
Sampling method	Random sampling in high density area of the city	GPS random sampling	Face-to-face interview	FGD
Type	questionnaire	questionnaire	open ended interview	open ended interview
Number of samples	153	45	24	3

Then, the questionnaire was tested with 10 residents through face to face surveys to detect suitability, comprehensibility, and amount of time required for response.

Finally, the modified questionnaire contained: knowledge, awareness, experience, trust, evacuation behavior, and socio-demographic characteristics (gender, age, education, income, religion).

For FGDs an open ended interview method were selected. The participants were asked about their experience in various natural hazards, their knowledge, awareness about existing mitigation plans in their living area.

3.4 Summary

In this section a general methodology to incorporate the identified uncertainties were discussed. Makran was introduced as an strategic area for the country and its feature makes it potential to absorb population and more development will happen in the next few years. Hence, tsunami hazard assessment were suggested for entire coastline irrespective of population density. A combination of statistical approach, historical assessment, and numerical model was introduced to incorporate both epistemic uncertainty and aleatory variability and assess hazard for entire Makran coast in different return periods. Epistemic uncertainty were incorporated using event trees and ensemble modeling. While aleatory variability were considered directly to probability equations. The selection of return periods were based on various stakeholders' interest and

information on a specific aspect of the tsunami hazard in the MSZ. Results for this part are explained in Chapter 4.

Finally, to cover uncertainties in soft measure and considering heterogeneity in community factors introduced in Chapter 2 were evaluated and empirical data was provided in four places in the MSZ. A mixed methodology, including questionnaire and interviews among residents were used. Results for this part are explained in Chapter 5.

4 PROBABILISTIC TSUNAMI HAZARD ASSESSMENT

In this chapter, tsunami hazard was assessed using the probabilistic approach described in Chapter 3 for the Makran subduction zone (MSZ), considering all identified and aforementioned uncertainties in Fig. 8.

First, the epistemic uncertainties of fault source for the assessment of mean annual rates of earthquakes at different magnitude levels were quantified. Despite the more classical approaches commonly used in literature, the combination of event tree and ensemble modeling was used, which is based on a method initially introduced for PSHA studies (Marzocchi et al., 2015). To develop the original event tree for the area, available seismic, geodetic, and historical catalogue data were utilized to better understand the potential seismogenic zone, maximum magnitude, and recurrence model for the MSZ. Next, rupture complexity, namely, dimensions, slip distribution, and possible earthquake locations, were considered to develop scenarios. Then, a high-resolution tsunami numerical model was used to propagate tsunami waves resulting from these scenarios. Finally, the aleatory variability associated with tidal variations, tsunami numerical and bathymetric models, and scaling relations were considered through statistical methods. These specific intermediate steps were followed to derive the probability of tsunami height occurrence and exceedance for a given exposure time along the Iran and Pakistan coasts.

Fig. 10 demonstrates a summary of the framework. As it is explained in Chapter 3 a combination of statistical, historical, and numerical model assessment was used to cover all the uncertainties. The development of method and its results are provided in this chapter.

Results are presented for different return periods for insurance activity, land use and city planning, critical facility design, mitigation measure design and implementation. Moreover, some sensitivity analysis were made, for example the results obtained in the presence and absence of the aleatory variability were compared (see section 4.8.3). Also, slip distribution in its uniform form and heterogeneous were demonstrated (see section 4.5.3).

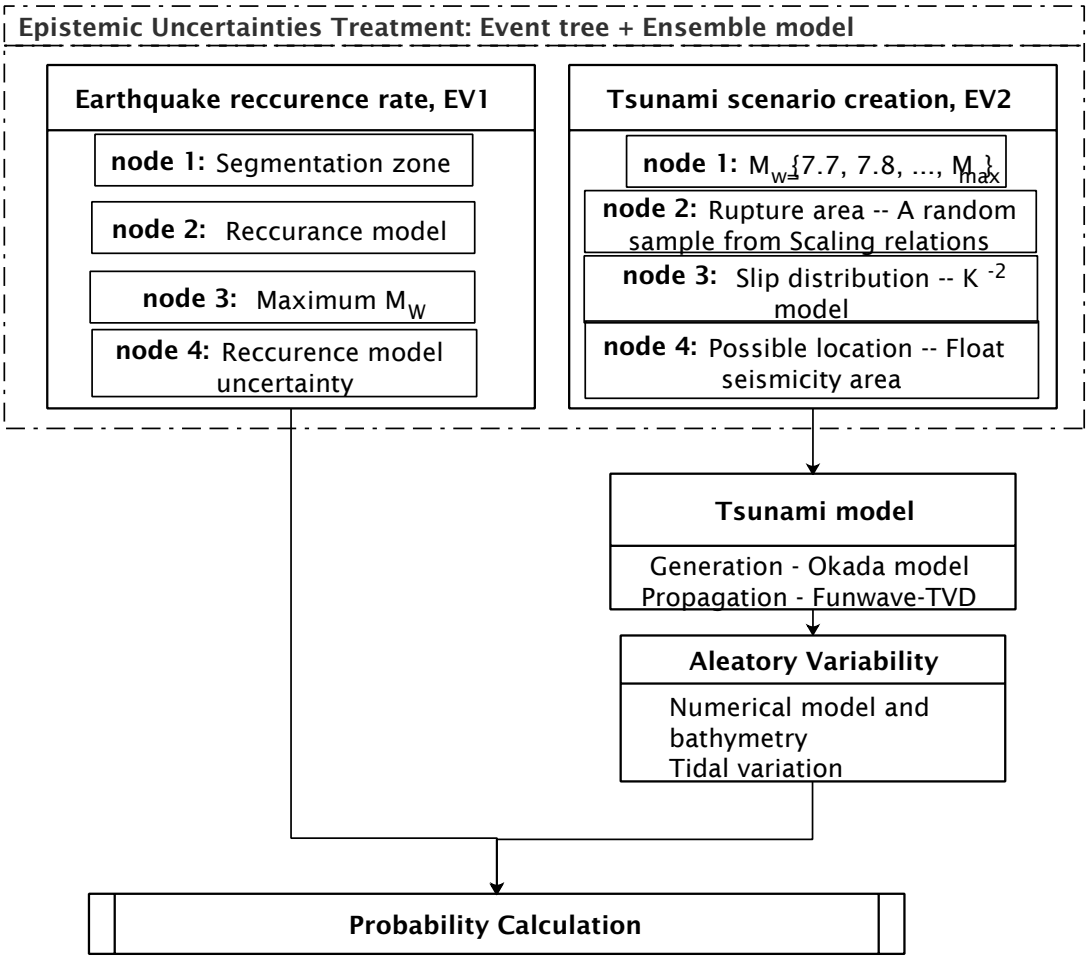

Fig. 10 Methodology framework. First, the fault geometry was defined using SLAB 2.0, and the source was discretized into smaller segments. Next, two event trees were developed to define the earthquake recurrence rate and create tsunami scenarios; then, the Okada model and `Funwave-TVD` were used to calculate tsunami heights for the scenarios. Finally, considering the aleatory variability, the probability of exceedance was derived.

4.1 Treatment of uncertainties

Both aleatory and epistemic uncertainties had been taken into consideration. for the latter, two event trees were developed based on determination of information contents, through statistical, historical and geometry facts. the former one had been directly affected probability calculation. The detail of developed methodology and results are described in due courses.

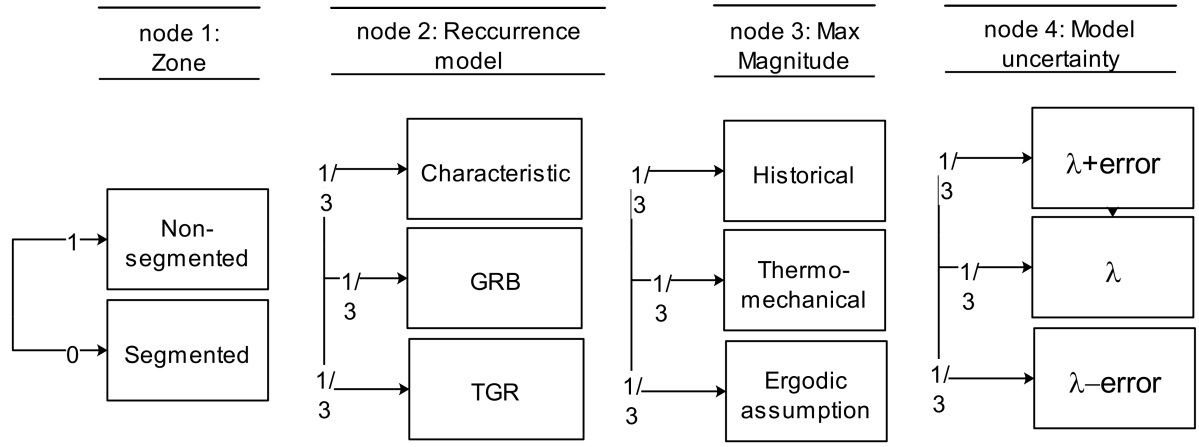

(a)

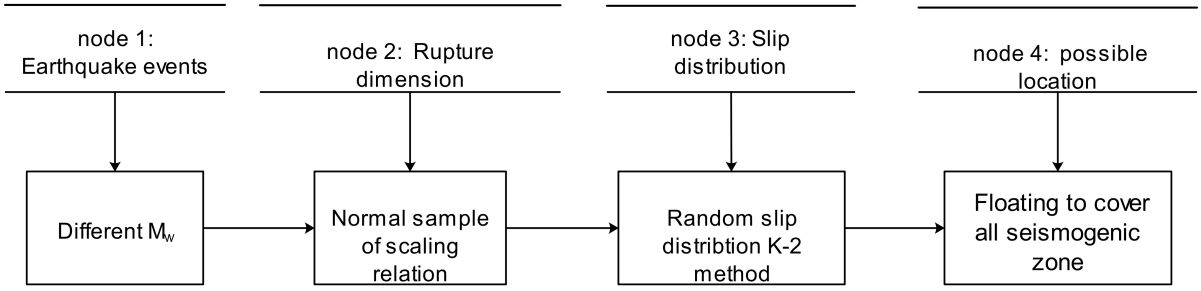

(b)

Fig. 11 Developed event trees for (a) source recurrence model; (b) rupture complexity and tsunami scenario creation.

4.1.1 Epistemic

Two event trees based on scientific facts in MSZ were developed as bellow: (See Fig. 11)

(i) Focusing on the fault source recurrence model for the assessment of mean annual rates of earthquakes at different magnitude levels with 36 branches. It consists of two zonations [segmented and none, section 4.4.1]; three approaches for the seismicity model [Gutenberg–Richter–Bayes (GRB) (Kijko et al., 2016), truncated Gutenberg–Richter, and characteristic (Kagan, 2002), section 4.4.2]; three maximum magnitudes (M_{max}) [based on the Kijko–Sellevoll–Bayes method (Kijko, 2004), thermomechanical modeling (Smith et al., 2013) and ergodic assumption (Bird and Kagan, 2004), section 4.4.3]; and three for incorporating the uncertainty of the earthquake occurrence model.

(ii) Focusing on the bulk rupture parameters and rupture complexity. It consists of rupture length and width (see section 4.5.2), slip distribution (see section 4.5.3), and earthquake source location within the fault (see section 4.5.4).

4.1.2 Aleatory

The proper treatment of aleatory variability in tsunami wave heights is a prominent subject, and ignoring this typically leads to significant hazard underestimation (Bommer and Abrahamson, 2006). In the analysis, three main contributions, i.e., $\{\sigma_m, \sigma_s, \sigma_t\}$, to the aleatory variability have been identified:

1. The mismatch between tsunami height model and observed caused by the numerical and bathymetric model error (σ_m, see section 4.2)

2. The stochasticity in the earthquake dimensions imposed by the scaling relations (σ_s, see section 4.5.2.1),

3. The tide variation at tsunami arrival time (σ_t, see section 4.3)

4.2 Numerical model and bathymetry mismatch (σ_m)

Due to the lack of field data and background information on the MSZ, the 2011 Tohoku earthquake of Japan was modeled, and the results were compared with the available measured data to quantify the mismatch between the observed and computed tsunami heights. This uncertainty is described as the standard deviation of a log-normal distribution with a zero mean (Aida, 1978; Thio et al., 2007):

$$\begin{aligned} \sigma_m = \log \kappa &= \sqrt{\frac{1}{n}\sum_{i=1}^{n}(\log K_i)^2 - (\log K)^2}, \\ \log K &= \frac{1}{n}\sum_{i=1}^{n}\log\left(\frac{H_{obs}}{H_{model}}\right). \end{aligned} \tag{4.1}$$

Here, $K_i = H_{obs}/H_{model}$ with H_{obs} and H_{model} are the measured and simulated tsunami heights, respectively.

4.2.1 The 2011 Japan tsunami modeling

The 2011 Tohoku tsunami was simulated using the same bathymetry and numerical model as the ones used for the MSZ to obtain H_{model} . Moreover, in order to only consider the mismatch between modeled and observed tsunami height resulted because of numerical model and bathymetry a very precise initial condition needed to be used. Accordingly, to get better accuracy an inverted source that had goodness of fit was used from (Fujii et al., 2011b; Hossen et al., 2015). Fig. 12 shows initial condition used for the 2011 tsunami Japan.

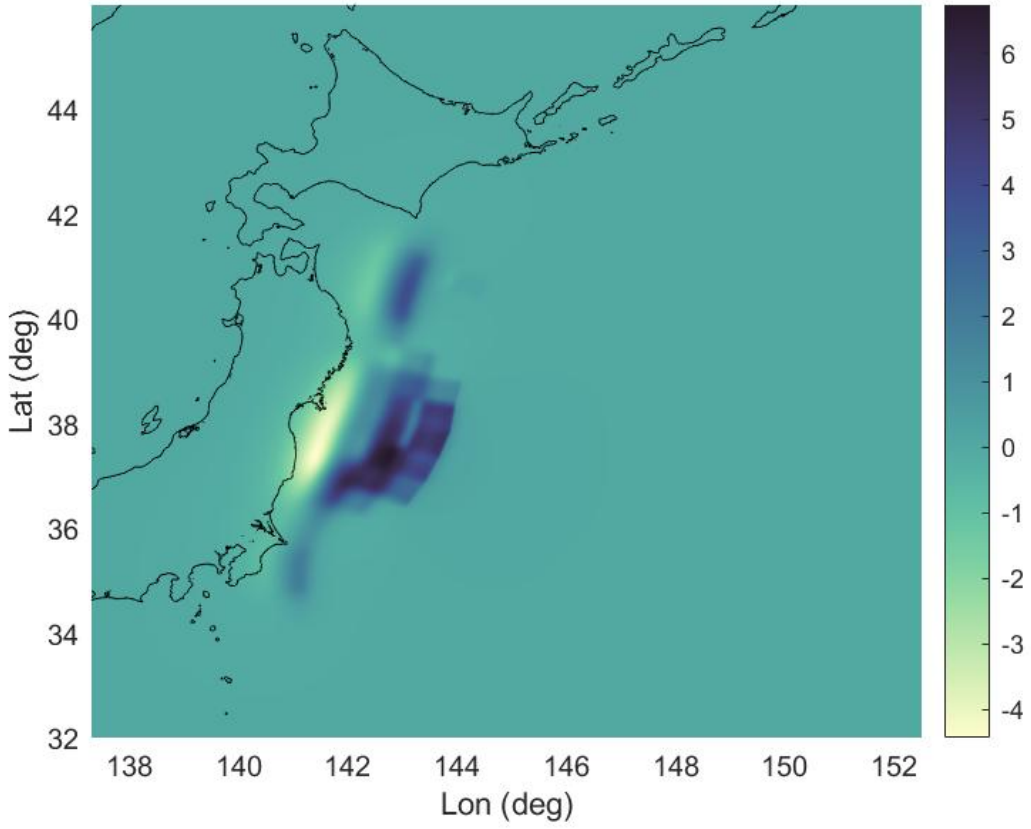

Fig. 12 Inverted initial condition of the 2011 Japan tsunami the maximum 8.7 and minimum −5.

4.2.1.1 Field data – H_{obs}

Many field measurements were made during and after the tsunami. The methods of measurements have their own uncertainties caused by survey measuring tools. Hence, to avoid them,

for H_{obs}, only the measured tsunami height at GPS (Yamazaki et al., 2011), DART buoys (Lay et al., 2011), and tide and wave gauges (Kawai et al., 2013) were used.

4.2.1.2 Propagation model inputs

`FUNWAVE-TVD` was used in its Cartesian implementation to simulate the tsunami propagation from the source to the Japan coast. GEBCO 2020 (global bathymetric model based on ship-track data) with 15 arcsec resolution was used. The computation domain and bathymetry data are showed in Fig. 13. A 600 m resolution was used for the computational domain, which is a trade-off between precision and practical feasibility. To prevent non-physical reflection from the boundaries, sponge layers were specified with 50 km thickness within the computational domain along the north, east and south boundaries. Also, to avoid the triggering of instabilities because of sharply varying bathymetry during wetting-drying, the critical depth for wetting-drying was set to 1 cm, and the bottom drag coefficient to 0.01. All the inputs were validated by comparison between differences between modeled height and field observation and computation time. The final inputs parallels with those suggested by (Bakhsh, 2014). A summary of the inputs are shown in Table 2.

Table 2 A summary of input variables for the 2011 tsunami Japan propagation model.

Variables	Inputs
Computational domain	137 - 152.5 ° E , 32 - 46 ° N
Bathymetry data	GEBCO 15 arcsec – 2020
Resolution	600 m
Sponge layers thickness	50 km in all directions
Drag coefficient	0.01
Wetting-drying (the critical depth)	1 cm

4.2.1.3 Results

Fig. 14 shows the comparison between the modeled and measured tsunami heights (top), Eq. (4.1) were then used to calculate the standard deviation of a log normal distribution showing

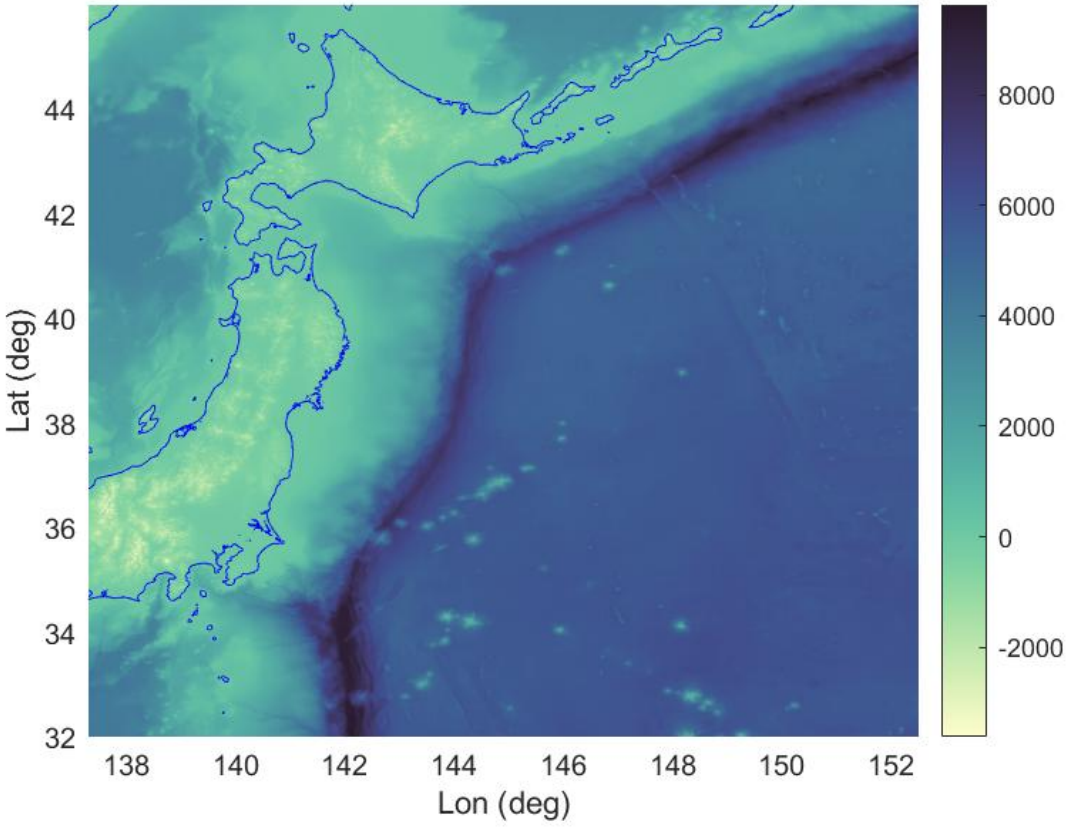

Fig. 13 Bathymetry and computational domain of the 2011 Tohoku tsunami.

the mismatch of modeled and measured tsunami height. It resulted $\sigma_m = 0.376$. The value derived here is somewhat smaller than the one previously reported by (Thio, 2010) (i.e. 0.595). The difference is due to the simplified uniform-slip representation of the tsunami source and Green's approach that were used in the latter reference.

4.3 Tidal variation (σ_t)

Because the tide level at tsunami arrival time is unknown, tidal variation variability must be included in the PTHA. In the Makran region, the tidal variation is notable, and the peak to peak tidal amplitude is as high as 2-3 m. For this task, the probability of exceedance of mean sea level (MSL) from the tidal record at each point of interest (PoI) was calculated.

To calculate tidal record probability, a relatively long time-series of record measured by tidal gauges for each PoI was used. For PoIs in which a tidal record is not available, a linear interpolation of the closest tidal gauges was used. This choice seems reasonable because the

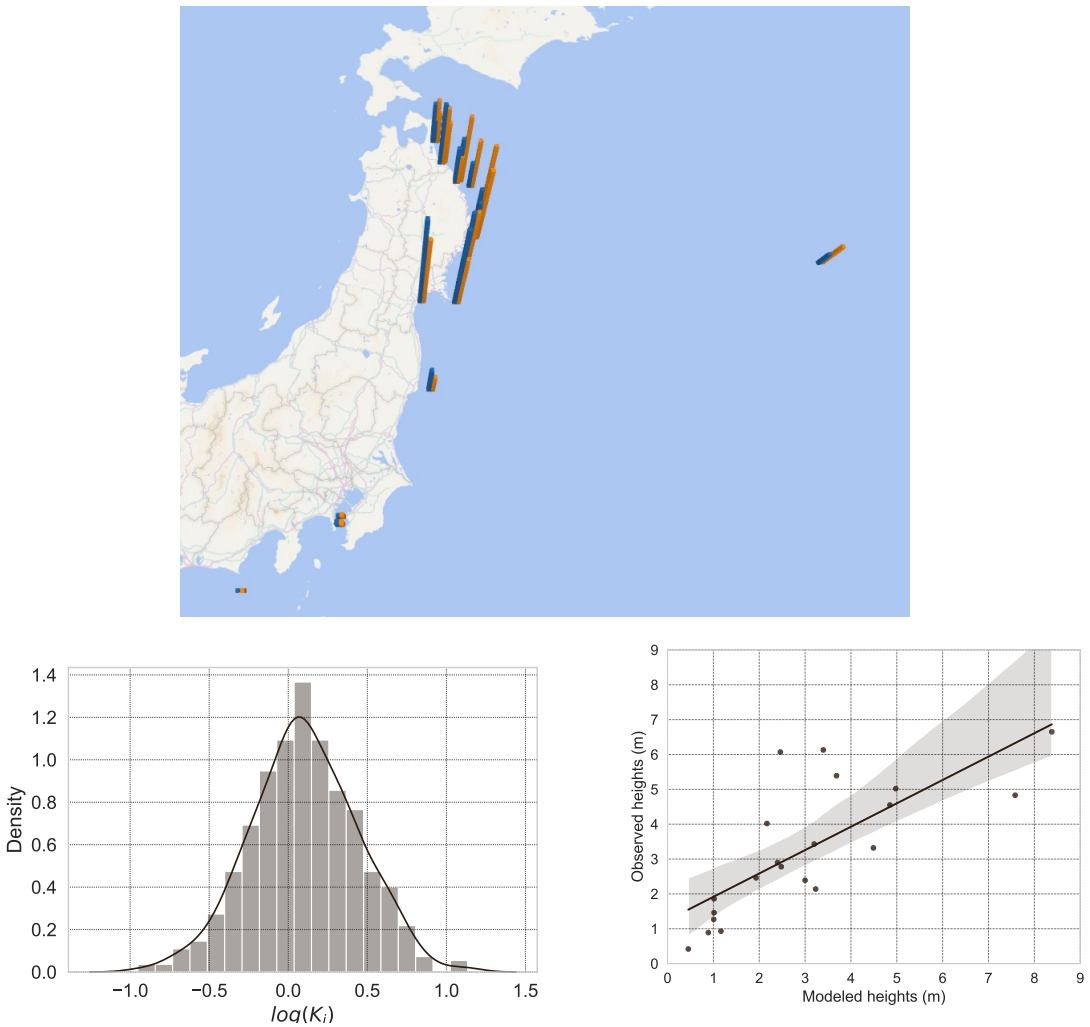

Fig. 14 Comparison between modeled and measured tsunami height for the 2011 Japan tsunami at 15 stations recorded by GPS, DART buoys, tide and wave gauges; regression line for modeled versus measured height (bottom right); histogram of errors in log tsunami height and corresponding normal distribution (bottom left).

differences in tidal levels along the Makran coast are not significant (Akbari et al., 2017). Mean is equal to MSL which had been used in tsunami propagation modeling and standard deviation is calculated for each PoIs. Fig. 14 illustrates some example of the methodology for some of the PoIs, namely Beris, Jask, Chabahar, and Konarak. The dynamic interaction between tides and tsunami waves was disregarded.

4.4 Source

For any earthquake induced tsunamis the probability of earthquake for different magnitudes is needed to be considered. The mean annual rates (ν_j) of earthquakes at different magnitudes

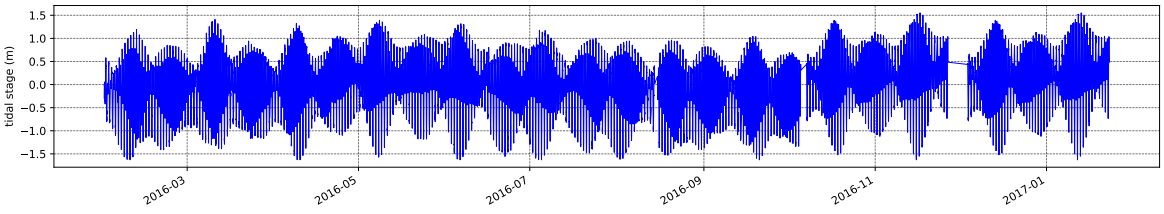

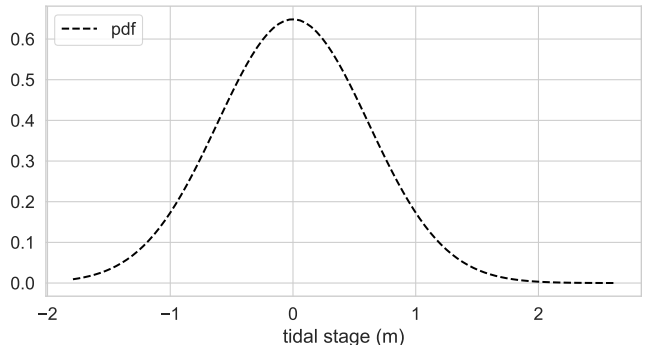

(Beris, for this PoI, $\sigma_t = 0.612$.)

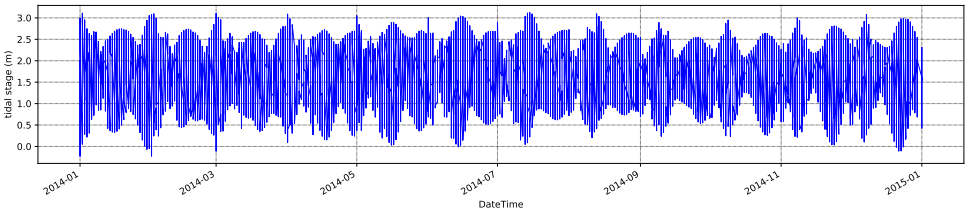

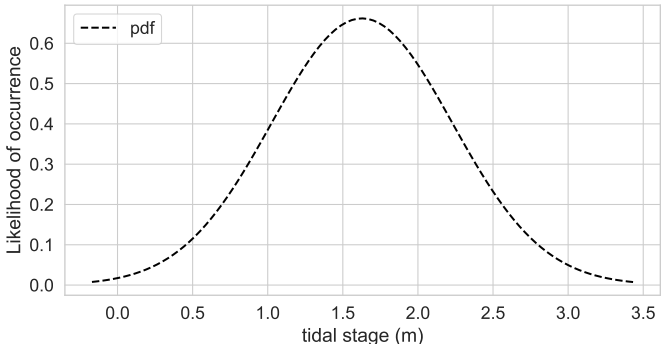

(Jask, for this PoI, $\sigma_t = 0.602$.)

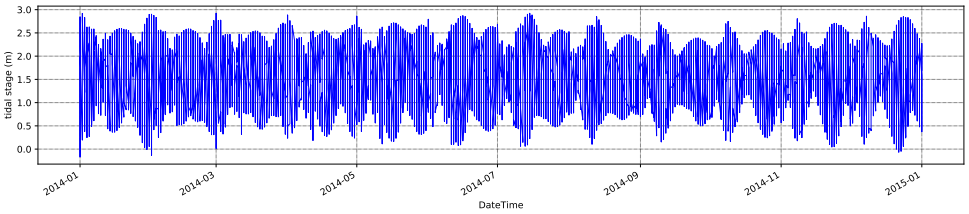

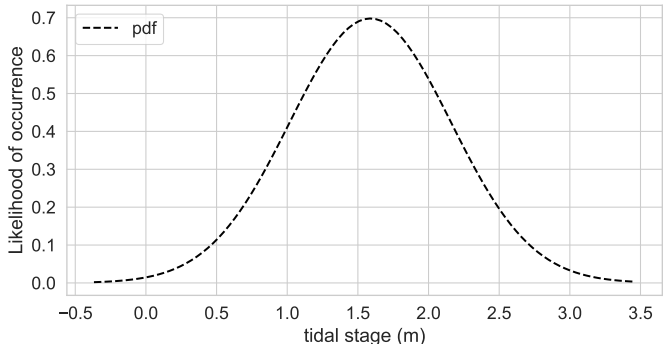

(Chabahar, for this PoI, $\sigma_t = 0.571$.)

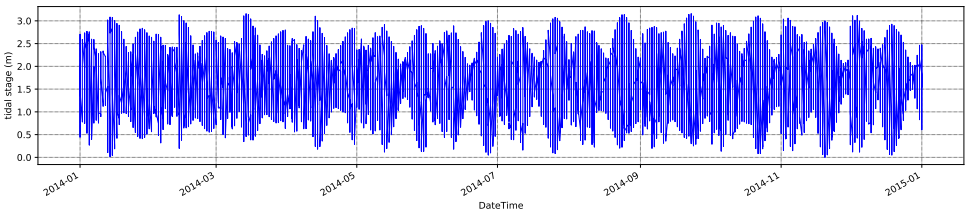

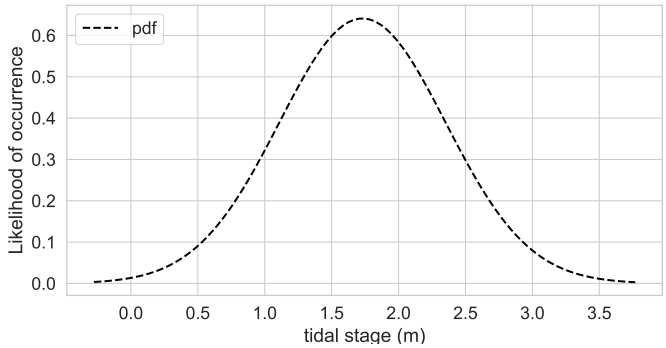

(Konarak, for this PoI, $\sigma_t = 0.622$.)

Fig. 14 Tidal time series record of one year for Beris, Jask, Chabahar, and Konarak; and their corresponding normal distributions.

can be assessed as

$$\nu_j = \lambda_{\min}(1 - F_M(M|M_{\min}, M_{\max})) \,. \tag{4.2}$$

$M_{\min}$ is minimum magnitude of interest (7.7), $M_{\max}$ is maximum magnitude (see section 4.4.3 and $\lambda_{\min}$ refers to the parameter of the Poisson distribution and describes activity rate of earthquake occurrence. $F_M(M|M_{\min}, M_{\max})$ is provided by different methods in section 4.4.1.

Uncertainties are highly depend on the underlying assumptions of earthquake physics. To do so the mean annual rates (ν_j) of earthquakes at different magnitudes was calculated considering all the associated uncertainties. As it is mentioned in Chapter 3 the MSZ is located on the south-eastern coasts of Iran and southern coasts of Pakistan. This zone extends east from the Strait of Hormoz to the Ornch–Nal Fault in Pakistan. It experienced the deadliest tsunami that has occurred in the Indian Ocean prior to 2004, and recent smaller earthquakes suggest seismicity on the megathrust. However, poor historical records have led to significant uncertainty and complicated hazard potential estimation. Therefore, to incorporate the uncertainties associated with the fault source, an event tree (EV1) to assess the mean annual rates (ν_j) of earthquakes at different magnitude levels was developed, as described below.

4.4.1 Zone: node 1 in EV1

The eastern and western parts of the MSZ exhibit extremely different seismicity patterns (Aldama-Bustos et al., 2009). This, along with its unrecognized bathymetric trench, makes the MSZ a unique subject of analysis. (Al-Lazki et al., 2014) argued that the eastern MSZ is underlain by an oceanic lithosphere, while the western part is possibly underlain by a continental or very low velocity oceanic lithosphere. This, along with the more historical seismicity activity at the eastern part, form the hypothesis of east-west segmentation of the MSZ. However, it remains a controversial issue whether the MSZ should be considered segmented in hazard studies because the existence of late Holocene marine terraces along the eastern and western halves suggests that both can generate megathrust earthquakes (Normand et al., 2019).

Both the segmented and non-segmented zone in node 1 of EV1 are presented. However, owing to the above mentioned related controversy, the hypothesis of the segmented the MSZ was neglected as it leads to a strong hazard underestimation. Note that treating Tohoku as a

segmented zone led to strong underestimation of the devastating 2011 tsunami (Kagan and Jackson, 2013). Accordingly, the segmented and non-segmented zones were weighted as 0 and 1, respectively. However, in this methodology framework one can change it as their interests.

4.4.2 Recurrence rate model: node 2 in EV1

The severity of a large earthquake is determined by the tail of a frequency distribution. Earthquake catalogues are limited at large magnitudes for a particular fault zone. This makes the accurate estimation of the PTHA through the recurrence interval of seismic history impossible and inaccurate. In particular, for the MSZ with poor and incomplete catalogues, a simple linear regression of the historical cumulative distribution is known to be biased (Power et al., 2012). Accordingly, several models exist that can be used to define the distribution of earthquake magnitudes for incomplete catalogues. In this study, three seismicity models were used to define the behavior of the MSZ using its earthquake catalogues (see section 4.4.4):

(i) Gutenberg–Richter–Bayes(GRB) (Kijko et al., 2016). Seismicity was determined using the `HA3` application built in `MATLAB`. The applied procedure of the seismic hazard considers the incompleteness of the seismic catalogues, uncertainty in magnitude estimation, and variation in seismicity. The code accepts mixed data catalogues, namely, paleo, historical, and instrumental with different completeness magnitudes, magnitude uncertainties, and time periods. This method employs a mixed (Bayesian) Poisson-gamma distribution as a model of earthquake occurrence over time.

$$\Phi_M = 1 - F_M = \begin{cases} 1 - C_\beta \left[1 - \left(\frac{p}{p + M - M_{\min}} \right)^q \right], & M_{\min} \leq M \leq M_{\max} \\ 0, & M > M_{\max} \end{cases}, \tag{4.3}$$

where p and q are gamma function parameters and C_β being the normalization coefficient.

(ii) Characteristic (Kagan, 2002). [1] The characteristic distribution has the cumulative complementary function (Φ_M) truncated on both ends and is characterized by the following

[1] Caution: there is another "Characteristic" Gutenberg-Richter model (Youngs and Coppersmith, 1985) which is conceptually similar to the Kagan, but it spreads the rate of the highest magnitude event over a small interval

equation

$$\Phi_M = 1 - F_M = \begin{cases} e^{-\beta(M-M_{\min})}, & M_{\min} \leq M \leq M_{\max} \\ 0, & M > M_{\max} \end{cases}, \tag{4.4}$$

(iii) Truncated Gutenberg-Richter (TGR). The cumulative complementary function (Φ_M), which is truncated at both ends, is expressed as

$$\Phi_M = 1 - F_M = \begin{cases} \frac{e^{-\beta(M-M_{\min})} - e^{-\beta(M_{\max}-M_{\min})}}{1-e^{-\beta(M_{\max}-M_{\min})}}, & M_{\min} \leq M \leq M_{\max} \\ 0, & M > M_{\max} \end{cases}, \tag{4.5}$$

where $M_{\min}$ is the level of magnitude completeness, $M_{\max}$ is the maximum possible earthquake magnitude and $\beta = b \log 10$, and b is the parameter of the Gutenberg-Richter relation.

The simplest method to obtain parameters for power law, i.e., β and $\lambda_{\min}$ is the least square method (LS) of historical catalogues. The disadvantages of this method is that it usually overestimates β that causes the rates of large earthquake to be underestimated. Moreover, due to the lack of historical and modern tools in the MSZ, incompleteness and uncertainty in data need to be considered. Hence, in this study β and $\lambda_{\min}$ were calculated using earthquake catalogues and `HA3` application to cover both incompleteness and uncertainties in catalogues. (see section 4.4.4).

Fig. 15 shows an example of the earthquake curves generated by the aforementioned recurrence models with one specific $M_{\max} = 8.1$. All of these models are modifications of the "pur" Gutenberg-Richter. The original formulation is for any events with magnitude more than zero, while the modified distributions are used in truncated form – because earthquakes like most other natural hazards are size limited. Because an upper magnitude bound for any finite source is presumably an associated maximum magnitude. As it can be seen in Fig. 15, in case of characteristic model the limit at the tail of the distribution is "hard", while the other two distributions, i.e., GRB and TGR apply a "soft" exponential taper to the distribution tail.

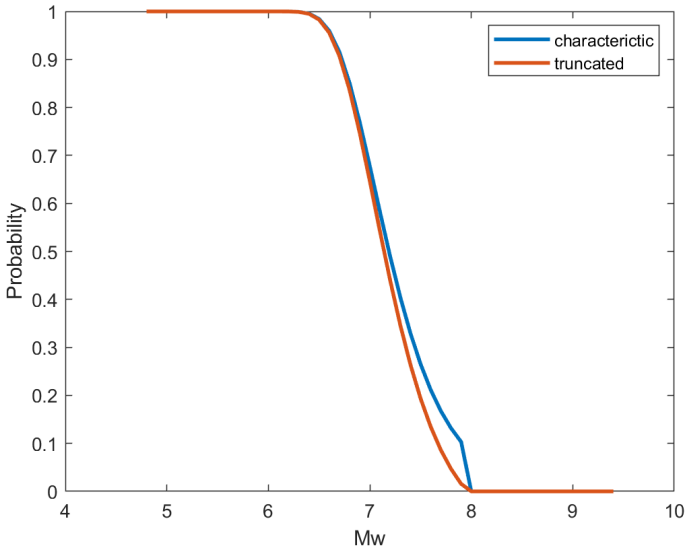

Fig. 15 An example of the earthquake curves (the probability of earthquake at different magnitude level) generated by the different recurrence models with one specific $M_{\max} = 8.1$.

4.4.3 M_{max}: node 3 in EV1

PTHAs are more sensitive to $M_{\max}$ than PSHAs because with increasing magnitude, tsunami heights do not saturate but seismic ground motion does (Thio et al., 2007). $M_{\max}$ based on instrumental catalogues may underestimate the maximum magnitude event due to their short records. Here, to include this uncertainty, three maximum magnitude ($M_{\max}$) methods were used based on three different methodology:

$M_{\max}$ = 8.2: Kijko-Sellevoll-Bayes method (Kijko, 2004): the maximum magnitude was calculated base on earthquake catalogues in section 4.4.4 and using the `HA3` application. Their code calculates maximum magnitude via an iterative solution of a Bayesian estimator with the equation:

$$M_{\max} = M_{\max}^{\text{obs}} + \frac{\delta^{\frac{1}{q}+2} e^{\frac{n \cdot r^q}{1-r^q}}}{\beta} \left[\Gamma\left(-\frac{1}{q}, \delta \cdot r^q\right) - \Gamma\left(-\frac{1}{q}, \delta\right) \right], \tag{4.6}$$

where $\Gamma(\cdot,\cdot)$ denotes the incomplete Gamma function, p and q are gamma function parameters, and

$$r = \frac{p}{p + M_{\max} - M_{\min}}, \qquad \delta = nC_\beta, \tag{4.7}$$

with $C_\beta = 1/(1-r^q)$ being the normalization coefficient. The worse case scenario recorded in earthquake catalogue in the MSZ was $M_{\max}^{\text{obs}} = 8.1$ and using above equations $M_{\max} = 8.2$ was obtained.

$M_{\max}$ = 9.22: Thermomechanical model: (Smith et al., 2013) using a 2 - D thermal model of the subduction zone showed that high sediment thickness leads to high temperature in boundaries making the megathrust potentially seismogenic to a shallow depth and shallow dip leads to high seismogenic zone area. For the full length of subduction zone they observed a potential of $M_{\max} = 9.22$.

$M_{\max}$ = 9.58: Ergodic theory says:

$$\lim_{T\to\infty} \frac{1}{2T} \int_{-T}^{T} x(t)dt = \lim_{N\to\infty} \frac{1}{N} \sum_{k=1}^{N} x_k(t_0)\,, \tag{4.8}$$

the time of process x at a particular geographic point is equal to the average at a particular rim (t_0) over an ensemble of points (x_k) (Anosov, 2001). Using the concept of this theory, it can be assumed that by compiling all subduction zones data in world for a century, enough information may be available to extract average seismicity properties in local zones with a confidence that is small enough to cover uncertainties. (Bird and Kagan, 2004) suggested $M_{\max} = 9.58$ for subductions based on their statistical analysis for a number of faults worldwide in a century.This value also meets the MSZ seismicity area limit.

4.4.4 Earthquake catalogues

Earthquake data employed in this study were derived from various sources:

(i) International Seismological Centre (ISC),

(ii) Incorporated Research Institutions for Seismology (IRIS),

(iii) The United States Geological Survey Online bulletin (USGS), which includes information from the National Ocean and Atmospheric Administration (NOAA) and Preliminary

Determination of Epicentres (PDE) provided by the National Earthquake Information Center (NEIC),

(iv) Iranian Seismological Center (IRSC),

(v) Global Historical Earthquake Archive (GEM).

Extra efforts have been made to extract more data from the literature regarding earthquakes with magnitudes beyond 6.5. This includes information from the Pakistan Meteorological Department (PMD) (Department], 2007) and (Ambraseys and Melville, 1982).

4.4.4.1 Pre-processing catalogues

The ZMAP7 analysis tool (Reyes and Wiemer, 2019) was used for the pre-processing data from different catalogues mentioned in section 4.4.4. First, the catalogues were compiled for a region that lies in the plate interface, excluding nonsubduction seismicity (see Fig. 22). The catalogues cover the period from 825 BCE to mid-2020 CE. Table 3 shows different catalogues periods along with the sources for historical records.

Table 3 The time period of different catalogues and the sources for historical records

Catalogue name	The time period
ISC	1907/07/04 — 2016/10/31
IRIS	2013/03/03 — 2020/04/26
USGS	1909/10/20 — 2020/04/26
IRSC	1902/07/09 — 2000/12/26
Historical records from: GEM, PMD, IRSC, (Murty and Rafiq, 1991), (Pararas-Carayannis, 2006), (Dominey-Howes et al., 2007), (Ambraseys and Melville, 1982), (Quittmeyer and Jacob, 1979)	825 BCE — 1899 CE

These catalogues are different in terms of magnitude scale. When available, the moment magnitude, M_w, was used; otherwise, the published magnitudes, e.g., teleseismic magnitudes (M_s, m_b) and modified Mercalli intensity (MMI) were converted to M_w. Table 4 shows comparison of MMI scale and M_w (Allen et al., 2012). For other teleseismic magnitudes the empirical

laws proposed by (Lolli et al., 2014) were used as below:

$$M_w = \begin{cases} \exp(2.133 + 0.063M_s) - 6.205, & M_s \leq 5.5 \\ \exp(-0.109 + 0.229M_s) + 2.586, & M_s > 5.5 \end{cases}, \tag{4.9}$$

$$M_w = \exp(0.741 + 0.210m_b) - 0.758\,. \tag{4.10}$$

Table 4 The degrees of the MMI scale compare to magnitude M_w

Magnitude	modified Mercalli intensity (mmi)
1 – 3	I
3 – 3.9	II – III
4 – 4.9	IV – V
5 – 5.9	VI – VII
6 – 6.9	VII – VIII
7 and higher	IX or higher

Then, following the assumption that seismicity obeys a Poisson process, it is necessary to decluster the catalogues by removing all dependent events, namely, precursors and aftershocks. Hence, the cluster approach proposed by Reasenberg (Reasenberg, 1985) was employed to eliminate dependent shocks. Then, duplicate events from different catalogues were removed. Subsequently, the plot of the cumulative number of events allowed to split the working catalogues into prehistorical, historical, and three sub-instrumental categories (i.e., sub1, sub2, and sub3). Each has a different magnitude of completeness (M_c) and magnitude uncertainty. Fig. 16 shows 3 sub-instrumental categories events. It can be seen the differences in event number thus magnitude of completeness (M_c) of each.

4.4.4.2 Statistical analysis of compiled catalogue

Fig. 17 shows all three instrumental sub-catalogues together and divided limited to the subduction area and the number of events in each. The number of recorded earthquake events had been

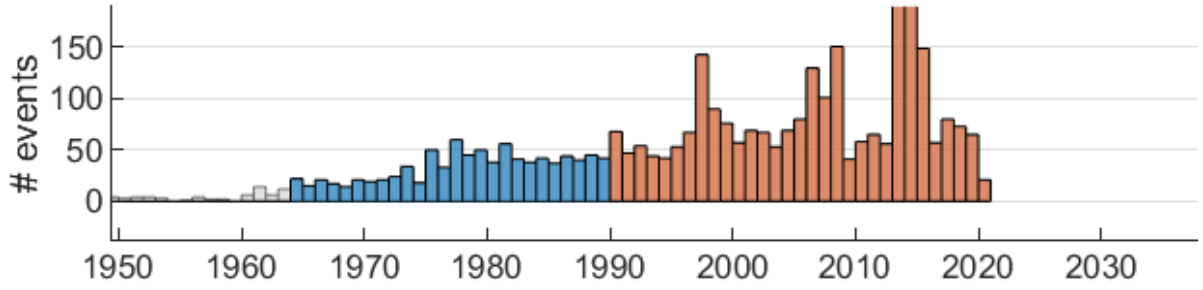

Fig. 16 The number of event for three different 3 sub-instrumental categories through years. White: sub1, blue: sub2, and red: sub3.

increasing over years. Another interesting analysis is longitude histogram to more understand the activity of east and west part of the MSZ. Fig. 18 (a) shows the number of events along the subduction trench with 0.5 km interval. The number of event at the west part is more than other parts, while the center shows historically less active than other parts. Of course, the magnitude intensity needs to be taken into consideration in order to have a reasonable judgment about activity rate, however, limited earthquake catalogues makes it nor possible neither precise. This is why along with the other aforementioned reasons in section 4.4.1 both east and west part of the MSZ weighted equal in this study. Fig. 18 (b) shows histogram of number of event with the magnitude sizes in the compiles catalogue. It is trivial that the number of events increases in the middle of the interval between the completeness and maximum magnitude.

Finally, to calculate a `prior` value for b for the recurrence Bayesian model for each catalogue an analysis of b_value from events had been done using The `ZMAP7` analysis tool.

4.4.4.3 Results of statistical analysis

In this section the results of two previous subsections are provided. Table 5 shows extracted values for magnitude of completeness (M_c), error, and b-value from `zmap` for different working catalogues. Moreover, the time period for each time catalogue is provided. Because seismic network capabilities have improved year by year, the completeness magnitude of data and error values decrease as the observation period becomes more recent. These values had been used in the recurrence models introduced in section 4.4.2.

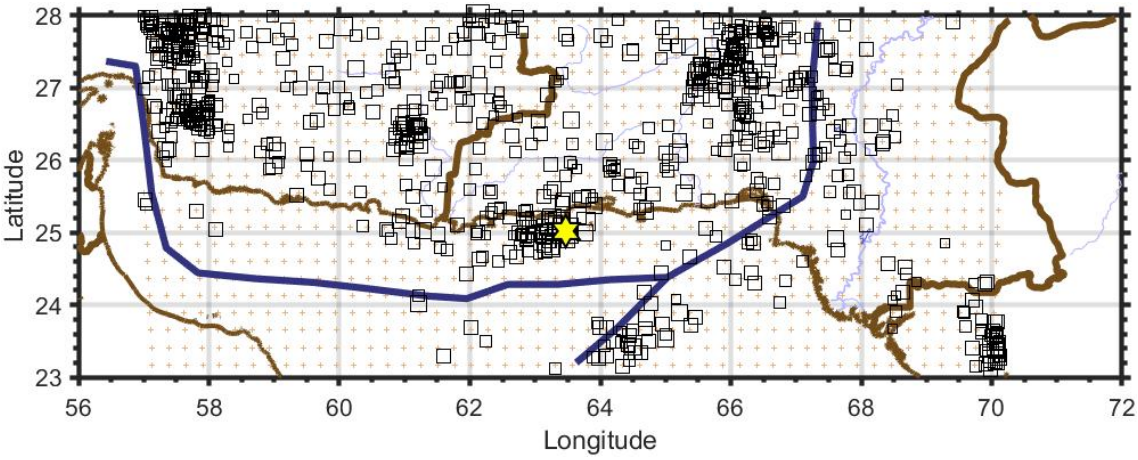

(a) all the sub catalogues

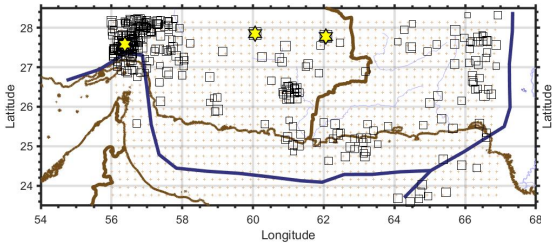

(b) sub-catalogue 2

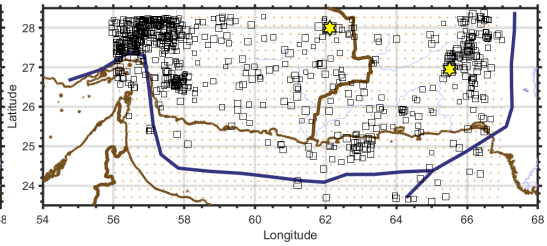

(c) sub-catalogue 3

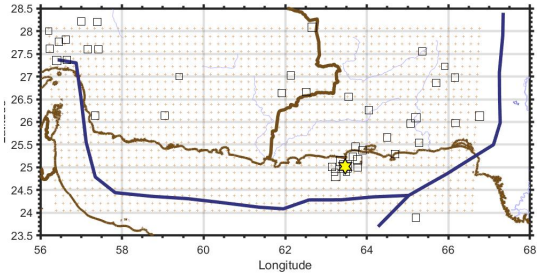

(d) sub-catalogue 1

Fig. 17 Earthquake events catalogue map

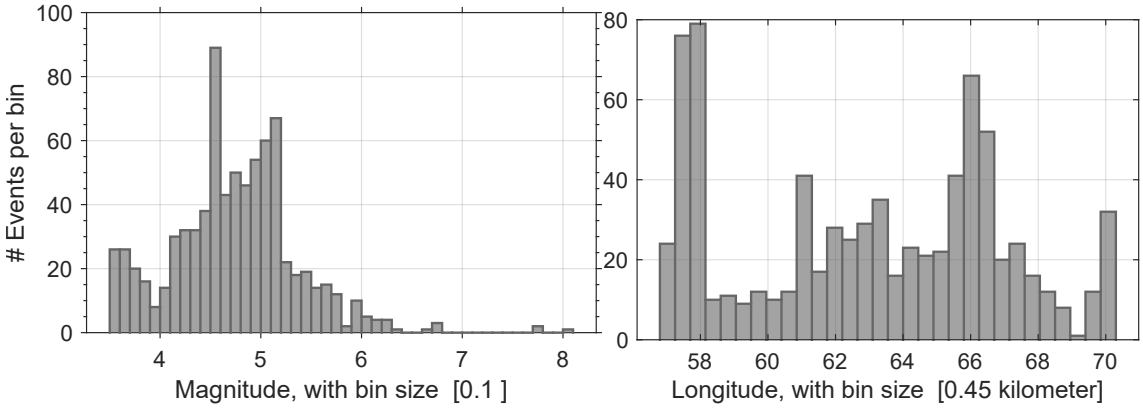

(a) Magnitude histogram

(b) Longitude histogram

Fig. 18 The number of earthquake events in different: (a) magnitude and (b) longitude

Table 5 Extracted values for magnitude of completeness (M_c), error, and b-value from `zmap` for different working catalogues.

	prehistorical	historical	sub-catalogue 1	sub-catalogue 2	sub-catalogue 3
period	326 BC – 1020 AD	1480 – 1899	1900 – 1963	1964 – 1989	1990 – 2020
M_c	—	5.5	5.7	4.8	4.8
error value	0.6	0.5	0.45	0.35	0.25
prior b-value	0.91 ± 0.04				

4.5 Tsunami scenarios

To create possible tsunami scenarios and incorporate rupture and location uncertainties, event tree 2 (EV2) was developed (see Fig. 11). The branches of EV2 are introduced in section 4.1.1; here, a more detail description are provided:

4.5.1 Source discretization

The subduction zone geometry represent a keystone in determining the spatial extent and the size of subduction zone earthquakes. In this study, similar to (Davies and Griffin, 2019), fault geometry was defined using a three-dimensional source zone fault-plane, SLAB 2.0 – a comprehensive subduction zone geometry model (Hayes et al., 2018). Fig. 19 shows dip, rake, strike, and depth of the MSZ calculated for the first time for the MSZ using a three-dimensional geometry.

The MSZ has an extremely shallow subduction angle (dip) and thick sediment pile (≈ 7 km) that leads to a wide potential seismogenic zone (Smith et al., 2013). Following the suggestion of (Berryman et al., 2015) and (Safari et al., 2017), the seismogenic zone was constrained from 0 km (i.e., trench) to 38 km depth as a preferred down-dip limit. This assumption leads to define a seismogenic zone for the MSZ as shown in Fig. 22.

Then, to obtain a better representative of the MSZ fault geometry, the seismogenic zone was discretized into 50×50 km^2 segments. A 20×8 unit source was created. The area of segments

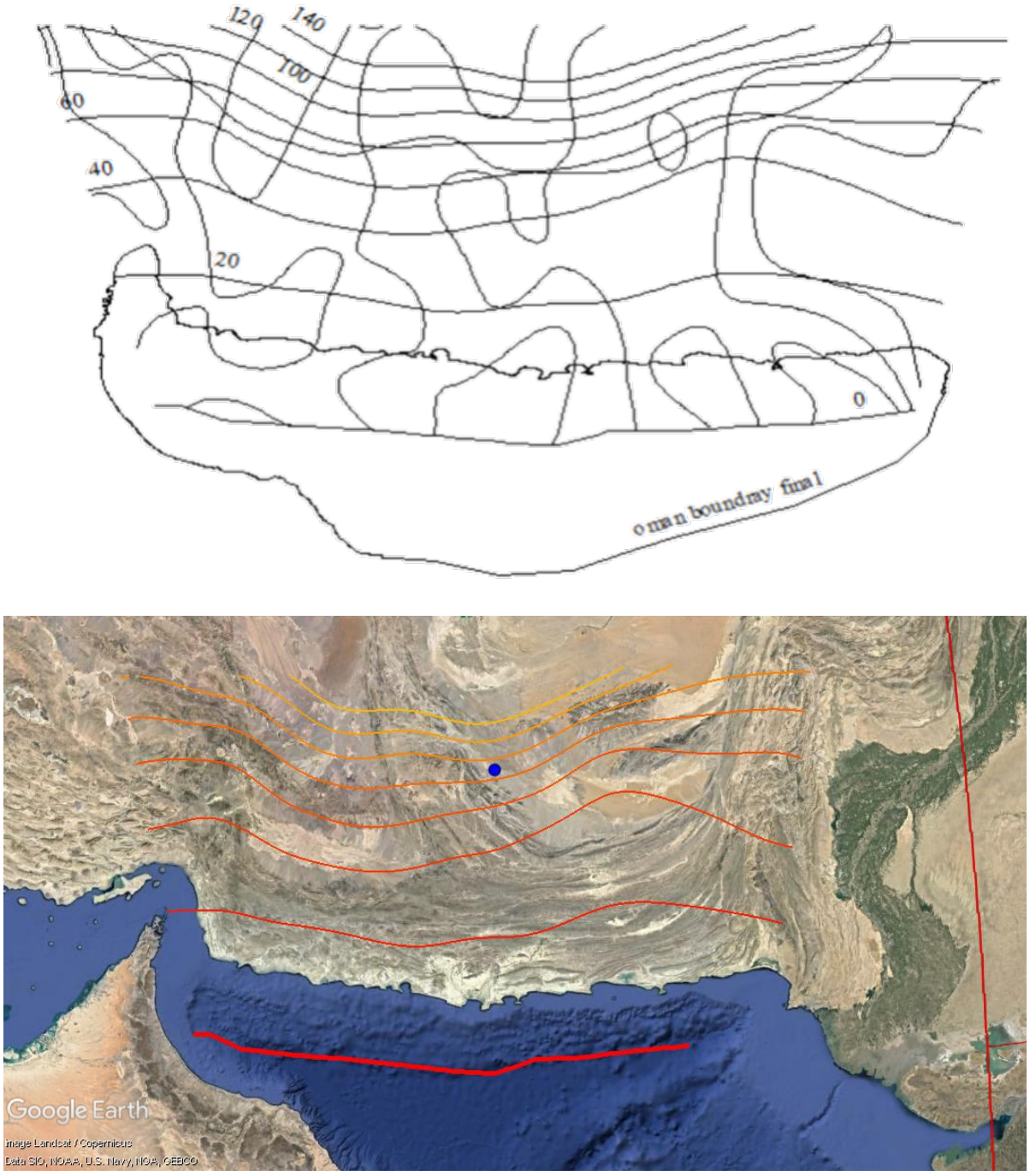

Fig. 19 Three - dimensional MSZ geometry showing the contour of dip, rake, strike, and depth of the MSZ.

varies slightly around 50 km to fit the MSZ geometry. Finally, dip, rake, strike, and depth for each segment were identified from the geometry model in Fig. 19 for use in the Okada model (Okada, 1985) to generate the initial tsunami conditions.

4.5.2 *Rupture area: node 1 and 2 in EV2*

For each magnitude ranging from $M_w = 7.7$ [2] to $M_w = 9.5$ with a regular magnitude interval of 0.1, i.e., $M_w \in \{M_{w,\min}, M_{w,\min} + 0.1, \ldots, M_{w,\max} - 0.1, M_{w,\max}\}$, the rupture length (L) and width (W) were calculated using the scaling relation derived from the regression analysis of historical subduction events worldwide:

$$\begin{aligned} \log_{10} L &= (a + b \times M_w), \\ \log_{10} W &= (c + d \times M_w), \end{aligned} \tag{4.11}$$

a, b, c, and d are the regression coefficients. Table 6 shows the rupture coefficient for five different scaling relation. The results of these five scaling relation for different magnitude levels were compared in Fig. 20. Fig. 20 (a) and (b) demonstrates different length and width calculated from the five scaling relations in vertical axis and different magnitude level in horizontal axis. It can be seen the differences in rupture length derived from the different scaling relation is not significant. While, the differences in the widths is significant and This difference is underscored by increasing the magnitude level. Finally, (Strasser et al., 2010) relation owing to its better fit to the trust events was used to calculate rupture area.

Table 6 Rupture scaling coefficient for five different scaling relations

Scaling relation	L		W	
	a	b	c	d
(Strasser et al., 2010)	-2.477	0.585	-0.882	0.351
(Blaser et al., 2010)	-2.37	0.57	-1.56	0.41
(Allen and Hayes, 2017)	-2.9	0.63	-0.86	0.35
(Goda et al., 2016)	-2.16	0.549	-0.689	0.289
(Wells and Coppersmith, 1994)	-2.42	0.58	-1.61	0.41

[2] $M_w = 7.7$ considered as the minimum magnitude capable of causing a noticeable tsunami.

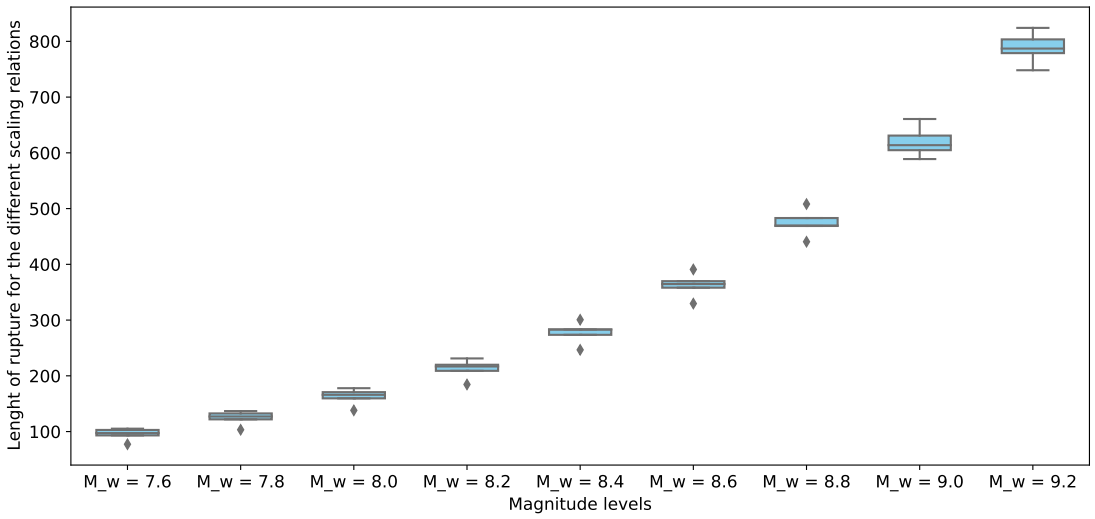

(a) Length

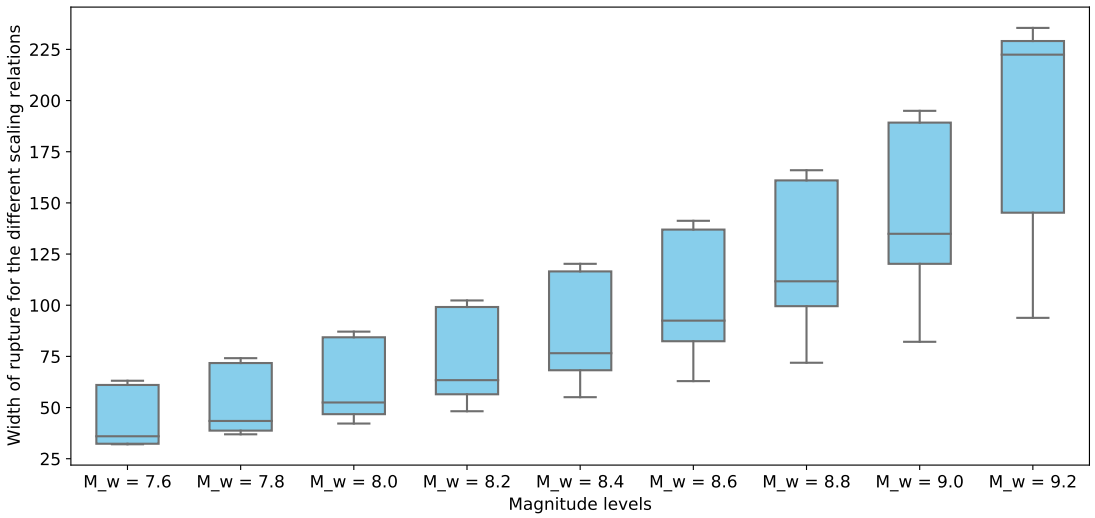

(b) Width

Fig. 20 Length (a) and width (b) calculated from the five scaling relations in vertical axis and different magnitude level in horizontal axis

4.5.2.1 Scaling relations uncertainty (σ_s)

Given the earthquake magnitude, rupture length and width were derived by evaluating the scaling relations as explained. To account for stochasticity in the earthquake dimensions imposed by the scaling relations, For $M_w \leq 8.7$, uncertainties associated with the use of the scaling relation for earthquake dimensions were included as aleatory variability directly in

probabilistic equations. To do so the standard deviations associated with the equations, which were $\sigma_s = 0.173$ and $\sigma_s = 0.180$ for length and width, respectively were used. However, the variability enlarges with growing magnitude. Hence, for $M_w > 8.7$, rather than using only one value for rupture length and width, a random sample was selected from a log-normal distribution. The initial intention was to consider the dependence of the variance of rupture length and width, and sample from a two-dimensional multivariate normal distribution (Blaser et al., 2010). However, the range of variation was quite small and considering the segmentation size (i.e., 50×50 km^2), the independent random selection of length (L) and width (W) were generated form normal distributions according to

$$\begin{aligned} \log_{10} L &\sim \mathcal{N}(-2.477 + 0.585 M_w, 0.18)\,, \\ \log_{10} W &\sim \mathcal{N}(-0.882 + 0.351 M_w, 0.173)\,. \end{aligned} \tag{4.12}$$

$\mathcal{N}(\mu, \sigma)$ is a normally distributed of random variable with mean μ and standard deviation σ; notation $\sim$ denotes the equivalence of distributions.

4.5.2.2 Rupture area and entangled segments (n_s, n_l)

For each length and width the number of segments downdip (n_s) and along-strike (n_l) were calculated. To do so, first the area (A) was calculated from:

$$\log_{10} A = (-3.476 + 0.952 \times M_w)\,. \tag{4.13}$$

Then, four pair of (n_s, n_l) were investigated. Two pairs from round up and down n_s and setting n_l to best match A calculated form Eq. (4.13) and the other two from round up and down n_l and setting n_s to best match A. The one pair that minimize the bellow aspect ratio error was selected (for more detail see (Davies et al., 2018)):

$$\left(\log_{10} \left(\frac{n_s \bar{l}_s}{n_d \bar{l}_d} \right) - \log_{10} \left(\frac{L}{W} \right) \right)^2 . \tag{4.14}$$

An example of above method for $M_w = 8$ and $L = 159.59$, $W = 84.33$ is shown in Table 7. In this case $n_s = 3$ and $n_l = 2$ was selected as the rupture area and segments entanglements.

Table 7 Example of segments involvement calculation method for $M_w = 8$ and rupture area of $L = 159.59$, $W = 84.33$.

Pairs	n_s	n_l	Aspect ratio
1	4	1	0.10564
2	3	2	0.01018
3	3	2	0.01018
4	5	1	0.17803
Minimum ratio	0.1018, pair number 2 with $n_s = 3$ and $n_l = 2$		

4.5.3 Slip distribution: node 3 in EV2

Slip distribution significantly affects tsunami heights nearshore. Recently, different studies have shown that maximum nearshore wave height varies by a factor of 2 or more due to heterogeneity in earthquake slip (Butler et al., 2017; Goda et al., 2014; Løvholt et al., 2012; Mueller et al., 2015; Sugino et al., 2015). However, owing to its convoluted nature and computation complexity, tsunami hazard assessments are usually based on idealized uniform slip earthquakes. In this study, a uniform slip for $M_w \leq 8.6$, where the effect of spatial slip distribution is not significant was used. 15 heterogeneous slip distribution for $M_w \geq 8.7$, where the heterogeneity of slip notably varies tsunami heights at the PoIs was used. This trade-off was specified to account for the effect on tsunami heights and optimize the number of scenarios through a sensitivity analysis. The number of scenarios and differences among modeled tsunami heights at PoIs were compared for a fixed scenario, but with varying M_w, starting from $M_w = 7.7$. This observation is relatively similar to (Sugino et al., 2015) in which, for the Japan PTHA, earthquakes with $M_w > 8.9$ were considered large, and the authors included three levels of spatial slip in their model.

Average slip was computed for each scenario with magnitude M_w employing the scaling relation as follows:

$$M_w = \frac{\log M_o - 9.1}{1.5}, \qquad S = \frac{M_o}{\mu \times A}, \tag{4.15}$$

where M_o is the seismic moment, μ the shear modulus, and A the area of each scenario. μ was set to 3×10^{11} dyn cm^{-2} as it is appropriate for crustal rocks and shallow depth faults (Deif and El-Hussain, 2012). Then the evaluated S from Eq. (4.15) as a uniform slip was used for $M_w \leq 8.6$; whereas for $M_w > 8.6$, the slip for each sampled (L,W)-scenario was created randomly using the `PTHA18` code built in `R`. The `PTHA18` code uses the SNCF model of (Davies et al., 2015) for generating random slip distribution for a given segment dimension and number. This model is a variant on the widely used K^2 model.

Let S_{nm} be an image representing a 2-D planar slip distribution, it can be represent via its 2-D discrete Fourier transform:

$$S_{nm} = \frac{1}{n_s \times n_l} \sum_{j=0}^{n_s-1} \sum_{l=0}^{n_l-1} \eta_{j,l} \exp\left(2\pi i \left(\frac{nj}{n_s} + \frac{ml}{n_l}\right)\right), \tag{4.16}$$

$$\eta_{j,l} = \sum_{n=0}^{n_s-1} \sum_{m=0}^{n_l-1} S_{nm} \exp\left(2\pi i \left(\frac{nj}{n_s} + \frac{ml}{n_l}\right)\right), \tag{4.17}$$

with n_s,n_l segments in the along-strike (x) and down-dip (y) directions respectively, segment dimensions Δx,Δy, length $L = n_s \Delta x$ and width $W = n_l \Delta y$. Further implementation details can be found in (Davies, 2019) and (Davies et al., 2015). Fig. 21 demonstrates 15 randomly selected slip distribution generated from the 2 - D planner distribution – Eq. (4.16) – for one of the scenarios with magnitude $M_w = 8.9$. The distributions are scattered in the MSZ seismicity zone along - strike ($n_s = 20$) and down-dip ($n_l = 8$).

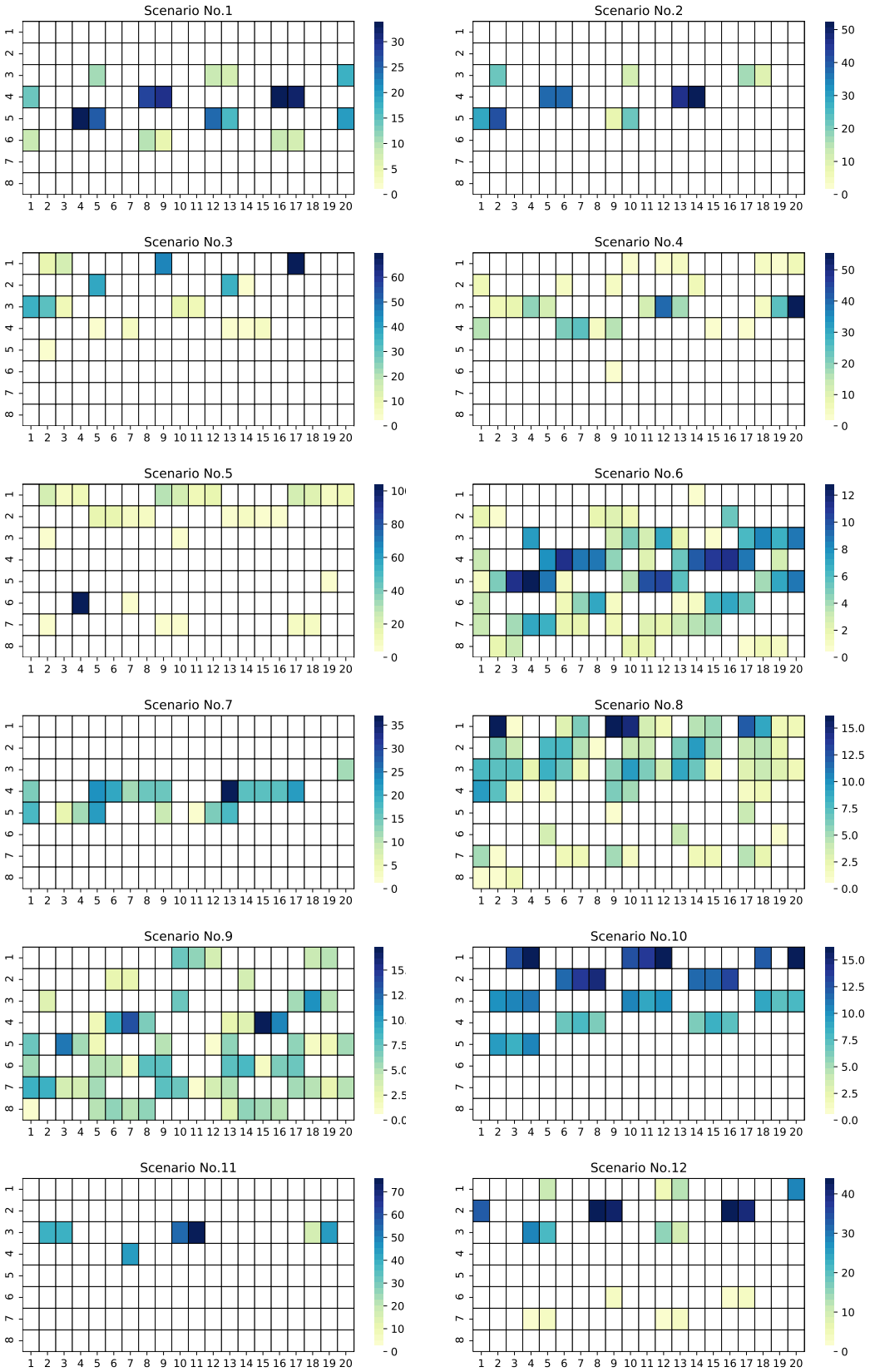
Scenario No.1
Scenario No.2
Scenario No.3
Scenario No.4
Scenario No.5
Scenario No.6
Scenario No.7
Scenario No.8
Scenario No.9
Scenario No.10
Scenario No.11
Scenario No.12

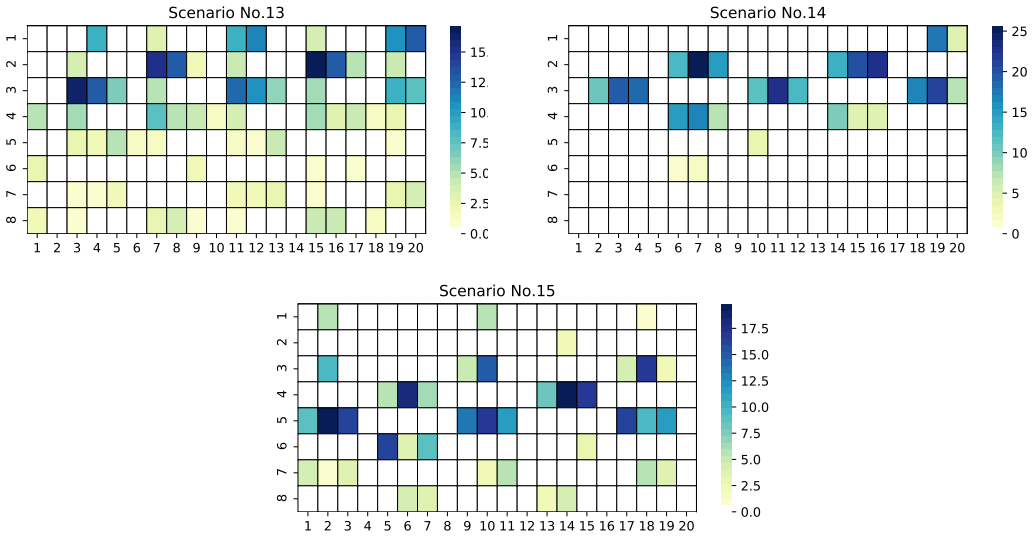

Fig. 21 Fifteen randomly selected slip distribution generated from the 2 - D planner distribution, Eq. (4.16) for one of the scenarios with magnitude $M_w = 8.9$.

4.5.4 Possible location: node 4 in EV2

To cover all the seismogenic zone for each magnitude and sampled length and width, the calculated $n_s \times n_l$ were floated through all possible locations of the MSZ seismicity area, shown in the blue mesh in Fig. 22. Table 8 shows the number of scenarios for different magnitude level based on the method described in sections 4.5.2 and 4.5.3. For each magnitude and number of segments along-strike and down-dip, scenarios were created by floating through all the seismicity zone (20×8).

In total, 5275 scenarios were created using the approach discussed considering the branches of EV2 for different magnitudes, which were randomly sampled from the rupture area, slip distribution, and all possible locations.

It is assumed that the occurrence of a specific magnitude was equally probable in all possible locations; therefore, an equal weight was assigned to the branches of EV2.

4.6 Tsunami model

For each scenario, numerical simulations of tsunami generation and propagation were performed using the models and techniques described in Chapter 3, section 3.2.3.

Table 8 The number of scenarios for each magnitude considering the heterogeneity of slip.

M_w	n_s	n_l	Possible scenarios along-strike	Possible scenarios down-dip	Total Possible scenarios	Total Possible Heterogeneity's scenarios
7.7	2	2	19	7	133	133
7.8	2	2	19	7	133	133
8.0	3	2	18	7	126	126
8.2	4	2	17	7	119	119
8.4	6	2	15	7	105	105
8.6	7	3	14	6	84	84
8.7	8	3	13	6	78	1170
8.8	9	3	12	6	72	1080
8.9	11	3	10	6	60	900
9.0	13	4	8	5	40	600
9.1	15	4	6	5	30	450
9.2	16	4	5	5	25	375
Sum					1024	5275

Here, `FUNWAVE-TVD` was used in its Cartesian implementation. To prevent non-physical reflection from the boundaries, sponge layers were specified with 10 km thickness within the computational domain. A 600 m resolution was used for the computational domain, which is a trade-off between precision and practical feasibility.

To guarantee representative bathymetry, three bathymetric models were evaluated. In particular, Etopo-v1 (based on satellite gravity data), GEBCO (global bathymetric model based on ship-track data), and SRTM+ (space shuttle radar mapping) with measured data provided by the Ports and Maritime Organization of Iran (PMO) were compared. It appears that the latest released data of the GEBCO model with 15 arc-second resolution are the best among the aforementioned models and exhibit a smoother transition between deep and shallow water. This contrasts the results of (Thio et al., 2007) while agreeing with those of (Marks and Smith, 2006). The former can be due to the heterogeneous characteristic of each site or/and the latest update of the bathymetry data. Hence, GEBCO-2020 with 15 arc-second resolution has been used for the tsunami simulations. Each scenario has been simulated for 8 h, and for each computational time step, a time series of tsunami wave has been recorded at 84 hazard points. These PoIs are located at 5 to 0 m isobath at approximately $10-12$ km intervals along the Iran and Pakistan coastline. The PoIs are shown in Fig. 22.

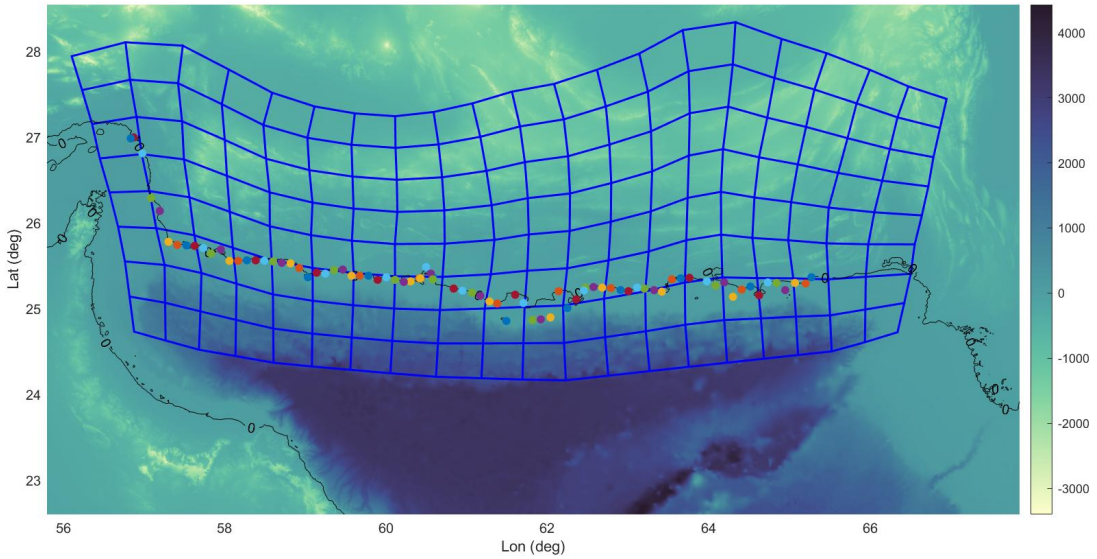

Fig. 22 Bathymetry model and computational domain; dots represent PoIs located at 0 m isobath along the coast; blue mesh indicates the seismogenic zone and source discretization into 50×50 km^2.

Table 9 A summary of input variables for the MSZ propagation model.

Variables	Inputs
Computational domain	55.8 - 67.8 ° E , 22.6 - 28.5 ° N
Bathymetry data	GEBCO 15 arcsec – 2020
Resolution	600 m
Sponge layers thickness	10 km in all directions
Drag coefficient	0.01
Wetting-drying (the critical depth)	1 cm

4.6.1 Propagation result

Fig. 23 shows initial condition and propagation waves for one of the scenarios with the magnitude $M_w = 8.7$. Tsunami waves are arriving to the coast 25 min to 45 min after earthquake in different PoIs. depend on the location of the event. In this example, earthquake was located at the east part of the MSZ.

Fig. 24 demonstrates tsunami wave time series for the same scenario as above - mentioned in four PoIs as an example. PoIs in Fig. 24 (a) and (b) are located at the west part of the MSZ,

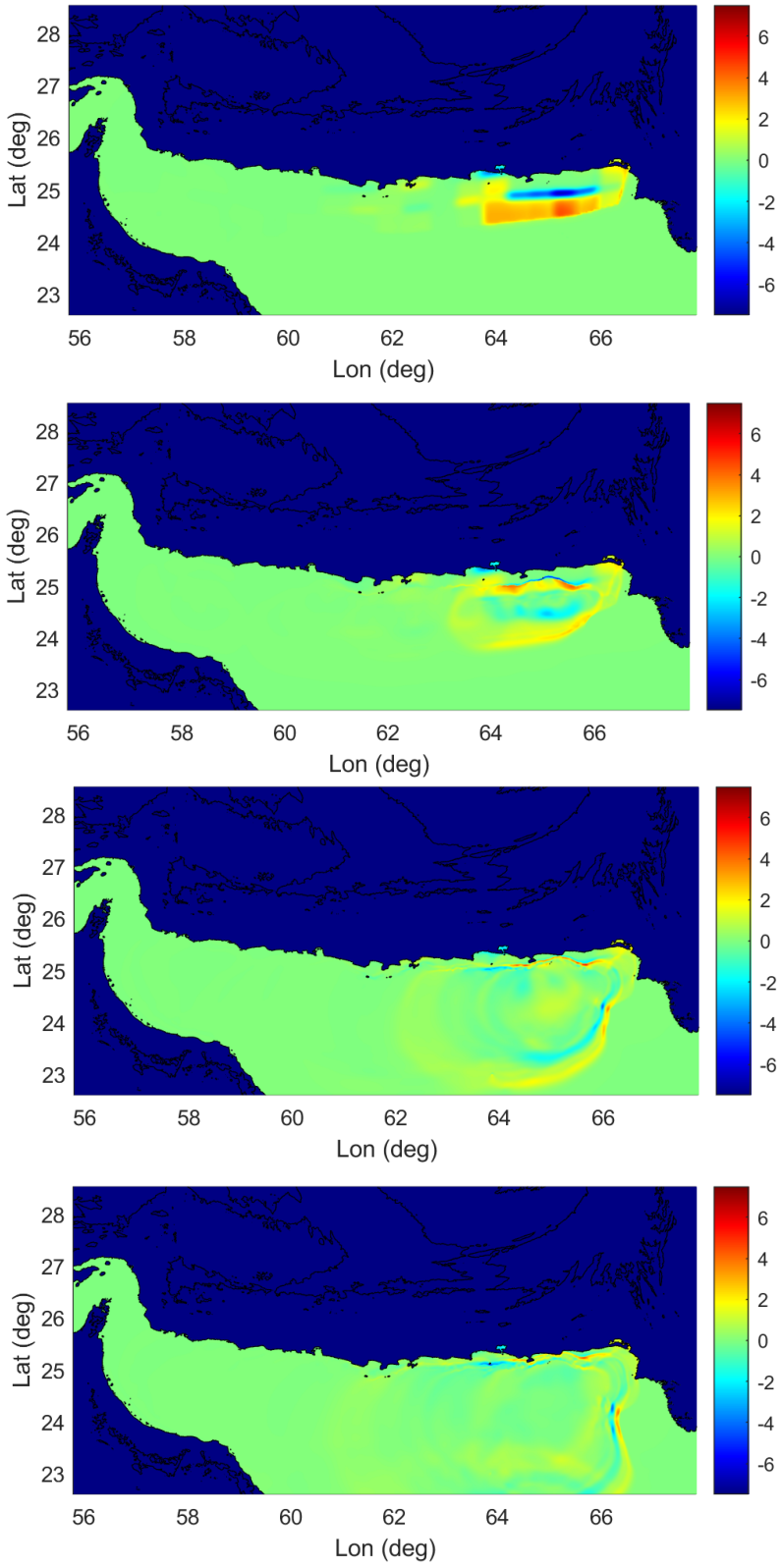

Fig. 23 Propagation results for one of the scenarios with magnitude $M_w = 8.7$ in $t = 0$, $t = 5$ min, $t = 10$ min, and $t = 20$ min.

and PoIs in 24 (c) and (d) are at the eat part. Tsunami waves are arriving to the east part around 25 min later while in the west part it takes more than 35 min to be affected by the first wave of

tsunami. It is because of the epicenter of earthquake which in this particular example (scenario) is located at the east part of the MSZ. With changing the scenario and locations the arrival time will significantly change in the PoIs. Recalling that all the possible earthquake locations were weighted the same (see section 4.5.4).

Considering the same chance in all the location tsunami waves will arrive to the coast within 15 min to 45 min for different magnitude levels and mitigation planers must consider it in their designs.

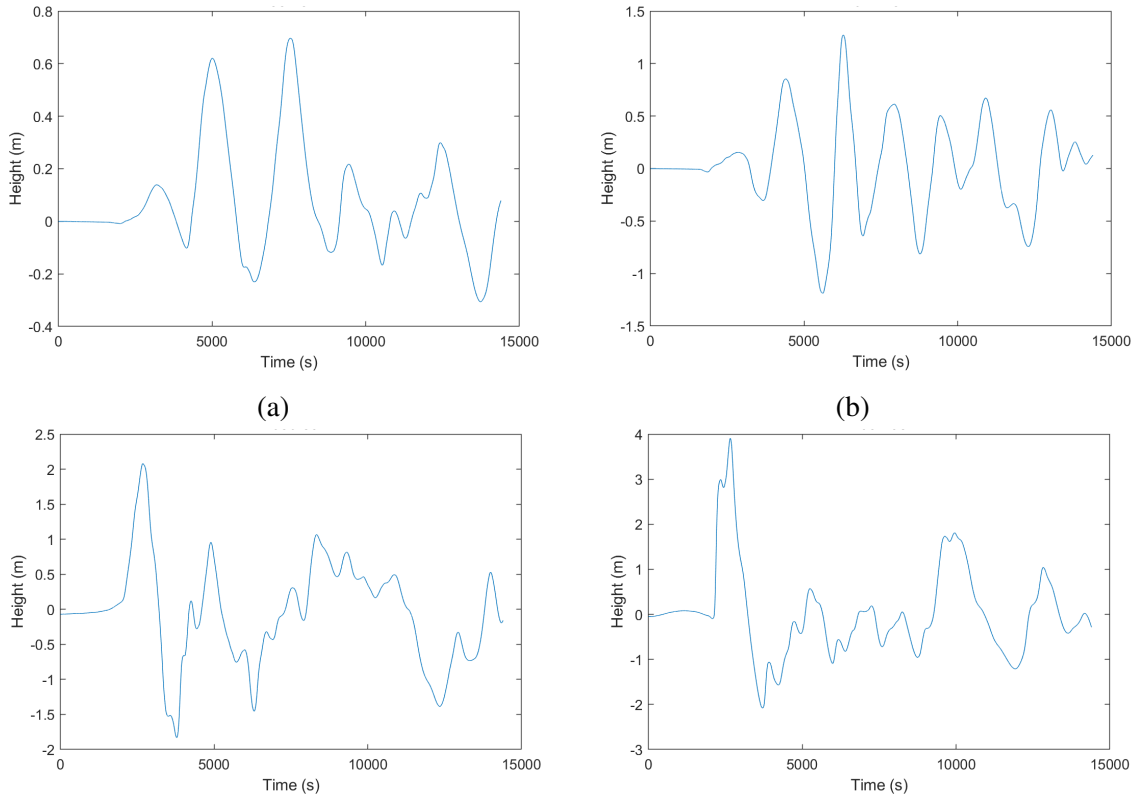

Fig. 24 The timeserie results of one of the scenarios with magnitude $M_w = 8.7$ at four PoIs: (a) and (b) are located at the west part of the MSZ and (c) and (d) are located at the east part.

4.7 Deriving the probability of exceedance

For a given exposure time (ΔT), PTHA was performed by deriving the exceedance of maximum tsunami height (ψ) at each PoI form a threshold value (ψ_t). Considering a total of J possible

magnitudes, the total probability of exceedance was defined

$$P^{\text{tot}}(\psi > \psi_t, \Delta T, \text{PoI}) = 1 - \prod_{j=1}^{J} \left(1 - \mathscr{P}(E_j, \Delta T) P(\psi > \psi_t | E_j)\right) , \tag{4.18}$$

where $\mathscr{P}(E_j, \Delta T)$ is the probability that at least one event (E_j) occurs in the return period ΔT. Assuming that the occurrence of earthquakes conforms to a stationary Poisson process with the annual recurrence rate ν_j, it can be assessed as

$$\mathscr{P}(E_j, \Delta T) = 1 - \exp\left(-\nu_j \times \Delta T\right) . \tag{4.19}$$

Considering the uncertainties on rupture dimensions, locations, and slip distribution in EV2, each E_j can cause different scenarios ($\mathscr{S}_A^{(j)}$). The probability that tsunami height (ψ) exceeds a threshold (ψ_t) when the event E_j occurs is then given by

$$P(\psi > \psi_t | E_j) = \sum_{A=1}^{A_j} P\left(\mathscr{S}_A^{(j)} | E_j\right) P\left(\psi > \psi_t | \mathscr{S}_A^{(j)}\right) . \tag{4.20}$$

Here, $P\left(\mathscr{S}_A^{(j)} | E_j\right)$ is the probability of occurrence of the scenario $\mathscr{S}_A^{(j)}$, and in the absence of aleatory variability,

$$P\left(\psi > \psi_t \middle| \mathscr{S}_A^{(j)}\right) = \begin{cases} 0, & \psi < \psi_t \\ 1, & \psi \geq \psi_t \end{cases} , \tag{4.21}$$

While in the presence of the aleatory variability that was discussed in section 4.1.2 (Thio, 2010),

$$P\left(\psi > \psi_t \middle| \mathscr{S}_A^{(j)}\right) = 1 - \Phi\left(\log(\psi_t) \middle| \left[\log(\psi_{\mathscr{S}_A^{(j)}})\right], \sigma\right) . \tag{4.22}$$

Φ is the cumulative distribution function for a log-normal distribution with the mean equal to the modeled tsunami height at each PoI and standard deviation σ, given value of a $\log(\psi_t)$. From (Thio, 2010), σ can be computed by combining the aleatory variability terms $\sigma = \sqrt{\sigma_{\text{m}}^2 + \sigma_{\text{t}}^2 + \sigma_{\text{s}}^2}$.

4.7.1 Ensemble model

In this section, how to incorporate the uncertainties from EV1 and obtain $\mathscr{P}(E_j, \Delta T)$ using the ensemble model (Marzocchi et al., 2015) is explained. As it is explained in Chapter 3, section 3.2.1.1 To calculate the probability that at least one earthquake E_j occurs for the selected ΔT, an event tree was developed as described in section 4.4 and Fig. 11. The branches of EV1 were treated in the framework of ensemble modeling, as introduced in (Marzocchi et al., 2015). Ensemble modeling presumes that epistemic uncertainty is greater than that evaluated by one event tree, and treats the branches of the event tree as an unbiased sample from a parent distribution. This distribution, $f(\theta)$, describes the variable θ simultaneously considering the aleatory variability and epistemic uncertainty.

Here, branches of EV1 are a small sample size, and their few probability outcomes can be replaced by a parametric distribution. A natural choice is the beta distribution that is commonly used in hazard literature. In this case, variable $\theta^{(E_j)}$ is set to $\mathscr{P}(E_j, \Delta T)$ so that the variable will be the hazard curve. Different $\theta^{(E_j)}$ are the branches of EV1 that are now a sample of a Beta (α, β) distribution. Parameters α and β are related to the average and variance of $\theta^{(E_j)}$ as

$$\mathrm{E}[\theta^{(E_j)}] = \frac{\alpha}{\alpha+\beta}, \qquad \mathrm{Var}[\theta^{(E_j)}] = \frac{\alpha\beta}{(\alpha+\beta)^2(\alpha+\beta+1)}. \tag{4.23}$$

$\mathrm{E}[\theta^{(E_j)}]$ and $\mathrm{Var}[\theta^{(E_j)}]$ denote, respectively, the weighted average and variance of the exceedance probabilities of the jth magnitude for the selected ΔT. Inverting equations Eq. (4.23), the parameters of the Beta distribution were found for each magnitude j. Finally, calculating the Beta parameters of the exceedance probability for a set of magnitudes, the full hazard curves was plotted. Fig. 25 shows beta distribution of the 50 yrs exceedance probability calculated for four different magnitude levels. This beta distributions were generated from $\mathscr{P}(E_j, \Delta T)$ of EV1 and calculated beta parameters from Eq. (4.23). After, calculating all the beta distributions for all the magnitude levels, statistical description, mean, and the 16th-86th percentiles confidence intervals was calculated and used for further calculation.

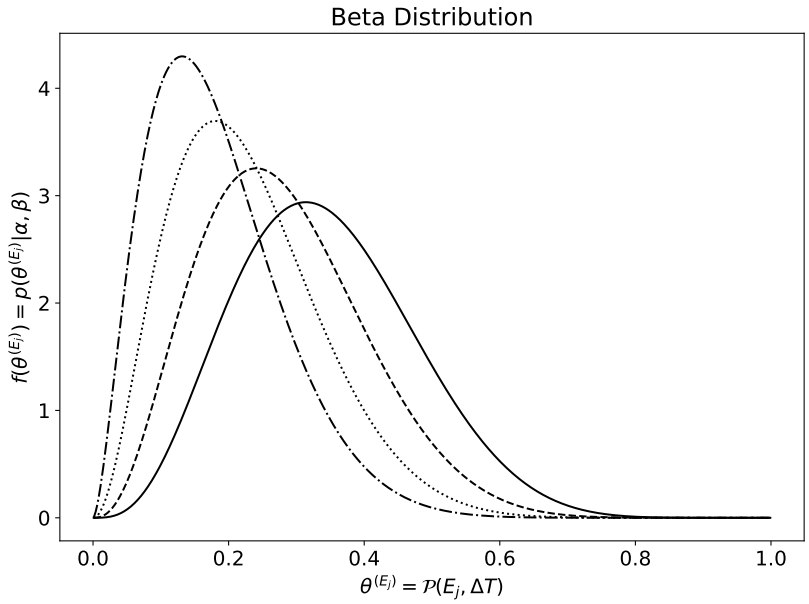

Fig. 25 The calculated beta distribution of 50 yrs exceedance probability for four different magnitude levels.

4.8 Probability of exceedance results

In this section, the results obtained from the analyses and modeling presented in previous sections are presented for the coastal area of the MSZ. The main results are presented by earthquake and tsunami probability exceedance curves and tsunami probability maps for the selected return time periods. In this study, return periods are set to $\Delta T = \{50, 100, 250, 500, 1000\}$ years; each choice interests different stakeholders and provides information on a specific aspect of the tsunami hazard in the MSZ.

As it was mentioned in Chapter 3, section 3.2.4, $\Delta T = 500$ and $\Delta T = 1000$ years for city planing and designing critical facilities (e.g. nuclear power plant), respectively, had been selected for further analysis and discussion. However, the results for $\Delta T = \{50, 100, 250\}$ are also provided for the sake of other stakeholders' interest.

Furthermore, besides the sensitivity analysis in sections 4.2, 4.4.2, 4.5.2, and 4.5.3, in this section another sensitivity analysis has been done comparing the results obtained in the presence and absence of the aleatory variability.

4.8.1 Earthquake probability exceedance curves

The earthquake probability of exceedance for the selected ΔTs are depicted in Fig. 26. The ensemble model results from section 4.7.1 is shown through its statistical description, its mean, and the 16th-86th percentiles confidence intervals. For the sake of comparison, the branches of EV1 ($\theta^{(E_j)}$) are also shown in light gray. In nearly all cases, the statistical description of the mean ensemble model is a good representative of EV1 branches Fig. 26. Henceforth, the value of mean ensemble was used for each magnitude to calculate tsunami probability exceedance curves and probability maps. Notably, in this step, any other statistical description can be chosen for further analysis and using the probability codes.

4.8.1.1 $\Delta T = 500$ **years**

Each gray curves in Fig. 26 shows exceedance probability for different magnitude levels for one path of the EV1 branches (i.e. different recurrence model, maximum magnitude and the modeling error, see Fig. 11 (a)). Selection of the most appropriate curve which represents the true hazard has been a subject of discussion and controversies among scientists and risk managers (Marzocchi and Jordan, 2014). For example for 500 years return period, the probability of exceedance of $M_w = 8.1$ – the worst historically recorded magnitude – varies from nearly zero to 87% for different path of EV1.

Using the statistical description of ensemble modeling, the probability of exceedance of $M_w = 8.1$ is less than 10% for its 16^{th} percentile, 52% for 84^{th} percentile and its mean is 23%.

4.8.1.2 $\Delta T = 1000$ **years**

The probability of exceedance of $M_w = 8.1$ for return period of 1000, changes between 3% to 100%. Ensemble statistical descriptions are: 15% and 80% for 16^{th} and 84^{th} percentile, respectively. Its mean show a probability of 50% exceedance for $M_w = 8.1$. It is almost twice as the probability of exceedance for 500 year return period.

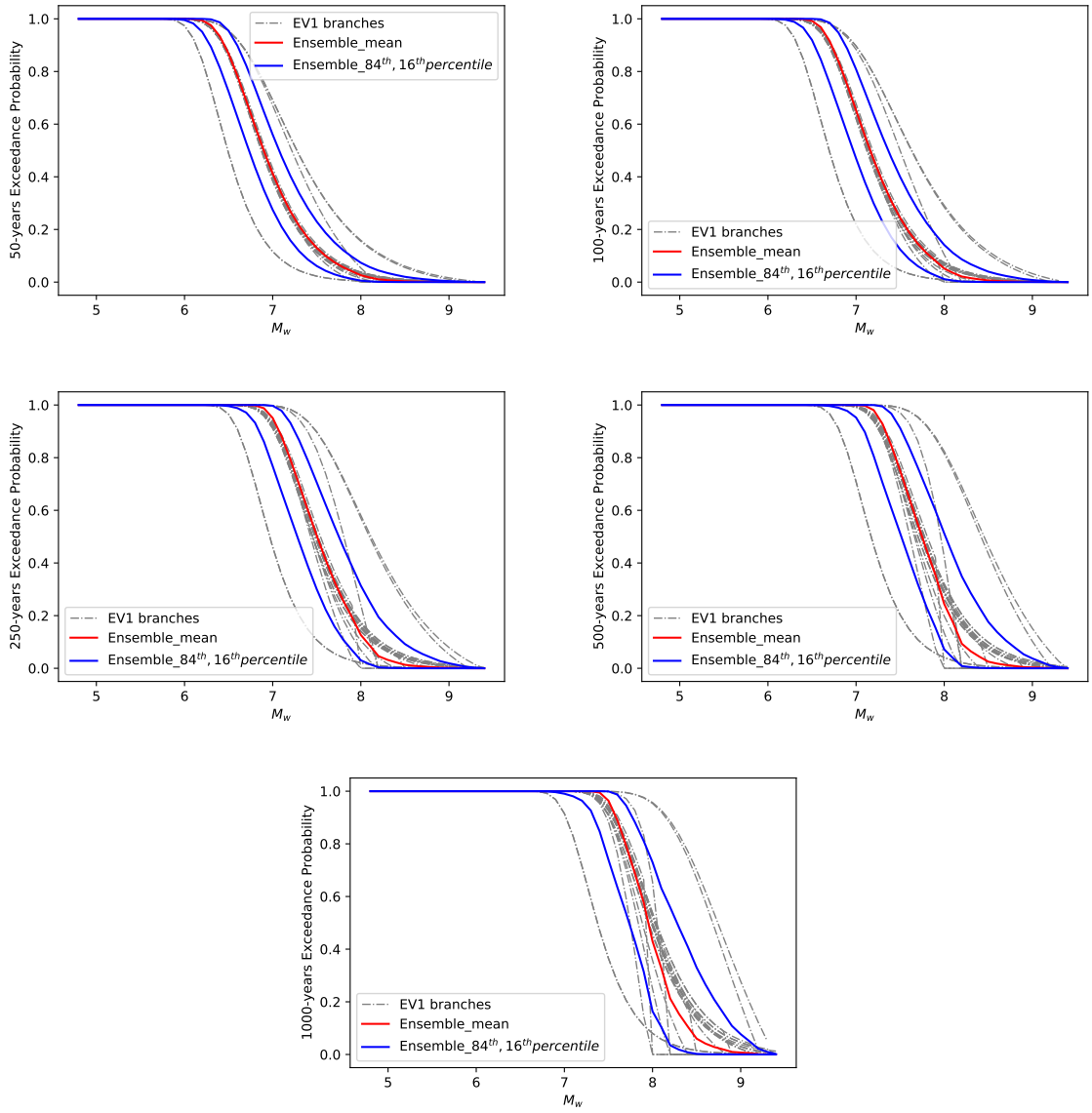

Fig. 26 Earthquake probability of exceedance for the sample of ΔTs: red and blue curves show the statistical description of ensemble model, i.e., mean and 16th-86th percentiles, respectively. For comparison, all outcomes of the EV1 branches are also displayed in light gray.

4.8.2 Tsunami probability exceedance curves

Using the equations described in section 4.7, and the mean value of ensemble modeling of the exceedance probability of earthquake in section 4.8.1, the probability of exceedance from a set of tsunami height thresholds $\psi_t = \{0.5, 1, 1.5, .., 5.5, 6\}$ m were calculated. Fig. 27 shows the generated hazard curves at different PoIs incorporating all uncertainties. The hazard curves for each PoI are shown in gray. The results show that the spread of hazard curves for different locations of the Makran coast is remarkably large. As an example, $P^{\text{tot}}(\psi > 3, \Delta T = 50)$

ranges from 0 to 16% for different PoIs. By increasing ΔT, this range opens up and it reaches $30\%, 58\%, 80\%$, and 95% for the return periods of 100, 250, 500, and 1000 years, respectively.

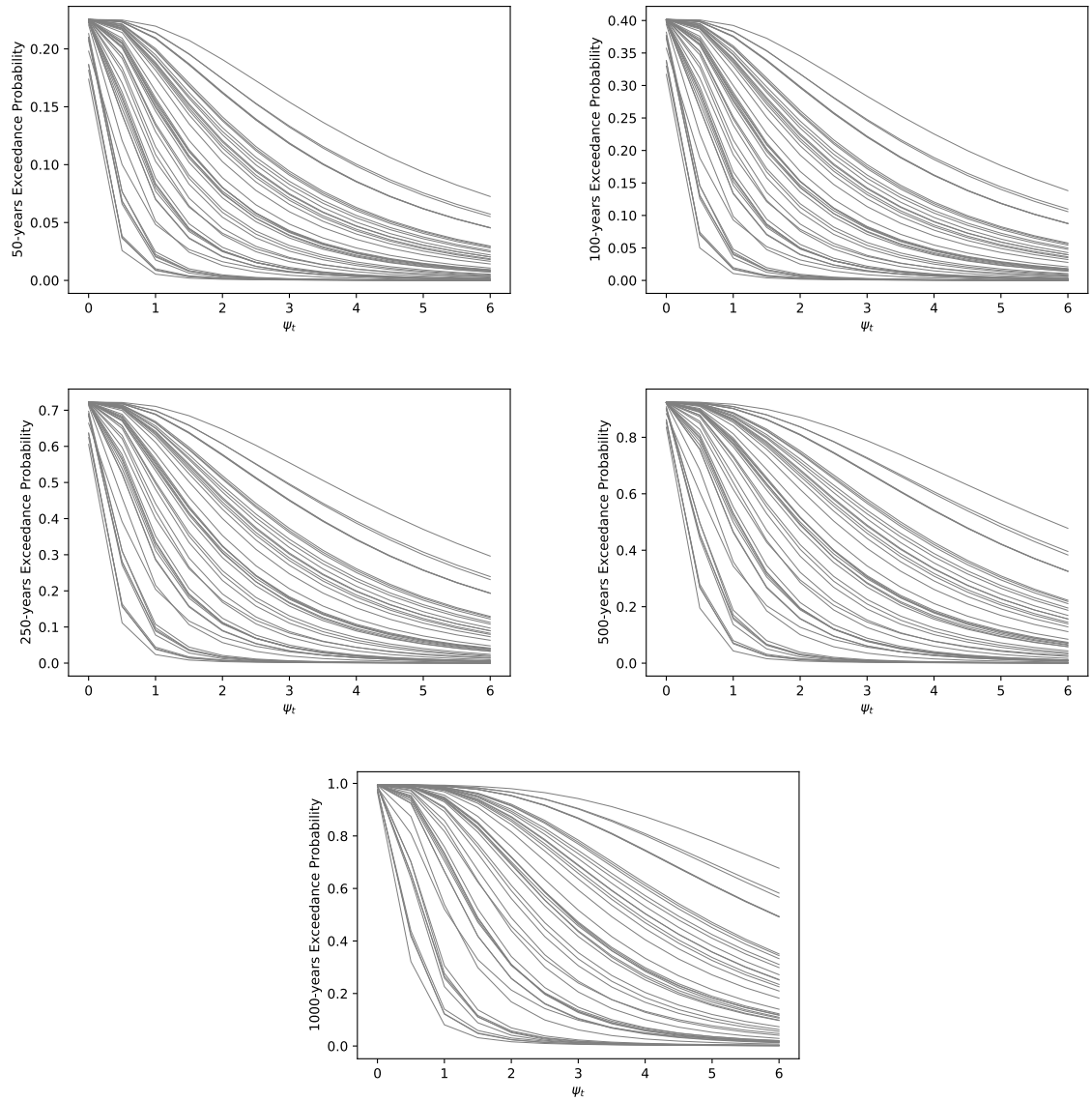

Fig. 27 Tsunami probability of exceedance for a sample of ΔTs at different PoIs along the Iran and Pakistan coasts.

$P^{\text{tot}}(\psi > 5, \Delta T = 500, 1000)$ ranges $0-60\%$ and $5-97\%$, respectively, in different PoIs along the coast of Iran and Pakistan. The range of the probability of tsunami exceedance is quit large and it is thus not wise to consider a mean (or percentile) of PoI hazard curves for any purpose in the coasts of Iran and Pakistan. Hence, six main PoIs close to the major cities of the Makran region, namely, Chabahar, Konarak, Jask, Ramin, Jiwani, and Gwadar, were selected to explore the results in detail.

Fig. 28 shows the tsunami probability exceedance curve at the above mentioned six major cities for different return periods. For a 50-year return period, the probability of exceedance does not vary much among different cities. However, this difference becomes significant with increasing ΔT. For instance, for $P^{\text{tot}}(\psi > 1, \Delta T = 1000)$, it ranges from 32% in the west (Gwadar) to 97% in the east (Jask). Moreover, the probability that tsunami height exceeds 4 m is low (less than 10%) near all major cities except for Jask, with the probability of 53%.

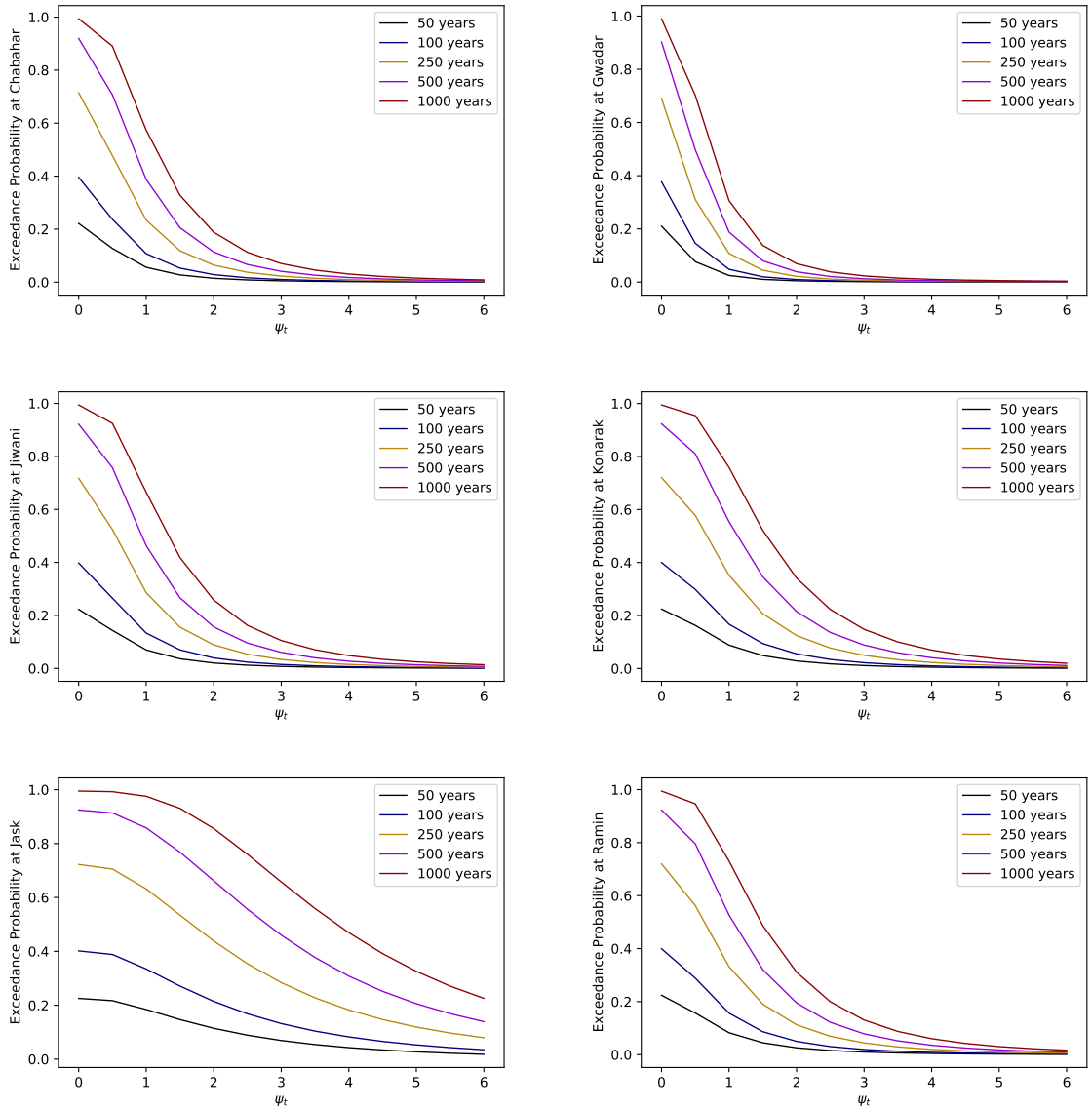

Fig. 28 Tsunami probability of the selected ΔTs exceedance for the selected six PoIs near main cities.

4.8.3 Sensitivity analysis

The effect of inclusion of the aleatory variability introduced in section 4.1.2 is shown in Fig. 29. Fig. 29 (a) illustrates the probability of exceedance in the presence and absence of the aleatory variability at one random PoI (i.e., Chabahar) for two return periods, 100 and 500 years. The inclusion of the aleatory variability has a significant effect on the probability of exceedance, which increases for a longer return period. As an example, the differences between $P^{\text{tot}}(\psi > 1, \Delta T, \text{Chabahar})$ with and without the aleatory variability are 8% and 26% for $\Delta T = 100$ and 500 years, respectively. To obtain a better interpretation, this difference for all PoIs and ΔTs were also calculated, see Fig. 29 (b). In summary, omitting the aleatory variability mostly leads to a noticeable underestimation with a median of 10% for all PoIs, reaching and it even reaches 40% at somewhere for 1000-year return period.

4.8.4 Probability maps

Probability maps were used to assess hazard along the entire coast irrespective of population density, which is crucial for prioritizing tsunami mitigation plans and city development in low-population areas, while most literature and mitigation plans focus on specific populated areas. Fig. 30 illustrates tsunami probability maps exceeding from three selective thresholds, $\psi_t = 1, 3$ m with different return periods. The probability of exceedance is much more intense in the west. Furthermore, in some rural areas (e.g., Tis and Tang) neighboring Chabahar, the probability that tsunami height will exceed 3 m for return periods of 100 and 1000 years is approximately 30% and 95%, respectively. Notably, this is almost 6 to 7 times higher than that in Chabahar. Owing to the small distances between these regions, the inundated area at Chabahar may be affected.

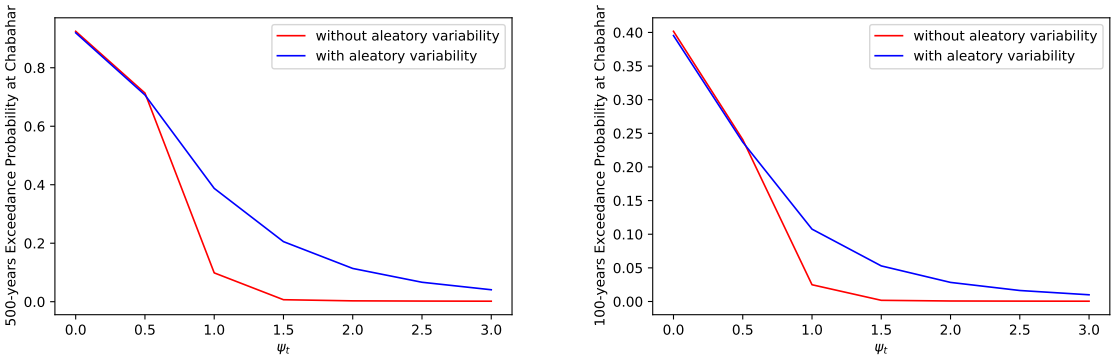

(a)

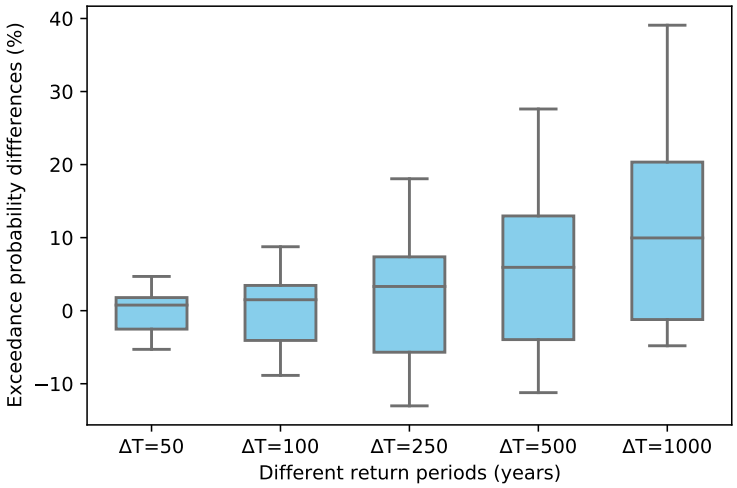

(b)

Fig. 29 (a) Exceedance curve of Chabahar as a random PoI for 100- and 500-year return periods; blue and red curves show the probability of exceedance in the presence and absence of the aleatory variability, respectively; (b) box plot showing the differences in exceedance probability (%) for different ΔTs with and without the presence of the aleatory variability for all PoIs.

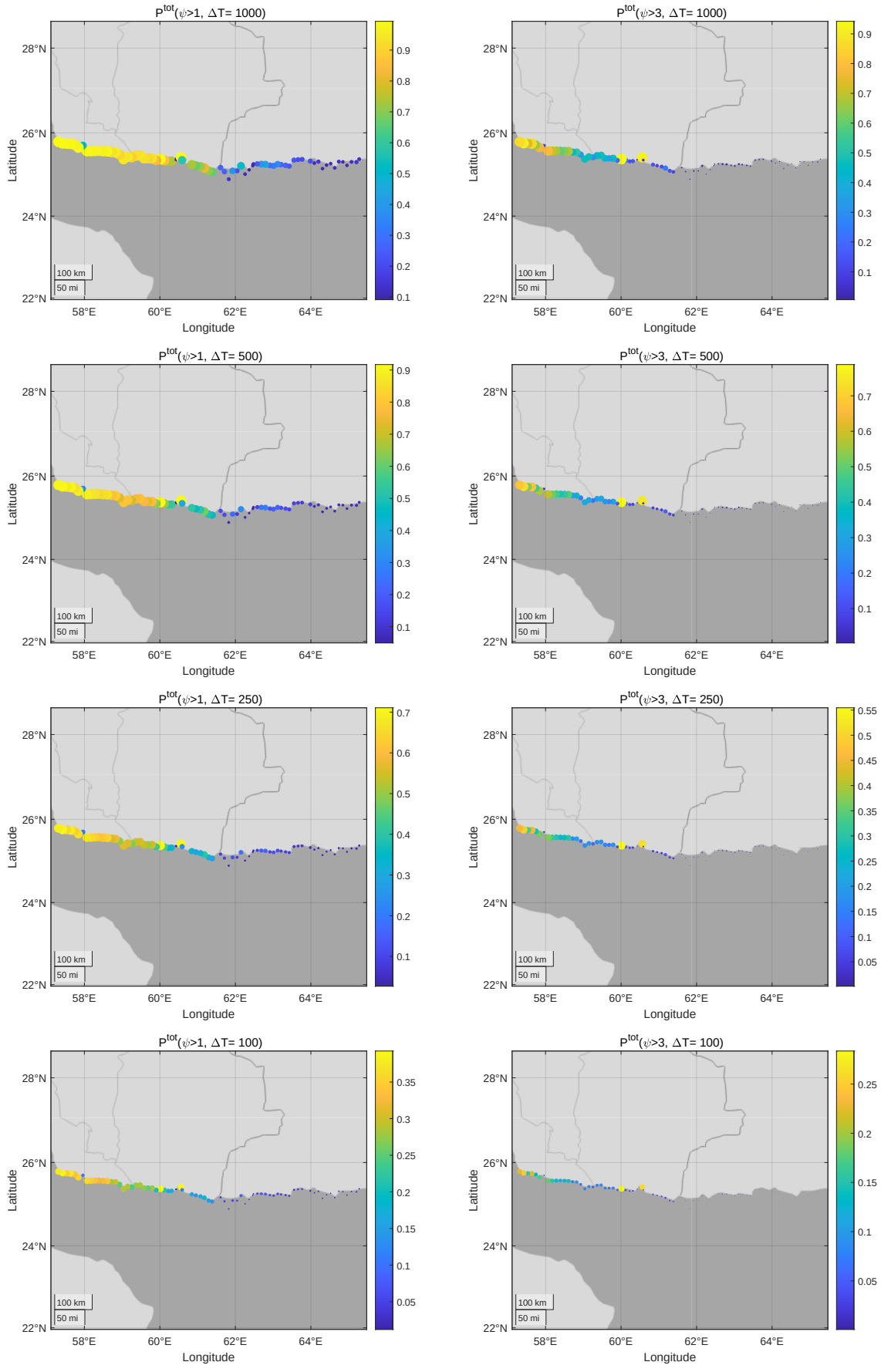

Fig. 30 Maps of tsunami probability exceeding 1 and 3 m for different ΔTs along the entire coast of Iran and Pakistan.

4.9 Summary

In this chapter, all the identified uncertainties in Chapter 2 associated with the potential tsunami were incorporated using PTHA approach. Moreover, different stakeholders' interests were taken into consideration by demonstrating the probability map for different return periods. To obtain more accurate and reliable results the combination of statistical, historical, geological and numerical assessment were considered. The epistemic uncertainties were incorporated by combining event tree and ensemble modeling, including uncertainties of fault source and rupture complexity (dimensions, slip distribution, and possible locations of earthquakes). The aleatory variability was identified from three main contributions (numerical model and bathymetry mismatch, tidal variation, and scaling relation), and incorporated directly into the probability equations, see Eq. (4.22). The results were demonstrated using hazard curves and probability maps. Moreover, several sensitivity analysis were performed in various stages of the work to find: (i) the optimal resolution of propagation model which is a trade-off between precision and practical feasibility, (ii) the best available bathymetry data which represent the real bathymetry of the area, (iii) the best source of tidal records, which was compared with the model constituents in the area, (iv) the threshold of M_w that after which a multitude number of rupture areas for each magnitude level was considered, (v) the threshold of M_w that after which a heterogeneous (instead of a uniform) slip distribution was used, (vi) the effect of the aleatory variability in probability of exceedance.

5 UNCERTAINTIES IN SOFT MEASURES

In this chapter, the uncertainties that had the most effect on vulnerability of communities in the past tsunamis and other hazards are evaluated in Makran. To propose mitigation and education plans, education strategy and disaster communication and must consider heterogeneity in community (Paton and Johnston, 2001). Accordingly, the present chapter provides emperical data about the this issue in an under-studied area, Makran, and thus expands upon the limited empirical data. Moreover, the heterogeneity of community was taken into account by interviewing risk experts in Iran and adding their suggested indices into the questionnaire.

Furthermore, this chapter engages to the literature (see Chapter 2) in 2 ways. First, it contributes issues with little attention in previous researches; second, it applies important indices, extracted from the literature in Chapter 2, to address local's knowledge, awareness, and attitudes about tsunamis. To do so, the the method explained in Chapter 3 was applied. Moreover, ANOVA and Chi-squared tests were used to find the variables that have a significant relationship. Understanding these variables can help development of optimal mitigation plans. Furthermore, mitigation and education plans can be resonate to more locals with lower effort and costs. This is essential considering the limited budget in the Makran and other vulnerable regions.

the following questions were assessed in this chapter:

1. What is the level of loval knowledge and awareness?

2. Correlation between awareness and other factors.

3. What is the willingness and intention of locals to evacuate?

4. What are the factors that affect the willingness of evacuation among locals and how are they correlated?

5.1 Study area

Using the results of Chapter 3 the most vulnerable areas in the southern coast of Iran, Makran can be recognized. To select the study area for doing survey the population and covering different characteristics of community were taken into account. Generally, the area is under developed and populated and big cities are few. The most populated cities are Chabahar, Konarak and Jask. Remarkably, above 65% of the population living in Makran coast in Iran side are rural population, which compare to the the country's norm with 74% urban population is significant. Therefore, both urban and rural areas were chosen to have a better representative of population. 4 sites were chosen to be investigated: Konarak and Chabahar, two densely populated coastal cities, and Tis and Ramin, two populated rural areas in the region (see Fig. 31). They are all located at Sistan and Baluchestan province.

Fig. 31 Study area along the Makran coast. Sources: Google Earth, Data SIO, NOAA, U.S. Navy, NGA, GEBCO.

5.1.1 Vulnerability of the study area

Tsunami maps near four selected study areas are provided in this section. Different return periods and tsunami wave threshold are shown in Fig. 32 to have a better understanding about the situation both in short and long time. The probability of exceedance from 1 m and 3 m for three return periods, $\Delta T = 100, 500, 1000$, are shown. The probability that tsunami waves exceed 1 m in 100 years is between 28% to 39%. In case of exceeding from 3 m for the same return period the probability is less than 19%. This probability increases with increasing return period, in which $P^{\text{tot}}(\psi > 1, \Delta T = 500) \in [37\%, 73\%]$ and $P^{\text{tot}}(\psi > 3, \Delta T = 500) \in [20\%, 48\%]$. The differences of the probability of exceedance for different areas are significant. It is much less in the PoIs close to Konarak and Chabahar than Tis and Ramin. Finally, in long term with 1000 return period the maximum probability of exceedance from 1 m and 3 m is 83% and 64%, respectively.

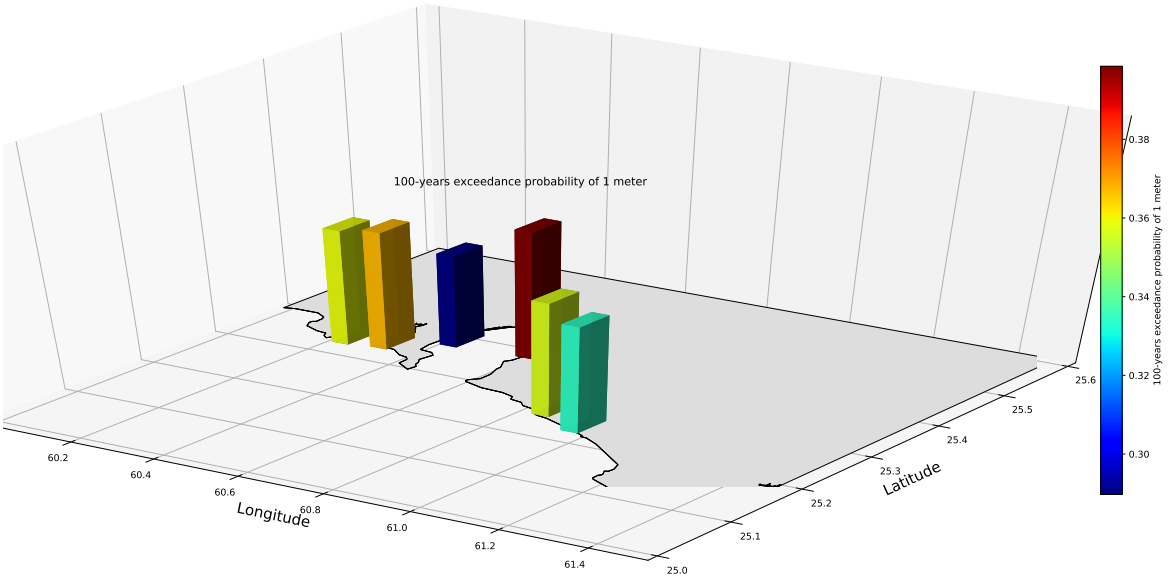

(a) $P^{\text{tot}}(\psi > 1, \Delta T = 100)$

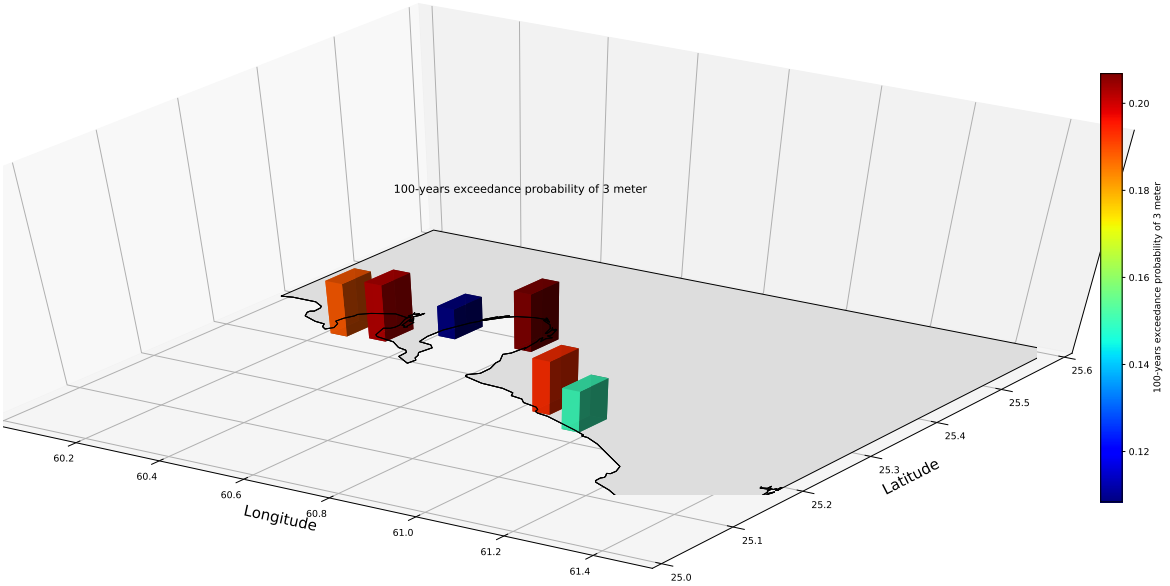

(b) $P^{\text{tot}}(\psi > 3, \Delta T = 100)$

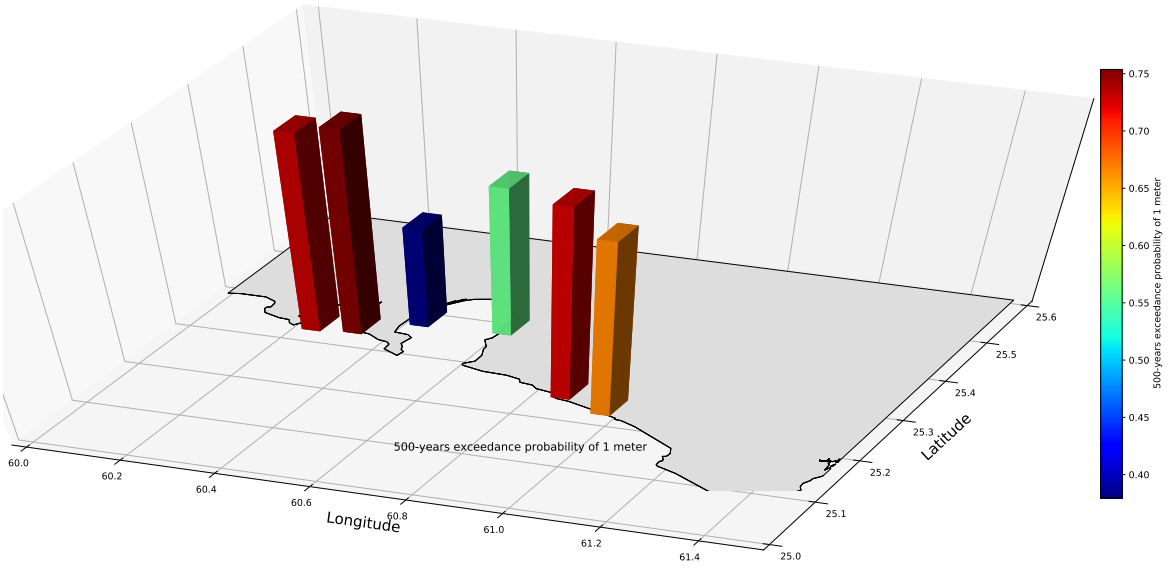

(c) $P^{\text{tot}}(\psi > 1, \Delta T = 500)$

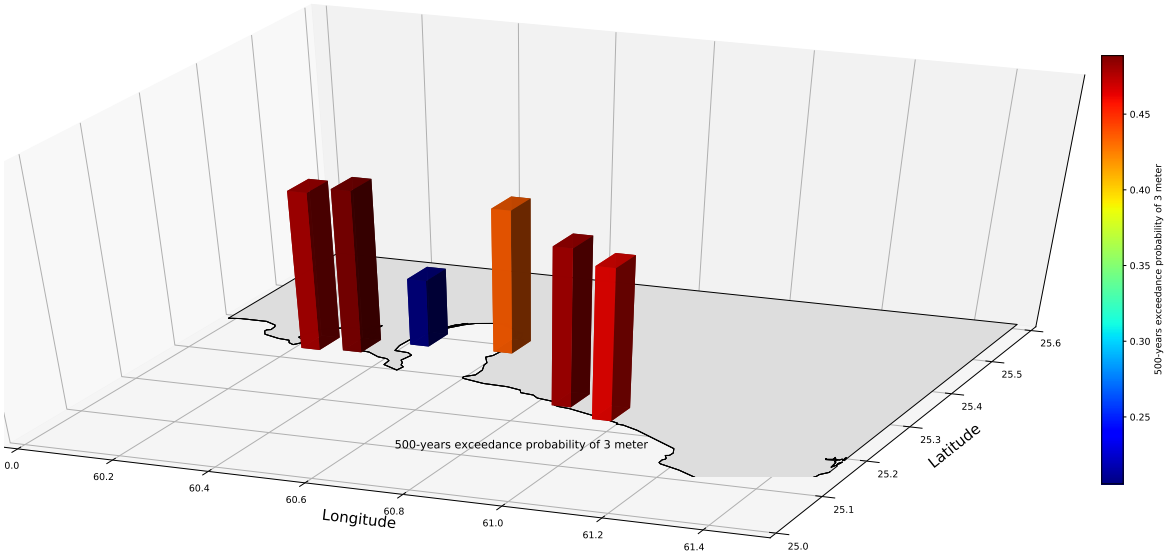

(d) $P^{\text{tot}}(\psi > 3, \Delta T = 500)$

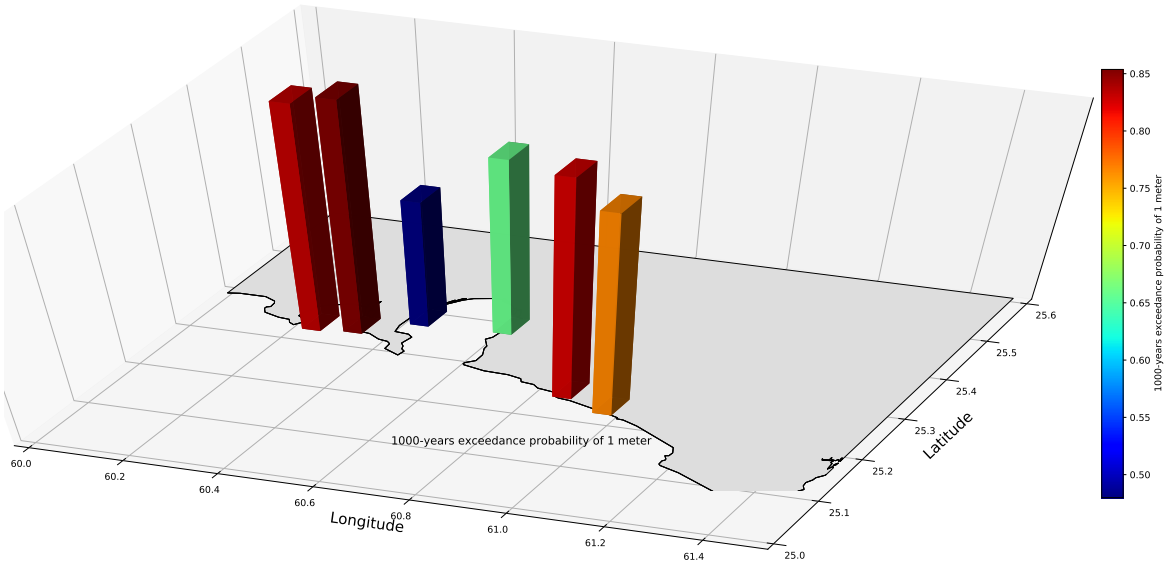

(e) $P^{\text{tot}}(\psi > 1, \Delta T = 1000)$

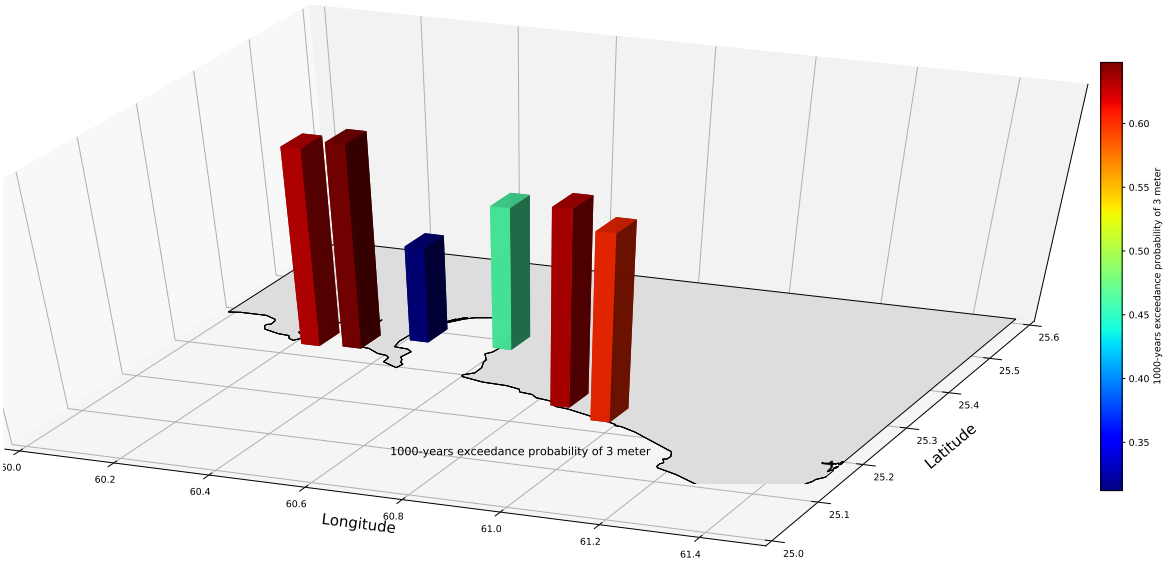

(f) $P^{\text{tot}}(\psi > 3, \Delta T = 1000)$

Fig. 32 The probability of exceedance from: (a) 1 m in 100 year; (b) 3 m in 100 year; (c) 1 m in 500 year; (d) 3 m in 500 year; (e) 1 m in 1000 year; (f) 3 m in 1000 year, for the areas close to Chabahar, Konarak, Tis, and Ramin.

Inundation area is dependent on the resolution of inundation model, high resolution of bathymetry and topography data, coast morphology, vegetation, land use and etc. since the latest researches have indicated that changing the aforementioned parameters have the highest impact on the simulation's accuracy, to predict the inundated area in each study area a comprehensive model is needed to cover all the factors. Otherwise, the results will be neither accurate nor reliable. To show how different the results can be Fig. 33 shows the final results extracted from the existing literature in the area (e.g. (Akbarpour Jannat et al., 2017; Payande et al., 2015; Rastgoftar and Soltanpour, 2016)). It had been shown for $M_w \geq 9.0$ a large inundated area where would affect all the study areas – Chabahar, Konarak, Tis, and Ramin. Although each study used different and limited number of scenarios, all are showing area is vulnerable if the worst case scenario happens.

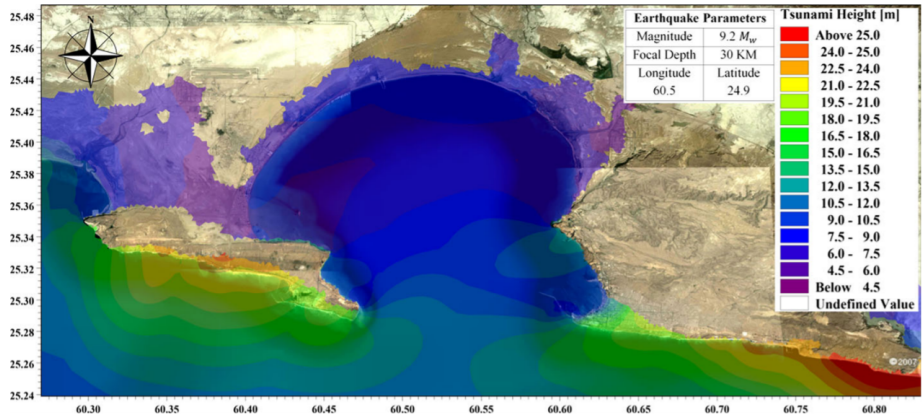

(a) Inundation area for $M_w = 9.2$ (Payande et al., 2015)

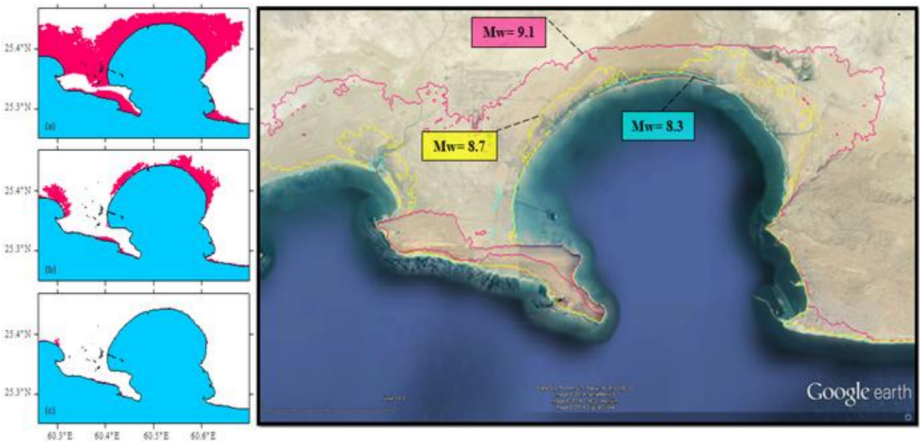

(b) Inundation area for $M_w = 8.7, 8.3, 9.1$ (Akbarpour Jannat et al., 2017)

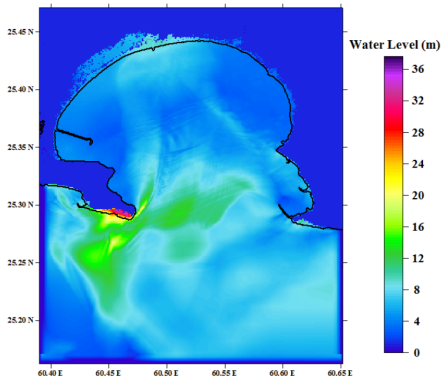

(c) Inundation area for $M_w = 9.0$ (Rastgoftar and Soltanpour, 2016)

Fig. 33 Inundation area resulted from literature for different scenarios in the study areas.

5.1.2 Demographic characteristics of population

The demographic characteristic of population for all the selected study areas are illustrated in this section. These information can be used to be compared with survey sample. The latest

census data were used if available (census, 2016) which had been conducted at 2016 by the government. Fig. 34 shows the population of the study areas with the separation of urban and rural population. Chabahar with 283,204 is the most populated city in Makran coast. The ration of rural population is significant with 68% of the total population. Konarak has 82,001 population. The population of Tis and Ramin are 6,348 and 3,821, respectively. Gender ratio

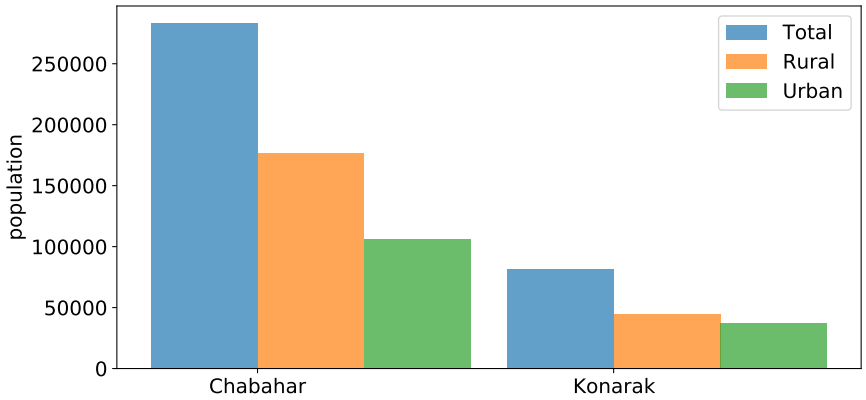

(a)

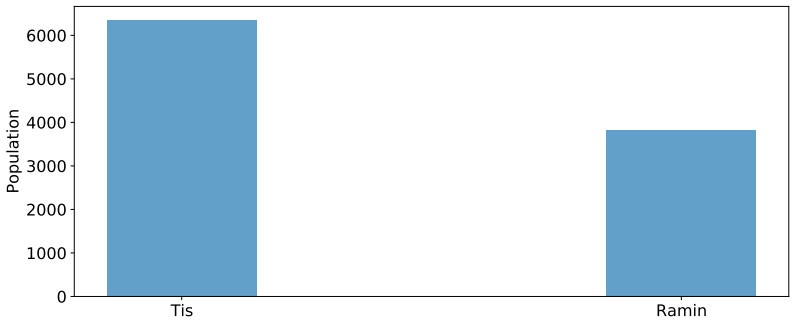

(b)

Fig. 34 (a) population of Chabahar and Konarak in total, rural and urban. (b) total population of two rural area, Tis and Ramin. Data were gathered using the raw sheets of 2016 country wide census.

in the study areas are shown in Table 10. A relative gender balance can be seen in all the areas.

Available census data for age and education distributions were only gathered and provided in county level (Chabahar and Konarak) not village level (Tis and Ramin). Fig. 35 (a) and Fig. 35 (b) show age and education distribution of population, respectively. Age groups were classified as 10-29, 30-49, and more than 50. Education distribution were divided into two groups: "with university education" and "without university education." It can be seen that

Table 10 Population gender ratio in four study areas.

Area	male	female
Chabahar	144482 (51%)	138722 (49%)
Konarak	40933 (49.9%)	41067 (50.1%)
Tis	3238 (51%)	3110 (49%)
Ramin	1982 (51.87%)	1839 (48.13%)

population is young with 67.44% and 67.78% under 30 years old in Konarak and Chabahar, respectively. The data shows more than 90% of population in both areas do not have university education.

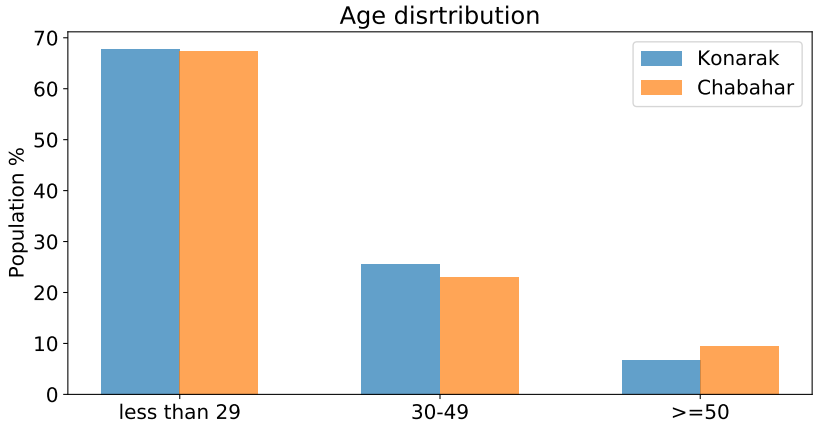

(a)

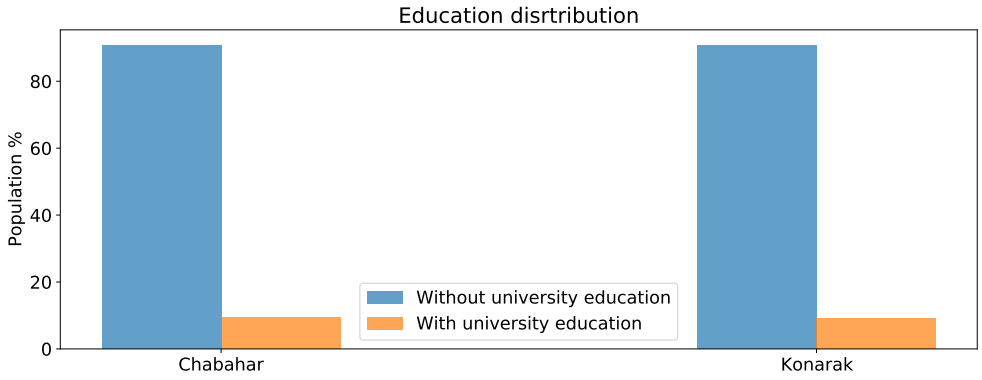

(b)

Fig. 35 (a) Age distribution; (b) education distribution of population in Chabahar and Konarak. Data were gathered using the raw sheets of 2016 country wide census.

5.1.3 Samples and analyze

The survey was conducted by different sampling methods at the 4 study areas in September, 2018. $(n_1 = 153)$ valid questionnaires were collected in Chabahar. In Konarak, GPS random spatial sampling method was used to choose households in the tsunami prone area. Due to the availability of respondents, $(n_2 = 45)$ households were questioned. In Ramin and Tis, face-to-face interview were collected due to the relatively low level of education, and 12 households in each were interviewed. Moreover, 3 focus group discussion (taking < 4 hrs) were held at 3 main fishery ports, Shahid Beheshty,Beris, and Ramin with local fishers and beach users.

5.2 Demographic characteristic of samples

The demographic characteristics of respondents in study areas are shown in Table 11 and Fig. 36. In urban areas, a relatively balanced gender ratio was obtained. The number of men respondents (Chabahar: 55.95%; Konarak: 57.42%) and women (Chabahar: 45.05%; Konarak: 42.22%) was similar. owing to gender prejudice which in rural area it is difficult to access and speak directly with women, there was an imbalance in the responses of the two rural areas (men: 70.83%; women: 29.17%). Respondents in urban areas were predominantly young, with 75% and 73.33% under the age of 40 in Chabahar and Konarak (cf. Fig. 35 (a)), respectively. In contrast, 66.67% of respondents in Ramin and Tis were older than 40. It is typical considering the recent migration of the youth to urban areas in Makran. Fig. 36 (a) is indicative of the typical education distribution according to the latest government census of the study area. In all sites, the majority of samples did not have a university education (Chabahar: 70.24%; Konarak: 93.44%; Ramin and Tis: 100%, cf. Fig. 35 (b)). The socioeconomic status of respondents was quite low, where the most reporting monthly household income was less than $30,000,000$ IRR (Iranian Rials) or 110 USD (Chabahar: 75%; Konarak: 91.25%), and all respondents in Tis and Ramin). Notably, the income distribution seems typical because the average monthly income of this province has been 46% greater than the country's average income of $12,460,000$ IRR for the past ten years.

Table 11 Demographic profile of samples.

		Chabahar (%)	Konarak (%)	Tis & Ramin (%)
Gender	Men	55.95	57.42	70.83
	Women	44.05	42.22	29.17
Age	10-19	20.24	4.44	8.33
	20-29	25	37.78	8.33
	30-39	29.76	31.11	16.67
	40-49	15.48	11.11	25
	50-59	5.95	8.89	25
	≥ 60	3.57	6.67	16.67
Education	No schooling	17.86	35.56	66.67
	Primary	15.48	31.11	25
	High school	36.9	26.67	8.33
	University	25	4.44	0
	Higher	4.76	2.22	0
Income (IRR)	$\leq 12,000,000$	44.05	75.6	83.33
	12,000,001 - 30,000,000	30.95	15.65	16.67
	30,000,001 - 50,000,000	17.86	6.67	0
	$> 50,000,000$	7.14	2.22	0

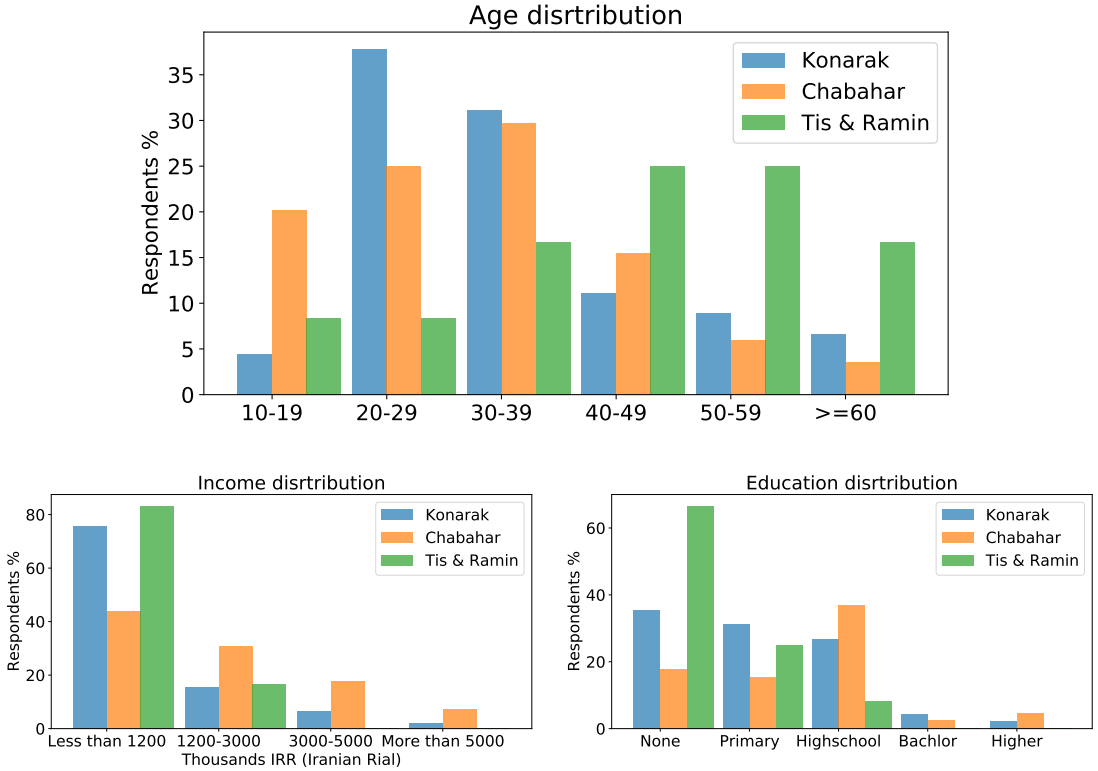

Fig. 36 Demographic profile of samples: age (top), income (bottom left), and education (bottom right).

5.3 Knowledge and awareness

Respondents were asked about their knowledge about the basic definition of a tsunami and their information sources of their knowledge. Results are demonstrated in Fig. 37. In both Chabahar and Konarak, $< 22\%$ of all respondents did not have the basic definition of a tsunami, while most of them had a basic knowledge (Chabahar: 61.9%; Konarak: 64.4%). In contrast, only 34.5% of respondents reported this same level of knowledge in Tis and Ramin. This may be the because of minimal access to information sources such as radio, tv, etc. in rural areas, as notedin the survey observations, and their low education level. Regarding to the information sources, a notable difference among study areas was observed. In Chabahar, 73% of respondents who had basic knowledge about tsunami, had obtained their knowledge from"internet." 43% of respondents in In Konarak indicated "Family/Friends," as their primary source of information. 27% "stated other sources not listed in the questionnaire," and only 16% the "internet." In Ramin and Tis, likely due to their minimum access to information sources, respondents obtained their basic knowledge either from "Family/Friends" or "Other sources not listed in the questionnaire."

5-point Likert scale question was asked to evaluate how respondents considered the degree of danger associated with tsunamis in their living area (from "Strongly disagree" to "Strongly agree"). Fig. 38 shows the results. most respondents with knowledge about tsunamis disagreed or strongly disagreed that tsunamis are a real danger to them (Chabahar: 66.66%; Konarak: 75.56%; Tis and Ramin: 85.72%). This low level of awareness may be attributed to the low experiences of a major coastal hazard, such as a tsunami. Moreover, it could be because of improper education plans where almost all of the respondents said that they had neither heard nor seen information about tsunamis and were not aware of public educations (as reported 97% of respondents).

5.4 Attitudes

There were considerable challenges during the pilot investigation, primarily related to the low number of tsunami events in the area. Therefore, to evaluate the intended evacuation behavior,

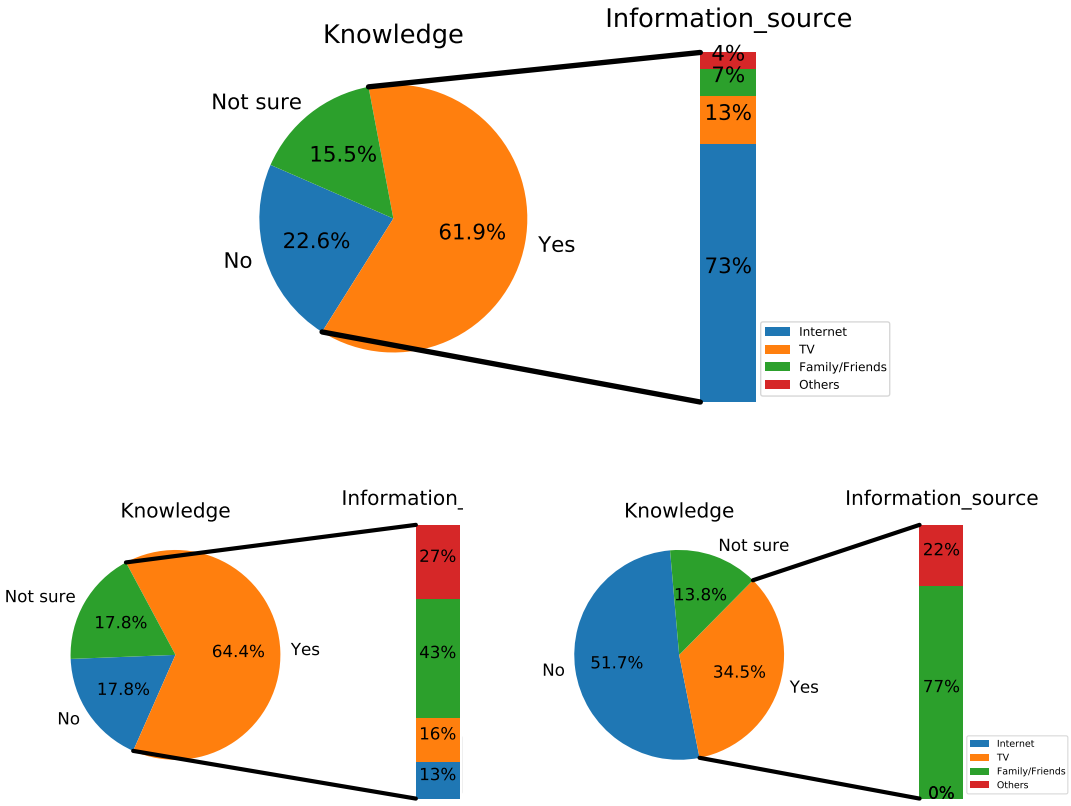

Fig. 37 Basic knowledge regarding tsunami definition and knowledge sources for Chabahar (top), Konarak (bottom left), and Tis and Ramin (bottom right).

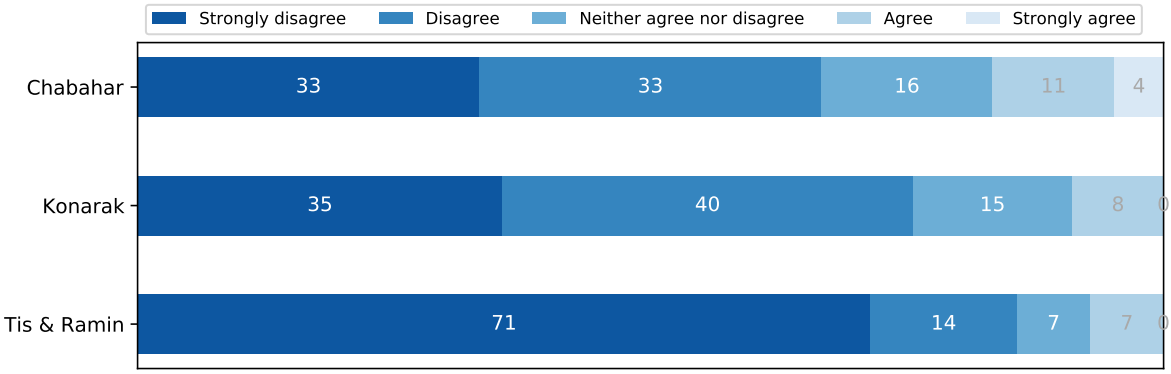

Fig. 38 Tsunami awareness believing it will not happen in their area and believing it is a threaten in their living area.

first respondents were asked whether they had experienced any natural hazards. $>82\%$ had experienced at least one natural hazard in their lifetime (for example flood, earthquake, storm, or tsunami). Then, respondents were asked what was their reactions during the hazards. See Fig. 39. more than half of them with the experience of natural hazards in their lifetime selected "not evacuated–trusting God will help" (Chabahar: 54.7%; Konarak: 65.8%; Tis and Ramin:

81.8%). In both cities, only 25% selected "evacuated immediately", whereas in Ramin and Tis, only 13.6% evacuated immediately. Respondents were then asked "whose actions would prevent loss of life during natural hazards?" $>$ 65% said God would prevent the loss of life. Remarkably, "individuals" and "the government" with less than 14.29% had almost the same ratio (Fig. 40).

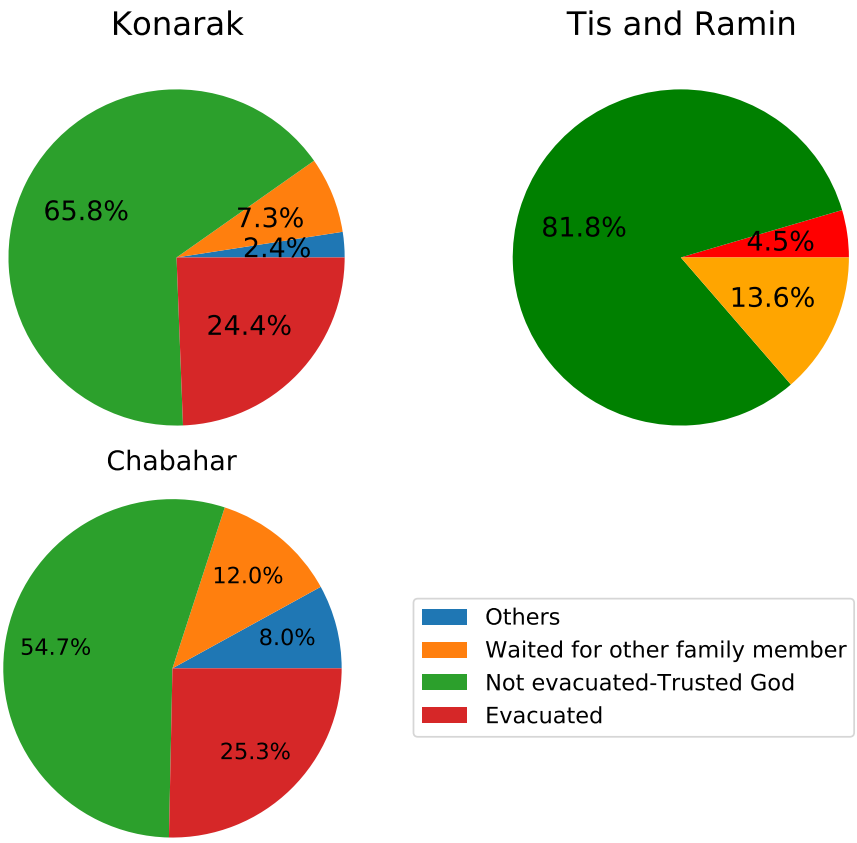

Fig. 39 Reactions of respondent during natural hazards.

another factor which is prominent is trust. It is a crucial in the effectiveness of policy for risk communication (Eiser et al., 2012). Based on experts' comments in Iran (see Chapter 3, section 3.3.2) and literature, trust is a multifaceted factor that can influence people's behavior toward action (Basolo et al., 2009). Therefore, the level of trust in the government in risk managements were assessed. The level of people's trust in the government's ability to manage a disaster in three states: before, after, and in disaster education plans is shown in Fig. 41. Majority of respondents either strongly disagreed or disagreed rather than being agreed/strongly agreed on trusting in the government's ability to manage hazards (Konarak, 74%; Chabahar, 60%; Ramin and Tis, 74%).

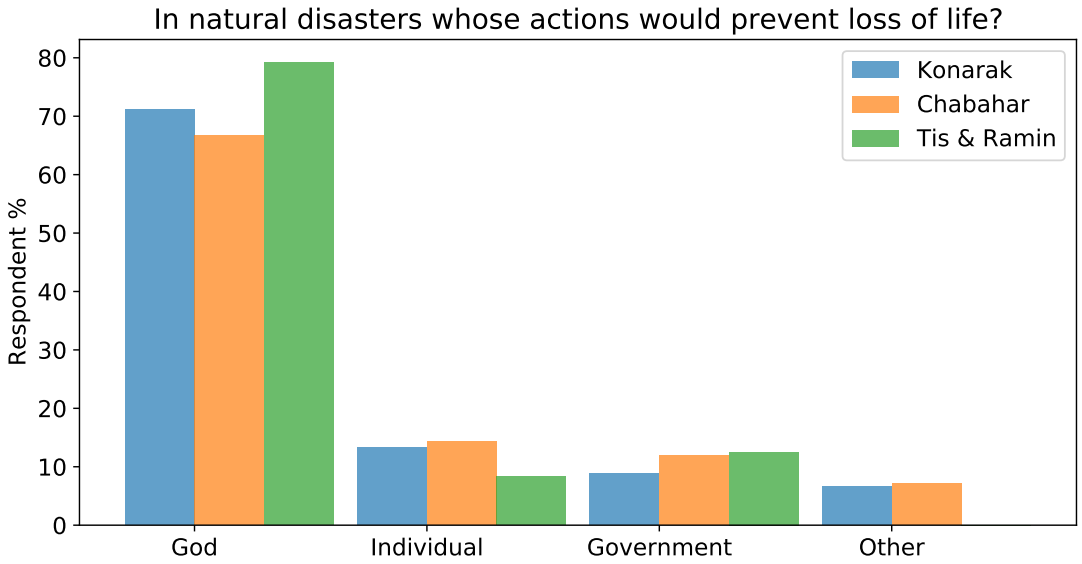

Fig. 40 Whose actions would prevent loss of life in natural hazards

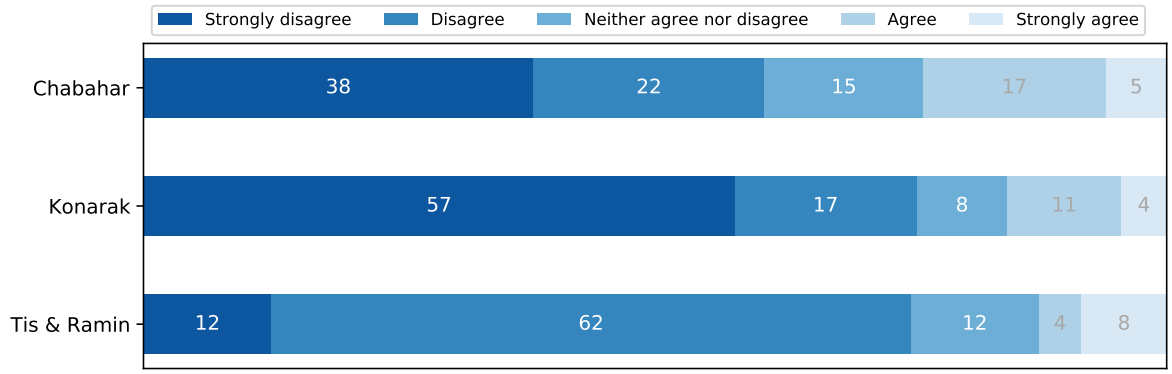

Fig. 41 The level of trust in government's ability to manage a natural hazard in 3 states: before, after, and in disaster education plans.

5.5 Statistical analysis

ANOVA and chi-square test were used to determine the dependency between the variables. The results were considered significant at the level of $p \leq 0.05$. The relationship between demographic factors and respondents' knowledge, awareness, reactions, and trust were assessed. All respondents from 4 areas were combined to meet computing needs. Second, to make comparisons easier and overcome the limited number of respondents in some categories, demographic factors were reclassified into new classification:

- **Age:** 10-29 ("young"), 30-49 ("middle-aged"), and $>$ 50 ("old").
- **Education:** two groups: "with university education" and "without university education."

- **Income:** Because most of respondents were in a poor status, respondents were categorized into 2 groups: household income $> 12,000,000$ IRR and $< 12,000,000$. The threshold was chosen based on the national minimum wage in 2018.

The results of p-value from ANOVA/chi-square tests are shown in Fig. 42. At the 0.05 significance level, 6 statistically significant relations were found. In regards with gender, the differences in knowledge and awareness of men and women were found to be significant ($p = 0.000$ and $p = 0.010$). Knowledge and awareness among men were higher compared with those of women, likely correlated to notable gender discrimination in the region (Sariolghalam, 2014). No significant relations between gender and their reaction during hazards or their trust level in the government were observed. The other statistical relationship was found to be between age and knowledge ($p = 0.007$). younger respondents had more knowledge about tsunami than other age groups. People with higher education levels tended to evacuate immediately in their previous disaster experiences. However, this difference was not significant compared with other relations ($p = 0.049$). respondents with university education had less trust in the government ($p = 0.028$). Finally, there was a significant association between respondents' income and their reaction to hazards ($p = 0.039$).

To understand whether differences in awareness could result in respondents' reactions further tests were conducted. The same test was applied for reaction and trust; and no significant relationships were found.

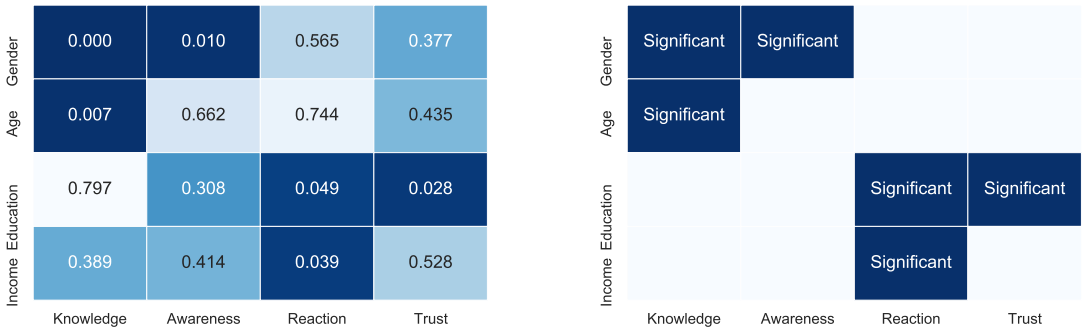

Fig. 42 p-values between variables and demographic characteristics (left).

5.6 Focus group discussion

3 focus group discussions were held with fishers and beach users to support the results from questionnaire survey. The interviewees were asked about their experiences in natural hazards. After the transcribed discussions were coded, “God” and “trust” were found to be among the most repeated terms. Some quotes from interviewees who had experienced cyclone Gonu in 2007 are presented below:

> We did not evacuate because we thought God will save us. (age 45, Ramin)
>
> The local government asked us to get on the buses and leave the area; my mom did not let us to do so, believing God will take care if we are innocent. (age 26, Ramin)
>
> My dad told us we have to stay and suffer to be forgiven because of our sins. (age 18, Ramin)
>
> We do not trust Shilat, governmental place in charge of coastal hazards in Makran. They asked people to get on the buses provided by them, but we did not. Shilat does not know where to take people. (age 42, Ramin)

The interviewees largely either trusted God to save them or believed the event to be some form of punishment or test. Moreover, distrusting the government was also among the main reasons respondents did not evacuate. These FGD findings were aligned with those of the questionnaire survey.

5.7 Summary

In this chapter, the uncertainty factors associated with soft measures in four areas along the Makran coast namely, Chabahar, Konarak, Tis, and Ramin were evaluated. First, the results of probability of exceedance for all these areas (which had been derived from Chapter 3) were investigated to have a better understanding on vulnerability of each areas. It has been observed that all the areas are extremely vulnerable areas and may experience waves higher than 3 m. The probability of having tsunami waves exceeding 3 m over a 100 year is 19% with a higher

chance for long term periods with maximum probability of 48% and 64% for period of 500 and 1000 year, respectively. However, based on the results from this work and literature in the area the first priority in the region should be given to the development of inundation maps and development of a regional tsunami warning system.

Then, local's knowledge, awareness, and attitudes toward tsunamis in the aforementioned areas were evaluated by conducting a field survey. All these factors were identified and classified in Chapter 2 that are playing an important role in risk and vulnerability assessment. The results indicated a low level of awareness and willingness to evacuate among residents and a low level of trust in the government in regard to risk management. Moreover, the results showed a significant religious attribution affecting respondents' risk perception and evacuation behavior, that along with the aforementioned factors increase residents' vulnerability.

6 DISCUSSION

The MSZ is one of the two sources of tsunamis in the Indian Ocean, and has the potential of generating large tsunamis that threaten neighboring countries of Iran, Oman, and Pakistan. However, a fortune lack of large tsunamis recently has led to a false sense of safety between community leaders and residents, which may negatively affect the area's vulnerability and resilience against future tsunamis. In this work, first a systematic literature review had been conducted to identify uncertainties and failure reasons of tsunami risk management around the world. Failure reasons were associated with both hard and soft measures. The indicators were then evaluated and assessed for the MSZ. In this chapter a summary of main findings are presented and discussed. Finally, a number of recommendations to improve risk management is proposed.

6.1 Uncertainties in hard measures

The potential seismogenic zone, maximum magnitude, and recurrence models were assessed at the MSZ using available seismic, geodetic, and historical catalogue data. Moreover, both aleatory and epistemic uncertainties were considered to obtain more accurate and reliable results. The findings are highlighted as follows.

1. The spread of hazard curves for different locations along the Makran coast is remarkably large. The probability that the tsunami height exceeds 3 m for return periods $\Delta T = \{50,\ 100, 250, 500, 1000\}$ ranges from 0 to $\{16, 30, 58, 80, 95\}$ percent, respectively, for different PoIs.

2. The probability of exceedance at PoIs near populated cities decreases and becomes insignificant for the exceedance threshold of 4 m (even for a long return period), except for Jask at the western coast of Iran. The results provide evidence that if consider the western part of the MSZ equally active and potential to the eastern part –similar to this paper, by weighting both parts the same in the developed event tree–the exceedance probability could be higher at the western part for a long return period. This can be

clearly seen from the probability maps where the exceedance probability of 3 m fluctuates and becomes maximum at the western part of the MSZ.

3. The inclusion of the aleatory variability has a significant effect on the probability of exceedance, and not including it mostly leads to a remarkable underestimation in the PTHA with a median of 10% difference for all PoIs. This difference is underscored by increasing the return periods and reaches 40% at somewhere for 1000-year return period in the presence and absence of the aleatory variability.

Owing to Makran's economical, geographical, and strategic importance, Iran approved a plan for developing the Makran Coast on December, 2016 titled "Makran Sustainable Development." This plan, along with the drought occurring recently in the neighboring cities, has led to an inevitable migration toward the coastlines, with Chabahar exhibiting 10% population rate growth last year and ranking among the highest population growth rates globally in 2019. Hence, the results are of vital for various stakeholders for developing and implementing tsunami risk mitigation activities and guiding risk-aware city planning.

6.2 Uncertainties in soft measures

The central findings of Chapter 5 are presented and compared with those found in literature. Moreover, based on the empirical data, a hypothesis framework for decreasing the vulnerability in the region was constructed.

6.2.1 Knowledge and awareness

The survey results revealed that the majority of people had a basic knowledge of tsunamis in Chabahar and Konarak. In contrast, around one-third of respondents maintained this level in Tis and Ramin. Following our expectations, awareness was rather low among respondents with basic knowledge of tsunamis. Some studies have focused on specific factors In Indonesia, Chile, and Japan that could influence awareness, such as experience (Mulilis et al., 2003; Norris et al., 1999; Weinstein, 1989), information sources, policies (Esteban et al., 2013a),different capitals (e.g. social and cultural (Bastaminia et al., 2017, 2018; Mavhura, 2017)), poverty

(Fothergill and Peek, 2004; Mavhura, 2017), and demographic indicators (Bodas et al., 2017; Mohammad-pajooh et al., 2014; Sjöberg, 2000). In the studied region, low awareness may stem from respondents' minimal experience with coastal hazards over the last 75 years in the area. Low awareness also may come from lack of data and tools such as evacuation maps and warning systems, and their improper distribution among locals. Almost all respondents ($> 97\%$) had neither received nor heard/seen any information about tsunami and were not aware of any public education program in their community.

Moreover, there are studies that considered the effect of demographic characteristics on hazard awareness. e.g., gender (Juran, 2012), education (Muttarak and Pothisiri, 2013), and age (Ngo, 2001). The relationship between respondents' demographic profiles and their awareness levels were investigated. There was a significant difference between different gender and their knowledge and awareness. Many studies have been confirmed the inequalities between genders and their awareness; however, the difference between men and women remains a controversial issue. Some researchers indicated that risks tend to be judged as lower by men than by women (Finucane et al., 2000), while others have rejected this hypothesis (Hines, 2007; Juran, 2012; Mohammad-pajooh et al., 2014). In societies with strong patriarchal values, such as those of middle eastern countries, women's influence in society and decision making is typically diminished, and this gender gap could intensify the disparity in knowledge and awareness, as indicated by the findings here.

6.2.2 Attitude

In previous studies, the prominent role of risk perception in evacuation behavior has been highlighted. How people perceive risks is shaped by their experience, feelings, values, and beliefs. In addition to a lack of awareness and experience, this study provided information on how other variables can affect people's attitudes regarding natural hazards, specifically religion and trust in the government.

Trust In the literature, trust influences people's risk perception and their acceptance of preventive actions. It has unique effects in each area and community examined. Even though absolute trust in civil protection may lead to neglecting self-protection, trust in the government

and information sources may improve disaster risk communication. Trust influences people's risk perception and their acceptance of preventive actions (Samaddar et al., 2012). In a review by (Wachinger et al., 2013) it is suggested that trust in authorities and experts have the most impact on risk perception. Some studies have shown that a high level of trust in government to manage a disaster and provide information sources is correlated with a higher level of perceived preparedness (Basolo et al., 2009), whereas in Japan, the high level of trust led to neglecting self-protection strategies. In the results of this thesis, respondents' trust in authorities regarding risk management in risk education, evacuation warning, and post-disaster management was evaluated. Results show that more than two third of respondents (strongly) disagreed with trusting the government to manage hazards. This lack of trust in the government may lead to greater vulnerability in the study area. For example, cyclone Sidr caused hundred of casualties along the Bangladeshi coasts because people did not trust the cyclone early warnings circulated by the local government and mass media (Paul, 2012). Based on the FGDs conducted in this study, the same attitude was reported by interviewees for not evacuating in 2007 during cyclone Gonu.

Religion In both the questionnaire and FGDs, the role of religion in respondents' attitudes toward hazards was highlighted. Most of respondents with experiencing natural hazards in their life, either trusted God to save them or thought it was a God's punishment. Moreover, >two-third of respondents believed if a natural hazard occurs, God will prevent loss of life. The absolute faith in destiny, together with one's lack of belief in his or her own free will and determination, are strong personal characteristics associated with those living in the Middle East and Muslim countries (Sariolghalam, 2014); however, there are similar findings in other parts of the world and other religions. For example, Sun *et al.* (Sun et al., 2019) found that in 2010, the religious attribution of earthquakes in Tibet had a negative impact on people's awareness and behavioral responses. Moreover, most of residentsin Trinidad and Tobago (57% of interviewees) had a perception that "God is a Trini", and believed that if a tsunami were to occur, God was most likely to prevent the loss of life (La Daana et al., 2016). In their study, it was argued that the religious attribution of natural hazards might come from a low

awareness and limited experience with tsunamis. However, several studies revealed that even in communities where individuals are familiar with scientific explanations of natural hazards, people still perceived it as "God's will or punishment," (e.g., Nepal (Sherry and Curtis, 2017; Welton-Mitchell et al., 2016), Ghana (Bempah and Øyhus, 2017) and Japan (McLaughlin, 2011).) Extra efforts have been made to extract information from the literature regarding the survivors' experiences following the 1945 Makran tsunami. This included a booklet of interviews from 2008 to 2015 under United Nations projects (Kakar et al., 2015). Several examples showed the strong religious attribution of the tsunami among interviewees (some are presented in Table 12). Similar findings were reported after a mosque and shrine survived the 2004 Indonesia and 2011 Japan tsunamis, respectively, where people had asserted that God(s) were protecting his house.

Table 12 Extracted quotes of survivors of 1945 Makran tsunami from literature.

Gender, age at 1945 (years old)	Indicative quotes
Male, 20	Only a mosque survived, and the rest of the town was destroyed.
Male, 20	We could not protect ourselves, but many of us prayed at the mosque that Allah may save us from any destruction.
Female, 20	The roof of the shrine fell because of the earthquake. The sea did not go further than the mosque; Allah (God) stopped it.
Male, 12	Before the sea went far onshore, I went to the mosque for dawn prayer; the first wave happened, but it was small, so we began the prayer.
Male, 13	This area was not flooded because of a shrine that would not allow the sea to enter.
Male, –	The story of the daughter of a just judge, she was either kidnapped or killed in Qalhaat, and thus causing the wrath of God upon the town.

Salient value similarity (SVS) The over-reliance on destiny and subsequent neglect of one's ability to control their own situation can lead to insufficient planning and dismissal of the role of risk management against natural hazards. Becoming blindly accustomed to any circumstance, together with "actions" that come with inaction, make change and acceptance of new thoughts and methods difficult . This situation is intensified when the level of trust in the government regarding risk management is rather low. Hence, It is suggested that leaders and disaster

management practitioners obtain help from religious leaders to improve risk awareness and perception among low-trust populations. In previous studies, the importance of local leaders, both religious and non-religious, in disaster risk reduction has been reported Said *et al.* (Said et al., 2011) found that a better tsunami mitigation strategy should involve local community leaders as the primary focus of attention. Furthermore, local religious leaders can transfer important information about disaster preparedness to people through religious studies as they possess the ability to accept and interpret the information into such terms (Sherry and Curtis, 2017). Several studies have demonstrated that people tend to trust those who share similar values. Evidence supporting the theory known as salient value sharing (SVS) (Siegrist et al., 2000) indicates that policies based on salient cultural values are more widely accepted (Cvetkovich, 2013). Based on the findings, a hypothesize framework to improve risk perception among residents were introduced (see Fig. 43). Religion and risk are interconnected, which can have both positive and negative influences on risk assessment and mitigation (Sherry and Curtis, 2017). the hypothesis framework suggests that the negative aspects can be turned into positive factors in risk management by seeking help from religious leaders. However, since the survey questions were not designed originally to reflect the construct of SVS and the final hypothesis model, validating them were beyond the scope of this study and shall be addressed in future work.

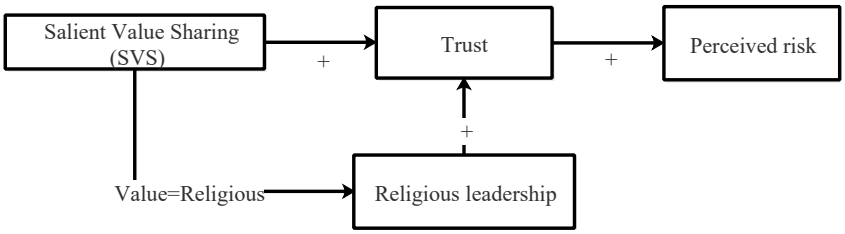

Fig. 43 Hypothesis based SVS framework for improving risk perception in Makran.

6.3 Limitations and future direction

This study is the first step toward comprehensive and reliable mitigation plans and activities; however, it is important to acknowledge its limitations. Tsunami sources beyond earthquakes

were not considered in this study. Notably, the only tsunami induced with combination of earthquake and landslide in word history occurred in Makran in 1945. Moreover, in September 2013, a landslide was recorded immediately following an earthquake in the MSZ (Heidarzadeh and Satake, 2014). This highlights the need to consider landslides (Rastgoftar and Soltanpour, 2016) and their combination with earthquakes in future PTHA studies. Moreover, the dynamic interaction between tides and tsunami waves was disregarded. This works for a tsunami wave with one isolated peak; however, it may lead to hazard underestimation when the tsunami has several peaks with significant heights. Finally, providing an accurate inundation map is paramount. an extensive data collection could be a better representative of the outcomes since the sample size of the study was quite small. Also, different sampling strategies were applied to each study area, which may limit the generalizability. Moreover, validating SVS model shall be addressed in the future work.

7 CONCLUSION

This study provides crucial information for developing comprehensive and reliable mitigation plans and activities addressing uncertainties in tsunami risk management for the southern coast of Iran, Makran. The Makran subduction zone is a hazardous tsunami-prone region; however, due to its low population density, it is not as prominent in literature. The results from the systematic literature review in Chapter 2 revealed that uncertainty indicators and failure roots are scattered in different fields and an multidisciplinary approach have been applied to evaluate and cover various aspects of it.

In Chapter 4 a methodology to cover the limitation of historical data and incorporating uncertainties (epistemic and aleatory) was applied using the combination of probabilistic approach, historical assessments, and numerical model –introduced in Chapter 3. The threat of tsunami hazard posed to the coast of Iran by the MSZ was assessed and a comprehensive PTHA for the entire coast regardless of population density was presented. Sources of epistemic uncertainties were accounted by employing event tree and ensemble modeling. Aleatory variability was also considered through probability density function. Further, the contribution of small to large magnitudes were considered and to create a multitude of scenarios as initial conditions. `Funwave-TVD` was employed to propagate these scenarios. The results demonstrate that the spread of hazard curves for different locations on the coast is remarkably large, and the probability that a maximum wave will exceed 3 m somewhere along the coast reaches $\{16, 30, 58, 80, 95\}\%$ for return periods $\{50, 100, 250, 500, 1000\}$, respectively. Moreover, the exceedance probability could be higher at the west part of Makran for a long return period, if consider it as active as the east part of the MSZ. Finally, the inclusion of aleatory uncertainty that was overlooked by the previous related studies demonstrated that the contribution of aleatory variability is significant, and overlooking it leads to a significant hazard underestimation, particularly for a long return period.

The results provides a reliable estimation of the associated hazard for designing a local early warning systems, site selection for critical infrastructures and prioritising necessary mitigation measures for existing infrastructures and critical regions.

Empirical data can also help to identify factors that decreases uncertainty in tsunami mitigation plans and evacuation process. Results of Chapter 5 provide as great help for a more evidence-based prediction, more informed, and cost-effective recommendations. The results presented in Chapter 5 indicate a low level of awareness and willingness to evacuate among residents and a low level of trust in the government in regard to risk management. Moreover, the results show a significant religious attribution affecting respondents' risk perception and evacuation behavior, that along with the aforementioned factors increase residents' vulnerability. Based on the findings, some recommendation were made to help policy-makers understand how to shape mitigation and evacuation plans such that they will become more evidence-based, sensitive, informed, and cost-effective.

Moreover, owing to the notable findings regarding the roles of religion, trust, and risk perception, new lines of research and discussion on this topic have been proposed. This exhibits a potential range of applicability that extends well beyond this region; however, further investigations in both Makran and other regions are still necessary. Risk reduction measures for one hazard should be compatible with those for other hazards. Therefore, the perspective presented in this study could be beneficial for developing disaster measures for other natural hazards.

References

Adams LM, LeVeque RJ, González FI (2015) The pattern method for incorporating tidal uncertainty into probabilistic tsunami hazard assessment (ptha). Natural Hazards 76(1):19–39

Aida I (1978) Reliability of a tsunami source model derived from fault parameters. Journal of Physics of the Earth 26(1):57–73

Akbari P, Sadrinasab M, Chegini V, Siadat Mousavi S (2017) Study of tidal components amplitude distribution in the persian gulf, gulf of oman and arabian sea using numerical simulation. Journal of Marine Science and Technology 16(3):27–41

Akbarpour Jannat MR, Rastgoftar E, Asano T (2017) Tsunami assessment for inundation risk management at chabahar bay facilities in iran. International Journal of Coastal and Offshore Engineering 1(2):27–39

Al-Lazki AI, Al-Damegh KS, El-Hadidy SY, Ghods A, Tatar M (2014) Pn-velocity structure beneath arabia–eurasia zagros collision and makran subduction zones. Geological Society, London, Special Publications 392(1):45–60

Aldama-Bustos G, Bommer J, Fenton C, Stafford P (2009) Probabilistic seismic hazard analysis for rock sites in the cities of abu dhabi, dubai and ra's al khaymah, united arab emirates. Georisk 3(1):1–29

Allen TI, Hayes GP (2017) Alternative rupture-scaling relationships for subduction interface and other offshore environments. Bulletin of the Seismological Society of America 107(3):1240–1253

Allen TI, Wald DJ, Worden CB (2012) Intensity attenuation for active crustal regions. Journal of seismology 16(3):409–433

Ambraseys N, Melville C (1982) A history of persian earthquakes cambridge univ. Press, New York

ANH LT, TAKAGI H, THAO ND, ESTEBAN M (2017) Investigation of awareness of typhoon and storm surge in the mekong delta–recollection of 1997 typhoon linda. Journal of Japan Society of Civil Engineers B3 (Ocean Engineering) 73(2):I_168–I_173

Annaka T, Satake K, Sakakiyama T, Yanagisawa K, Shuto N (2007) Logic-tree approach for probabilistic tsunami hazard analysis and its applications to the japanese coasts. In: Tsunami and its hazards in the Indian and Pacific Oceans, Springer, pp 577–592

Anosov D (2001) Ergodic Theory. In: M. Hazewinkel (Editor). Springer Science+Business Media B.V. / Kluwer Academic Publishers

Argote L (1982) Input uncertainty and organizational coordination in hospital emergency units. Administrative science quarterly pp 420–434

Bakhsh TST (2014) Improvements and Applications of State of the Art Numerical Models for Simulating Tsunami Hazard. University of Rhode Island

Basolo V, Steinberg LJ, Burby RJ, Levine J, Cruz AM, Huang C (2009) The effects of confidence in government and information on perceived and actual preparedness for disasters. Environment and behavior 41(3):338–364

Bastaminia A, Rezaei MR, Dastoorpoor M (2017) Identification and evaluation of the components and factors affecting social and economic resilience in city of rudbar, iran. International journal of disaster risk reduction 22:269–280

Bastaminia A, Safaeepour M, Tazesh Y, Rezaei MR, Saraei MH, Dastoorpoor M (2018) Assessing the capabilities of resilience against earthquake in the city of yasuj, iran. Environmental Hazards 17(4):310–330

Bayraktar HB, Ozer Sozdinler C (2020) Probabilistic tsunami hazard analysis for tuzla test site using monte carlo simulations. Natural Hazards and Earth System Sciences 20(6):1741–1764, DOI 10.5194/nhess-20-1741-2020, URL https://www.nat-hazards-earth-syst-sci.net/20/1741/2020/

Bempah SA, Øyhus AO (2017) The role of social perception in disaster risk reduction: beliefs, perception, and attitudes regarding flood disasters in communities along the volta river, ghana. International journal of disaster risk reduction 23:104–108

Berryman K, Wallace L, Hayes G, Bird P, Wang K, Basili R, Lay T, Pagani M, Stein R, Sagiya T, et al. (2015) The gem faulted earth subduction interface characterisation project, version 2.0, april 2015. Global Earthquake Model

Bird P, Kagan YY (2004) Plate-tectonic analysis of shallow seismicity: Apparent boundary width, beta, corner magnitude, coupled lithosphere thickness, and coupling in seven tectonic settings. Bulletin of the Seismological Society of America 94(6):2380–2399

Blaser L, Krüger F, Ohrnberger M, Scherbaum F (2010) Scaling relations of earthquake source parameter estimates with special focus on subduction environment. Bulletin of the Seismological Society of America 100(6):2914–2926

Bodas M, Siman-Tov M, Kreitler S, Peleg K (2017) Psychological correlates of civilian preparedness for conflicts. Disaster medicine and public health preparedness 11(4):451–459

Bommer JJ, Abrahamson NA (2006) Why do modern probabilistic seismic-hazard analyses often lead to increased hazard estimates? Bulletin of the Seismological Society of America 96(6):1967–1977

Burbidge D, Cummins PR, Mleczko R, Thio HK (2008) A probabilistic tsunami hazard assessment for western australia. In: Tsunami Science Four Years after the 2004 Indian Ocean Tsunami, Springer, pp 2059–2088

Butler R, Walsh D, Richards K (2017) Extreme tsunami inundation in hawai 'i from aleutian–alaska subduction zone earthquakes. Natural Hazards 85(3):1591–1619

census (2016) statistical center of iran. https://www.amar.org.ir, accessed: 2020-10-26

Chen Q, Dalrymple RA, Kirby JT, Kennedy AB, Haller MC (1999) Boussinesq modeling of a rip current system. Journal of Geophysical Research: Oceans 104(C9):20617–20637

Chen Q, Kirby JT, Dalrymple RA, Kennedy AB, Chawla A (2000) Boussinesq modeling of wave transformation, breaking, and runup. ii: 2d. Journal of Waterway, Port, Coastal, and Ocean Engineering 126(1):48–56

Comfort LK (2007) Crisis management in hindsight: Cognition, communication, coordination, and control. Public Administration Review 67:189–197

Cornell C (1968) Engineering seismic risk analysis, bulletin of the seismological society of america. ssss 27(2)

Crichton D (1999) Natural disaster management. The Risk triangle Tudor Rose, Leicester

Cubelos C, Kularathna A, Valenzuela B, Paolo V, Iliopoulos N, Quiroz M, Yavar R, Henriquez P, Bacigalupe G, Onuki M, et al. (2019) Understanding community-level flooding awareness in remote coastal towns in northern chile through community mapping. Geosciences 9(7):279

Cvetkovich G (2013) Social trust and the management of risk. Routledge

Dash N, Gladwin H (2007) Evacuation decision making and behavioral responses: Individual and household. Natural Hazards Review 8(3):69–77

Davies G (2019) Tsunami variability from uncalibrated stochastic earthquake models: tests against deep ocean observations 2006–2016. Geophysical Journal International 218(3):1939–1960

Davies G, Griffin J (2019) Sensitivity of probabilistic tsunami hazard assessment to far-field earthquake slip complexity and rigidity depth-dependence: Case study of australia. Pure and Applied Geophysics pp 1–28

Davies G, Horspool N, Miller V (2015) Tsunami inundation from heterogeneous earthquake slip distributions: Evaluation of synthetic source models. Journal of Geophysical Research: Solid Earth 120(9):6431–6451

Davies G, Griffin J, Løvholt F, Glimsdal S, Harbitz C, Thio HK, Lorito S, Basili R, Selva J, Geist E, et al. (2018) A global probabilistic tsunami hazard assessment from earthquake sources. Geological Society, London, Special Publications 456(1):219–244

Day SJ, Watts P, Grilli ST, Kirby JT (2005) Mechanical models of the 1975 kalapana, hawaii earthquake and tsunami. Marine Geology 215(1-2):59–92

Deif A, El-Hussain I (2012) Seismic moment rate and earthquake mean recurrence interval in the major tectonic boundaries around oman. Journal of Geophysics and Engineering 9(6):773–783

Department] PPM (2007) Seismic hazard analysis and zonation for pakistan, azad jammu and kashmir

Dominey-Howes D, Cummins P, Burbidge D (2007) Historic records of teletsunami in the indian ocean and insights from numerical modelling. Natural Hazards 42(1):1–17

Downes GL, Stirling MW (2001) Groundwork for development of a probabilistic tsunami hazard model for new zealand. In: International Tsunami Symposium 2001, Pacific Marine Environmental Lab. Seattle, Wash., pp 293–301

Eiser JR, Bostrom A, Burton I, Johnston DM, McClure J, Paton D, Van Der Pligt J, White MP (2012) Risk interpretation and action: A conceptual framework for responses to natural hazards. International Journal of Disaster Risk Reduction 1:5–16

El-Hussain I, Omira R, Deif A, Al-Habsi Z, Al-Rawas G, Mohamad A, Al-Jabri K, Baptista MA (2016) Probabilistic tsunami hazard assessment along oman coast from submarine earthquakes in the makran subduction zone. Arabian Journal of Geosciences 9(15):668

Esteban M, Tsimopoulou V, Mikami T, Yun N, Suppasri A, Shibayama T (2013a) Recent tsunamis events and preparedness: Development of tsunami awareness in indonesia, chile and japan. International Journal of Disaster Risk Reduction 5:84–97

Esteban M, Tsimopoulou V, Mikami T, Yun N, Suppasri A, Shibayama T (2013b) Recent tsunamis events and preparedness: Development of tsunami awareness in indonesia, chile and japan. International Journal of Disaster Risk Reduction 5:84–97

Esteban M, Thao ND, Takagi H, Valenzuela P, Tam T, Trang D, Anh L (2014) Storm surge and tsunami awareness and preparedness in central vietnam. In: Coastal Disasters and Climate Change in Vietnam, Elsevier, pp 321–336

Esteban M, Onuki M, Ikeda I, Akiyama T (2015a) Reconstruction following the 2011 tohoku earthquake tsunami: Case study of otsuchi town in iwate prefecture, japan. In: Handbook of coastal disaster mitigation for engineers and planners, Elsevier, pp 615–631

Esteban M, Takagi H, Shibayama T (2015b) Handbook of coastal disaster mitigation for engineers and planners. Butterworth-Heinemann

Esteban M, Valenzuela VP, Yun NY, Mikami T, Shibayama T, Matsumaru R, Takagi H, Thao ND, De Leon M, Oyama T, et al. (2015c) Typhoon haiyan 2013 evacuation preparations and awareness. J-SustaiN Journal 3:37–45

Esteban M, Valenzuela VP, Matsumaru R, Mikami T, Shibayama T, Takagi H, Thao ND, De Leon M (2016) Storm surge awareness in the philippines prior to typhoon haiyan: a comparative analysis with tsunami awareness in recent times. Coastal Engineering Journal 58(01):1640009

Esteban M, Bricker J, Arce RSC, Takagi H, Yun N, Chaiyapa W, Sjoegren A, Shibayama T (2018) Tsunami awareness: a comparative assessment between japan and the usa. Natural Hazards 93(3):1507–1528

Esteban M, Yamamoto L, Jamero L, Mino T (2020) Time-scale in framing disaster risk reduction in sustainability. In: Framing in Sustainability Science, Springer, Singapore, pp 133–151

Faulkner B (2001) Towards a framework for tourism disaster management. Tourism management 22(2):135–147

Finucane ML, Slovic P, Mertz CK, Flynn J, Satterfield TA (2000) Gender, race, and perceived risk: The'white male'effect. Health, risk & society 2(2):159–172

Fothergill A, Peek LA (2004) Poverty and disasters in the united states: A review of recent sociological findings. Natural hazards 32(1):89–110

Fraser S, Leonard G, Johnston DM (2013) Intended evacuation behaviour in a local earthquake and tsunami at Napier, New Zealand. GNS Science

Fujii Y, Satake K, Sakai S, Shinohara M, Kanazawa T (2011a) Tsunami source of the 2011 off the pacific coast of tohoku earthquake. Earth, planets and space 63(7):55

Fujii Y, Satake K, Sakai S, Shinohara M, Kanazawa T (2011b) Tsunami source of the 2011 off the pacific coast of tohoku earthquake. Earth, planets and space 63(7):55

Geist EL, Lynett PJ (2014) Source processes for the probabilistic assessment of tsunami hazards. Oceanography 27(2):86–93

Glimsdal S, Pedersen GK, Harbitz CB, Løvholt F (2013) Dispersion of tsunamis: does it really matter? Natural hazards and earth system sciences 13(6):1507–1526

Goda K, Mai PM, Yasuda T, Mori N (2014) Sensitivity of tsunami wave profiles and inundation simulations to earthquake slip and fault geometry for the 2011 tohoku earthquake. Earth, Planets and Space 66(1):105

Goda K, Yasuda T, Mori N, Maruyama T (2016) New scaling relationships of earthquake source parameters for stochastic tsunami simulation. Coastal Engineering Journal 58(3):1650010–1

Goda K, Mori N, Yasuda T, Prasetyo A, Muhammad A, Tsujio D (2019) Cascading geological hazards and risks of the 2018 sulawesi indonesia earthquake and sensitivity analysis of tsunami inundation simulations. Frontiers in Earth Science 7:261

González F, Geist EL, Jaffe B, Kânoğlu U, Mofjeld H, Synolakis C, Titov VV, Arcas D, Bellomo D, Carlton D, et al. (2009) Probabilistic tsunami hazard assessment at seaside, oregon, for near-and far-field seismic sources. Journal of Geophysical Research: Oceans 114(C11)

Gray-Graves A, Turner KW, Swan JH (2010) Sustainability of seniors: disaster risk reduction management. J Aging Emerg Econ 2(2):64–78

Gregg CE, Houghton BF, Paton D, Lachman R, Lachman J, Johnston DM, Wongbusarakum S (2006) Natural warning signs of tsunamis: human sensory experience and response to the 2004 great sumatra earthquake and tsunami in thailand. Earthquake Spectra 22(S3):671–691

Grezio A, Babeyko A, Baptista MA, Behrens J, Costa A, Davies G, Geist EL, Glimsdal S, González FI, Griffin J, et al. (2017) Probabilistic tsunami hazard analysis: Multiple sources and global applications. Reviews of Geophysics 55(4):1158–1198

Grilli ST, Ioualalen M, Asavanant J, Shi F, Kirby JT, Watts P (2007) Source constraints and model simulation of the december 26, 2004, indian ocean tsunami. Journal of Waterway, Port, Coastal, and Ocean Engineering 133(6):414–428

Hayes GP, Moore GL, Portner DE, Hearne M, Flamme H, Furtney M, Smoczyk GM (2018) Slab2, a comprehensive subduction zone geometry model. Science 362(6410):58–61

Heidarzadeh M, Kijko A (2011) A probabilistic tsunami hazard assessment for the makran subduction zone at the northwestern indian ocean. Natural hazards 56(3):577–593

Heidarzadeh M, Satake K (2014) Possible sources of the tsunami observed in the northwestern indian ocean following the 2013 september 24 m w 7.7 pakistan inland earthquake. Geophysical Journal International 199(2):752–766

Heidarzadeh M, Pirooz MD, Zaker NH, Yalciner AC, Mokhtari M, Esmaeily A (2008) Historical tsunami in the makran subduction zone off the southern coasts of iran and pakistan and results of numerical modeling. Ocean Engineering 35(8):774 – 786, DOI https://doi.org/10.1016/j.oceaneng.2008.01.017

Heidarzadeh M, Pirooz MD, Zaker NH (2009) Modeling the near-field effects of the worst-case tsunami in the makran subduction zone. Ocean Engineering 36(5):368–376

Hein P (2014) Expecting the unexpected: a case study on tsunami mitigation in fujisawa (japan). Environmental Hazards 13(1):1–20

Hines RI (2007) Natural disasters and gender inequalities: The 2004 tsunami and the case of india. Race, Gender & Class pp 60–68

Hoechner A, Babeyko AY, Zamora N (2016) Probabilistic tsunami hazard assessment for the makran region with focus on maximum magnitude assumption. Natural Hazards and Earth System Sciences (NHESS) 16:1339–1350

Hossen MJ, Cummins PR, Dettmer J, Baba T (2015) Tsunami waveform inversion for sea surface displacement following the 2011 tohoku earthquake: Importance of dispersion and source kinematics. Journal of Geophysical Research: Solid Earth 120(9):6452–6473

Juran L (2012) The gendered nature of disasters: women survivors in post-tsunami tamil nadu. Indian Journal of Gender Studies 19(1):1–29

Kagan YY (2002) Seismic moment distribution revisited: I. statistical results. Geophysical Journal International 148(3):520–541

Kagan YY, Jackson DD (2013) Tohoku earthquake: A surprise? Bulletin of the Seismological Society of America 103(2B):1181–1194

Kajiura K (1963) The leading wave of a tsunami. Bulletin of the Earthquake Research Institute, University of Tokyo 41(3):535–571

Kakar D, Naeem G, Usman A, Mengal A, Naderi Beni A, Afarin M, Ghaffari H, Fritz H, Pahlevan F, Okal E, et al. (2015) Remembering the 1945 makran tsunami; interviews with survivors beside the arabian sea. UNESCO-IOC Brochure 1:79

Kakimoto R, Fujimi T, Yoshida M, Kim H (2016) Factors promoting and impeding precautionary evacuation behaviour. International journal of urban sciences 20(sup1):25–37

Kanai M, Katada T (2011) Issues of tsunami evacuation behavior in japan: residents response in case of chilean earthquake in 2010. In: Solutions to Coastal Disasters 2011, pp 417–422

Katada T, Kanai M (2016) The school education to improve the disaster response capacity: A case of ?kamaishi miracle? Journal of disaster research 11(5):845–856

Kawai H, Satoh M, Kawaguchi K, Seki K (2013) Characteristics of the 2011 tohoku tsunami waveform acquired around japan by nowphas equipment. Coastal Engineering Journal 55(03):1350008

Kennedy AB, Chen Q, Kirby JT, Dalrymple RA (2000) Boussinesq modeling of wave transformation, breaking, and runup. i: 1d. Journal of waterway, port, coastal, and ocean engineering 126(1):39–47

Kijko A (2004) Estimation of the maximum earthquake magnitude, m max. Pure and Applied Geophysics 161(8):1655–1681

Kijko A, Smit A, Sellevoll MA (2016) Estimation of Earthquake Hazard Parameters from Incomplete Data Files. Part III. Incorporation of Uncertainty of Earthquake-Occurrence Model. Bulletin of the Seismological Society of America 106(3):1210–1222, DOI 10.1785/0120150252, URL https://doi.org/10.1785/0120150252, https://pubs.geoscienceworld.org/bssa/article-pdf/106/3/1210/3668777/1210.pdf

Kirby JT, Wei G, Chen Q, Kennedy AB, Dalrymple RA (1998) Funwave 1.0: fully nonlinear boussinesq wave model-documentation and user's manual. research report NO CACR-98-06

Kulikov E, Kuzin I, Yakovenko O (2014) Tsunamis in the central part of the caspian sea. Oceanology 54(4):435–444

La Daana KK, Singh D, Lauckner B, Ebi KL, Chadee DD (2016) Knowledge, attitude and practices of coastal communities in trinidad and tobago about tsunamis. Natural Hazards 81(2):1349–1372

Larsen J, Dancy H (1983) Open boundaries in short wave simulations—a new approach. Coastal Engineering 7(3):285–297

Lawshe CH (1975) A quantitative approach to content validity 1. Personnel psychology 28(4):563–575

Lay T, Yamazaki Y, Ammon CJ, Cheung KF, Kanamori H (2011) The 2011 m w 9.0 off the pacific coast of tohoku earthquake: Comparison of deep-water tsunami signals with finite-fault rupture model predictions. Earth, planets and space 63(7):797–801

Lindell MK, Perry RW (2012) The protective action decision model: theoretical modifications and additional evidence. Risk Analysis: An International Journal 32(4):616–632

Lindell MK, Prater CS, Gregg CE, Apatu EJ, Huang SK, Wu HC (2015) Households' immediate responses to the 2009 american samoa earthquake and tsunami. International journal of disaster risk reduction 12:328–340

Lolli B, Gasperini P, Vannucci G (2014) Empirical conversion between teleseismic magnitudes (mb and m s) and moment magnitude (m w) at the global, euro-mediterranean and italian scale. Geophysical Journal International 199(2):805–828

Lorito S, Selva J, Basili R, Romano F, Tiberti M, Piatanesi A (2015) Probabilistic hazard for seismically induced tsunamis: accuracy and feasibility of inundation maps. Geophysical Journal International 200(1):574–588

Løvholt F, Pedersen G, Bazin S, Kühn D, Bredesen RE, Harbitz C (2012) Stochastic analysis of tsunami runup due to heterogeneous coseismic slip and dispersion. Journal of Geophysical Research: Oceans 117(C3)

Løvholt F, Setiadi NJ, Birkmann J, Harbitz CB, Bach C, Fernando N, Kaiser G, Nadim F (2014) Tsunami risk reduction–are we better prepared today than in 2004? International journal of disaster risk reduction 10:127–142

Løvholt F, Griffin J, Salgado-Gálvez M (2015) Tsunami hazard and risk assessment on the global scale. Encyclopedia of complexity and systems science pp 1–34

Lynett P, Wei Y, Arcas DR (2016) Tsunami Hazard Assessment: Best Modeling Practices and State-of-the Art Technology. United States Nuclear Regulatory Commission, Office of Nuclear Regulatory ...

Mabuku MP, Senzanje A, Mudhara M, Jewitt G, Mulwafu W (2018) Rural households? flood preparedness and social determinants in mwandi district of zambia and eastern zambezi region of namibia. International journal of disaster risk reduction 28:284–297

Marks K, Smith W (2006) An evaluation of publicly available global bathymetry grids. Marine Geophysical Researches 27(1):19–34

Marzocchi W, Jordan TH (2014) Testing for ontological errors in probabilistic forecasting models of natural systems. Proceedings of the National Academy of Sciences 111(33):11973–11978

Marzocchi W, Taroni M, Selva J (2015) Accounting for epistemic uncertainty in psha: Logic tree and ensemble modeling. Bulletin of the Seismological Society of America 105(4):2151–2159

MAS E, SUPPASRI A, IMAMURA F, KOSHIMURA S (2012) Agent-based simulation of the 2011 great east japan earthquake/tsunami evacuation: An integrated model of tsunami inundation and evacuation. Journal of Natural Disaster Science 34(1):41–57, DOI 10.2328/jnds.34.41

Mavhura E (2017) Applying a systems-thinking approach to community resilience analysis using rural livelihoods: The case of muzarabani district, zimbabwe. International journal of disaster risk reduction 25:248–258

McLaughlin L (2011) In the wake of the tsunami: religious responses to the great east japan earthquake. CrossCurrents 61(3):290–297

Mileti DS, Darlington J, Passerini E, Forrest BC, Myers MF (1995) Toward an integration of natural hazards and sustainability. Environmental Professional 17(2):117–126

Mofjeld HO, González FI, Titov VV, Venturato AJ, Newman JC (2007) Effects of tides on maximum tsunami wave heights: Probability distributions. Journal of Atmospheric and Oceanic Technology 24(1):117–123

Mohammad-pajooh E, et al. (2014) Investigating factors for disaster preparedness among residents of kuala lumpur. Natural Hazards and Earth System Sciences Discussions 2 (2014), Nr 5

Mori N, Goda K, Cox D (2018) Recent process in probabilistic tsunami hazard analysis (ptha) for mega thrust subduction earthquakes. In: The 2011 Japan Earthquake and Tsunami: Reconstruction and Restoration, Springer, pp 469–485

Mueller C, Power W, Fraser S, Wang X (2015) Effects of rupture complexity on local tsunami inundation: Implications for probabilistic tsunami hazard assessment by example. Journal of Geophysical Research: Solid Earth 120(1):488–502

Mulilis JP, Duval TS, Rogers R (2003) The effect of a swarm of local tornados on tornado preparedness: A quasi-comparable cohort investigation 1. Journal of Applied Social Psychology 33(8):1716–1725

Murty T, Rafiq M (1991) A tentative list of tsunamis in the marginal seas of the north indian ocean. Natural Hazards 4(1):81–83

Muttarak R, Pothisiri W (2013) The role of education on disaster preparedness: case study of 2012 indian ocean earthquakes on thailand's andaman coast. Ecology & Society 18(4):1–16

Nakasu T, Ono Y, Pothisiri W (2018) Why did rikuzentakata have a high death toll in the 2011 great east japan earthquake and tsunami disaster? finding the devastating disaster?s root causes. International journal of disaster risk reduction 27:21–36

Ngo EB (2001) When disasters and age collide: Reviewing vulnerability of the elderly. Natural Hazards Review 2(2):80–89

Nomoto H (2016) Methodology of education for tsunami disaster prevention: Sharing the experiences of great east japan earthquake. The Journal of social sciences and humanities (512):15–31

Normand R, Simpson G, Herman F, Biswas RH, Bahroudi A (2019) Holocene sedimentary record and coastal evolution in the makran subduction zone (iran). Quaternary 2(2):21

Norris FH, Smith T, Kaniasty K (1999) Revisiting the experience–behavior hypothesis: the effects of hurricane hugo on hazard preparedness and other self-protective acts. Basic and Applied Social Psychology 21(1):37–47

Ohno R, Isagawa T (2012) How do coastal residents behave after a big earthquake? 9th International Conference on Urban Earthquake Engineering/ 4th Asia Conference on Earthquake Engineering

Okada Y (1985) Surface deformation due to shear and tensile faults in a half-space. Bulletin of the seismological society of America 75(4):1135–1154

Pararas-Carayannis G (2006) The potential of tsunami generation along the makran subduction zone in the northern arabian sea: Case study: The earthquake and tsunami of november 28, 1945. Science of Tsunami Hazards 24(5):358–384

Paton D (2003) Disaster preparedness: a social-cognitive perspective. Disaster Prevention and Management: An International Journal 12(3):210–216

Paton D, Johnston D (2001) Disasters and communities: vulnerability, resilience and preparedness. Disaster Prevention and Management: An International Journal 10(4):270–277

Paul BK (2012) Factors affecting evacuation behavior: The case of 2007 cyclone sidr, bangladesh. The Professional Geographer 64(3):401–414

Payande A, Niksokhan M, Naserian H (2015) Tsunami hazard assessment of chabahar bay related to megathrust seismogenic potential of the makran subduction zone. Natural hazards 76(1):161–176

Pidgeon N, Hood C, Jones D, Turner B, Gibson R, et al. (1992) Risk perception. Risk: Analysis, perception and management pp 89–134

Plomp T (2013) Educational design research: An introduction. Educational design research pp 11–50

Power W, Wallace L, Wang X, Reyners M (2012) Tsunami hazard posed to new zealand by the kermadec and southern new hebrides subduction margins: an assessment based on plate boundary kinematics, interseismic coupling, and historical seismicity. Pure and applied geophysics 169(1-2):1–36

Quittmeyer R, Jacob K (1979) Historical and modern seismicity of pakistan, afghanistan, northwestern india, and southeastern iran. Bulletin of the Seismological Society of America 69(3):773–823

Rastgoftar E, Soltanpour M (2016) Study and numerical modeling of 1945 makran tsunami due to a probable submarine landslide. Natural Hazards 83(2):929–945

Reasenberg P (1985) Second-order moment of central california seismicity, 1969–1982. Journal of Geophysical Research: Solid Earth 90(B7):5479–5495

Reyes C, Wiemer S (2019) Zmap7, a refreshed software package to analyze seismicity. In: Geophysical Research Abstracts, vol 21

Rikitake T, Aida I (1988) Tsunami hazard probability in japan. Bulletin of the Seismological Society of America 78(3):1268–1278

Rittichainuwat BN (2013) Tourists' and tourism suppliers' perceptions toward crisis management on tsunami. Tourism Management 34:112–121

Safari A, Abolghasem A, Abedini N, Mousavi Z (2017) Assessment of optimum value for dip angle and locking rate parameters in makran subduction zone. International Archives of the Photogrammetry, Remote Sensing & Spatial Information Sciences 42

Said AM, Mahmud AR, Abas F, et al. (2011) Community preparedness for tsunami disaster: a case study. Disaster Prevention and Management: An International Journal

Salah P, Soltanpour M (2014) Modeling of tsunami propagation and inundation at the north coast of gulf of oman due to earthquake in makran subduction zone. International conference on coasts, ports and marine structures (icopmas) 11

Salah P, Sasaki J, Soltanpour M (2020) Comprehensive probabilistic tsunami hazard assessment in the makran subduction zone. 2010.01284

Samaddar S, Misra BA, Tatano H (2012) Flood risk awareness and preparedness: the role of trust in information sources. In: 2012 IEEE International Conference on Systems, Man, and Cybernetics (SMC), IEEE, pp 3099–3104

Sariolghalam M (2014) Rationality and Iran's national development. Farzan

Satake K (2014) Advances in earthquake and tsunami sciences and disaster risk reduction since the 2004 indian ocean tsunami. Geoscience Letters 1(1):15

Science N, Council T (2003) Reducing disaster vulnerability through science and technology. An interim report of the Subcommittee on Disaster Reduction

Sepúlveda I, Liu PLF, Grigoriu M (2019) Probabilistic tsunami hazard assessment in south china sea with consideration of uncertain earthquake characteristics. Journal of Geophysical Research: Solid Earth 124(1):658–688

Sherry J, Curtis A (2017) At the intersection of disaster risk and religion: Interpretations and responses to the threat of tsho rolpa glacial lake. Environmental Hazards 16(4):314–329

Shi F, Kirby JT, Harris JC, Geiman JD, Grilli ST (2012) A high-order adaptive time-stepping tvd solver for boussinesq modeling of breaking waves and coastal inundation. Ocean Modelling 43:36–51

Shibayama T, Esteban M, Nistor I, Takagi H, Thao ND, Matsumaru R, Mikami T, Aranguiz R, Jayaratne R, Ohira K (2013a) Classification of tsunami and evacuation areas. Natural hazards 67(2):365–386

Shibayama T, Esteban M, Nistor I, Takagi H, Thao ND, Matsumaru R, Mikami T, Aranguiz R, Jayaratne R, Ohira K (2013b) Classification of tsunami and evacuation areas. Natural hazards 67(2):365–386

Siegrist M, Cvetkovich G, Roth C (2000) Salient value similarity, social trust, and risk/benefit perception. Risk analysis 20(3):353–362

Sjöberg L (2000) Factors in risk perception. Risk analysis 20(1):1–12

Smith GL, McNeill LC, Wang K, He J, Henstock TJ (2013) Thermal structure and megathrust seismogenic potential of the makran subduction zone. Geophysical Research Letters 40(8):1528–1533

Starrs R (2014a) When the Tsunami Came to Shore: Culture and Disaster in Japan. Global Oriental, URL https://books.google.co.jp/books?id=uqvynwEACAAJ

Starrs R (2014b) When the tsunami came to shore: Culture and disaster in Japan. Global Oriental

Strasser FO, Arango M, Bommer JJ (2010) Scaling of the source dimensions of interface and intraslab subduction-zone earthquakes with moment magnitude. Seismological Research Letters 81(6):941–950

Sugino H, Iwabuchi Y, Hashimoto N, Matsusue K, Ebisawa K, Kameda H, Imamura F (2015) The characterizing model for tsunami source regarding the inter-plate earthquake tsunami. Journal of JAEE 15(3):3_114–3_133

Sugiura M, Sato S, Nouchi R, Honda A, Ishibashi R, Abe T, Muramoto T, Imamura F (2019) Psychological processes and personality factors for an appropriate tsunami evacuation. Geosciences 9(8):326

Sun L, Su G, Tian Q, Qi W, Liu F, Qi M, Li R (2019) Religious belief and tibetans? response to earthquake disaster: a case study of the 2010 ms 7.1 yushu earthquake, qinghai province, china. Natural Hazards 99(1):141–159

Suppasri A, Shuto N, Imamura F, Koshimura S, Mas E, Yalciner AC (2013) Lessons learned from the 2011 great east japan tsunami: Performance of tsunami countermeasures, coastal buildings, and tsunami evacuation in japan. Pure and Applied Geophysics 170(6-8):993–1018

Suppasri A, Abe Y, Yasuda M, Fukutani Y, Imamura F (2015) Tsunami signs, memorials and evacuation drills in miyagi prefecture after the 2011 tohoku earthquake tsunami. In: Handbook of Coastal Disaster Mitigation for Engineers and Planners, Elsevier, pp 599–614

Suppasri A, Latcharote P, Bricker JD, Leelawat N, Hayashi A, Yamashita K, Makinoshima F, Roeber V, Imamura F (2016) Improvement of tsunami countermeasures based on lessons from the 2011 great east japan earthquake and tsunami—situation after five years. Coastal Engineering Journal 58(4):1640011–1

Suwa Y, Kato F (2009) Decision making on evacuation from the tsunami following the earthquake off kuril islands in 2006. Technical Report of the 41st Joint Meeting of of UJNR Wind and Seismic Structures

Takabatake T, Shibayama T, Esteban M, Ishii H, Hamano G (2017) Simulated tsunami evacuation behavior of local residents and visitors in kamakura, japan. International journal of disaster risk reduction 23:1–14

Takabatake T, Mäll M, Esteban M, Nakamura R, Kyaw T, Ishii H, Valdez J, Nishida Y, Noya F, Shibayama T (2018a) Field survey of 2018 typhoon jebi in japan: Lessons for disaster risk management. Geosciences 8(11):412

Takabatake T, Shibayama T, Esteban M, Ishii H (2018b) Advanced casualty estimation based on tsunami evacuation intended behavior: case study at yuigahama beach, kamakura, japan. Natural hazards 92(3):1763–1788

Takagi H, Mikami T, Fujii D, Esteban M, Kurobe S (2016) Mangrove forest against dyke-break-induced tsunami on rapidly subsiding coasts. Natural Hazards and Earth System Sciences 16(7):1629–1638

Tavares AO, Mendes JM, Basto E, Cunha L (2010) Risk perception, extreme events and institutional trust: a local survey in portugal. Reliability, risk and safety: theory and applications, London: Taylor & Francis Group, pp 1245Ā1252

Tehranirad B, Shi F, Kirby JT, Harris JC, Grilli S (2011) Tsunami benchmark results for fully nonlinear boussinesq wave model funwave-tvd, version 1.0. Center for Applied Coastal Research, University of Delaware, Tech Rep

Thio HK (2010) Urs probabilistic tsunami hazard system: A user manual. Technical Report URS Corporation, San Francisco, CA

Thio HK, Somerville P, Ichinose G (2007) Probabilistic analysis of strong ground motion and tsunami hazards in southeast asia. Journal of Earthquake and Tsunami 1(02):119–137

Thio HK, Wilson RI, Miller K (2014) Evaluation and application of probabilistic tsunami hazard analysis in california. AGUFM 2014:NH12A–01

Ukkusuri SV, Hasan S, Luong B, Doan K, Zhan X, Murray-Tuite P, Yin W (2017) A-rescue: An agent based regional evacuation simulator coupled with user enriched behavior. Networks and Spatial Economics 17(1):197–223

UNISDR (2015) Sendai framework for disaster risk reduction 2015–2030. http://www.preventionweb.net/files/43291_sendaiframeworkfordrren.pdf, accessed: 2017-05-20

Van Eck NJ, Waltman L (2010) Software survey: Vosviewer, a computer program for bibliometric mapping. scientometrics 84(2):523–538

Vasvári T, et al. (2015) Risk, risk perception, risk management–a review of the literature. Public Finance Quarterly 60(1):29–48

Vicente R, Ferreira TM, Maio R, Koch H (2014) Awareness, perception and communication of earthquake risk in portugal: Public survey. Procedia Economics and Finance 18:271–278

Viglione A, Di Baldassarre G, Brandimarte L, Kuil L, Carr G, Salinas JL, Scolobig A, Blöschl G (2014) Insights from socio-hydrology modelling on dealing with flood risk–roles of collective memory, risk-taking attitude and trust. Journal of Hydrology 518:71–82

Wachinger G, Renn O, Begg C, Kuhlicke C (2013) The risk perception paradox—implications for governance and communication of natural hazards. Risk analysis 33(6):1049–1065

Ward PJ, Blauhut V, Bloemendaal N, Daniell JE, de Ruiter MC, Duncan MJ, Emberson R, Jenkins SF, Kirschbaum D, Kunz M, et al. (2020) Natural hazard risk assessments at the global scale. Natural Hazards and Earth System Sciences 20(4)

Wei G, Kirby JT, Grilli ST, Subramanya R (1995) A fully nonlinear boussinesq model for surface waves. part 1. highly nonlinear unsteady waves. Journal of Fluid Mechanics 294:71–92

Weinstein ND (1989) Effects of personal experience on self-protective behavior. Psychological bulletin 105(1):31

Wells DL, Coppersmith KJ (1994) New empirical relationships among magnitude, rupture length, rupture width, rupture area, and surface displacement. Bulletin of the seismological Society of America 84(4):974–1002

Welton-Mitchell C, James L, Awale R (2016) Nepal 2015 earthquake: A rapid assessment of cultural, psychological and social factors with implications for recovery and disaster preparedness. International Journal of Mass Emergencies & Disasters 34(3)

Whitehead JC, Edwards B, Van Willigen M, Maiolo JR, Wilson K, Smith KT (2000) Heading for higher ground: factors affecting real and hypothetical hurricane evacuation behavior. Global Environmental Change Part B: Environmental Hazards 2(4):133–142

Wisner B, Blaikie PM, Blaikie P, Cannon T, Davis I (2004) At risk: natural hazards, people's vulnerability and disasters. Psychology Press

Wright N (2013) Background paper prepared for the global assessment report on disaster risk reduction 2013: Small island developing states, disaster risk management, disaster risk reduction, climate change adaptation and tourism. Geneva: UNISDR/GAR

Yamashita T, Matsushima H, Noda I (2014) Exhaustive analysis with a pedestrian simulation environment for assistant of evacuation planning. Transportation Research Procedia 2:264–272

Yamazaki Y, Lay T, Cheung K, Yue H, Kanamori H (2011) Modeling near-field tsunami observations to improve finite-fault slip models for the 11 march 2011 tohoku earthquake. Geophysical Research Letters 38(7)

Yasuda T, Hatayama M, Shimada H (2016) National questionnaire survey of surfers awareness about tsunami evacuation. Saf Sci Rev 2016:61–80

Youngs RR, Coppersmith KJ (1985) Implications of fault slip rates and earthquake recurrence models to probabilistic seismic hazard estimates. Bulletin of the Seismological society of America 75(4):939–964

Yun NY, Hamada M (2012) Evacuation behaviors in the 2011 great east japan earthquake. Journal of Disaster Research 7(7):458–467

Yun NY, Hamada M (2015) Evacuation behavior and fatality rate during the 2011 tohoku-oki earthquake and tsunami. Earthquake Spectra 31(3):1237–1265